

Physiological potential of the anaerobic  
naphthalene-degrading enrichment culture N47:  
Genomic, proteomic and stable isotope studies.

Franz D. Bergmann

Dissertation



TECHNISCHE UNIVERSITÄT MÜNCHEN

Lehrstuhl für Grundwasserökologie

Physiological potential of the anaerobic  
naphthalene-degrading enrichment culture N47:  
Genomic, proteomic and stable isotope studies

Franz Detlef Bergmann

Vollständiger Abdruck der von der Fakultät Wissenschaftszentrum Weihenstephan für Ernährung,  
Landnutzung und Umwelt der Technischen Universität München zur Erlangung des akademischen  
Grades eines

Doktors der Naturwissenschaften

genehmigten Dissertation.

Vorsitzende(r):

Univ.-Prof. Dr. W. Liebl

Prüfer der Dissertation:

1. Univ.-Prof. Dr. R. Meckenstock
2. Univ.-Prof. Dr. Th. Rattei  
(Universität Wien / Österreich)

Die Dissertation wurde am 13.07.2010 bei der Technischen Universität München eingereicht und  
durch die Fakultät Wissenschaftszentrum Weihenstephan für Ernährung, Landnutzung und Umwelt  
am 17.11.2010 angenommen.



## Summary

Anaerobic degradation of naphthalene is an important process during bioremediation of aromatic hydrocarbon spills as naphthalene is for example a major compound of coal tar. Naphthalene is potentially hazardous and a possible human carcinogen. Therefore, natural degradation potential is of particular interest. However, it is difficult to assess naphthalene degradation in the subsurface by established methods. On the other hand knowledge about anaerobic naphthalene degradation remains obscure. The initial activation reaction has not been elucidated yet, as well the knowledge about metabolic potential and physiology of organisms responsible for bioremediation is scarce.

Compound Specific Isotope Analysis (CSIA) has been shown to address the two research gaps of assessing degradation in the subsurface and enlightening the initial step of anaerobic transformation. Therefore, the carbon and hydrogen fractionation was measured during anaerobic naphthalene degradation under sulphate-reducing conditions for the two cultures N47 and NaphS2. The calculated enrichment factors were  $\epsilon_C = -5.0\text{‰} \pm 1.0\text{‰}$  and  $\epsilon_H = -100\text{‰} \pm 15\text{‰}$  for N47, and  $\epsilon_C = -0.7\text{‰} \pm 0.3\text{‰}$  and  $\epsilon_H = -73\text{‰} \pm 11\text{‰}$  for NaphS2, resulting in significantly different slopes of dual isotope plots,  $\Lambda = 29 \pm 8$  (N47) and  $\Lambda = 107 \pm 45$  (NaphS2). Opposed to carbon isotope analysis, the enrichment factors for hydrogen were surprisingly strong and consistent. This suggested hydrogen isotope fractionation measurements as a robust tool to qualitatively and quantitatively assess environmental biodegradation of naphthalene. Evaluating the slopes of the dual isotope plots did not provide further insights into the initial activation step of anaerobic naphthalene degradation.

Nevertheless, a proteogenomic investigation of sulphate-reducing enrichment culture N47 provided new insights. The alpha-subunit of a carboxylase protein was identified that was two-fold up-regulated in naphthalene-grown cells as compared to 2-methylnaphthalene-grown cells. A protein sequence based homology search of the putative naphthalene carboxylase resulted in 48% similarity to the anaerobic benzene carboxylase from an iron-reducing, benzene-degrading culture (BF) and 45% similarity to the alpha-subunit of phenylphosphate carboxylase of *Aromatoleum aromaticum* EbN1. In the genomic neighbourhood a second beta-subunit of putative naphthalene carboxylase has been identified and shown to be expressed during growth on naphthalene. A further strong hint for functional and structural consistency was that putative naphthalene carboxylase, benzene carboxylase, and phenylphosphate carboxylase subunits all contained the same carboxylase-related protein domain. Furthermore, several open reading frames (ORFs) were identified possibly encoding

a 2-naphthoate-CoA ligase and one of them was exclusively expressed during growth on naphthalene and 2-naphthoic. Such a naphthoate-CoA-ligase is obligate in anaerobic naphthalene degradation for activation of the carboxyl group with HS-CoA for the subsequent ring reduction.

Additional insight into metabolic potential of polycyclic aromatic hydrocarbon (PAH) degrading culture N47 was gained by sequencing the genome and mapping the proteome during growth on the PAHs naphthalene, 2-methylnaphthalene and 2-naphthoic acid to its predicted metabolic pathways. The sequencing, assembly and taxonomic binning resulted in 17 contigs of the dominant deltaproteobacterium of the culture. The metagenome covered most of the genome according to the presence of general clusters of orthologous groups (COGs). The genes present showed the potential of N47 to grow on D-mannose, D-fructose, D-galactose,  $\alpha$ -D-glucose-1P, starch, glycogen, peptidoglycan, and possesses the potential for butanoic acid fermentation. Contradictory to the existing genes for nitrate ammonification, N47 did not grow with  $\text{NO}_3^-$  as terminal electron acceptor. Furthermore it is the first bacterium containing a complete TCA cycle together with the carbon monoxide dehydrogenase pathway. However, it is not known if those pathways are used for either heterotrophic or autotrophic growth. The ability of genome evolution for the metagenome was mirrored by the significantly high percentage of repetitive sequences and transposase-related protein domains. The many unique putative genes with unknown function contained by N47 metagenome were meant to be candidates for yet unknown reaction pathways.

## Zusammenfassung

Anaerober Naphthalinabbau ist ein wichtiger Bestandteil von Bioremediationsabläufen, wenn aromatische Kohlenwasserstoffe in die Umwelt gelangen, da Naphthalin ein Hauptbestandteil von z.B. Steinkohlenteer ist. Naphthalinexposition ist potentiell gefährlich und wahrscheinlich krebserregend bei Menschen. Deshalb ist das natürliche Abbaupotential von besonderem Interesse. Allerdings ist es schwierig Naphthalinabbau unter der Erdoberfläche mit etablierten Methoden zu messen und zu berechnen. Andererseits ist Wissen über anaeroben Naphthalinabbau kaum vorhanden. Die anfängliche Aktivierungsreaktion wurde bisher nicht aufgeklärt. Genauso wenig weiß man über die metabolischen Möglichkeiten und die Physiologie solcher Bioremediationsorganismen.

In frühere Studien wurde bereits gezeigt, dass substanzspezifische Isotopenanalytik (CSIA) zwei wissenschaftliche Lücken schließen kann. Einerseits kann man Abbau im Untergrund messen und verfolgen, andererseits kann man damit den ersten Schritt von anaerobem Substanzabbau näher beleuchten. Deshalb wurde Kohlenstoff- und Wasserstofffraktionierung während des anaeroben Naphthalinabbaus unter sulfatreduzierenden Bedingungen für die zwei Kulturen N47 und NaphS2 gemessen. Die daraus errechneten Anreicherungsfaktoren sind  $\epsilon_C = -5.0\text{‰} \pm 1.0\text{‰}$  und  $\epsilon_H = -100\text{‰} \pm 15\text{‰}$  für N47, und  $\epsilon_C = -0.7\text{‰} \pm 0.3\text{‰}$  und  $\epsilon_H = -73\text{‰} \pm 11\text{‰}$  für NaphS2. Daraus resultierten signifikant unterschiedliche Steigungen für die zweidimensionalen Isotopemplots von  $\Lambda = 29 \pm 8$  (N47) und  $\Lambda = 107 \pm 45$  (NaphS2). Im Gegensatz zur Isotopenanalyse von Kohlenstoff, waren die Anreicherungsfaktoren für Wasserstoff erstaunlicherweise solide und konsistent. Dies wiederum zeigte, dass die Messung von Wasserstoffisotopenfraktionierung ein verlässliches Instrument ist um biologischen Abbau von Naphthalin sowohl qualitativ als auch quantitativ zu bestimmen. Betrachtet man die Steigungen der Regressionen in den zweidimensionalen Isotopenplots, so konnte man daraus keine weiteren gesicherten Erkenntnisse über den ersten Aktivierungsmechanismus beim anaeroben Naphthalinabbau gewinnen.

Im Gegensatz dazu gewährte ein proteogenomischer Ansatz mit der sulfatreduzierenden Anreicherungskultur N47 neue Einblicke in den anaeroben Naphthalinabbau. Die Alpha-Untereinheit eines Carboxylaseproteins konnte identifiziert werden. Diese war zweifach überexprimiert in Zellen, welche mit Naphthalin als Substrat gewachsen waren im Vergleich zu solchen, welche auf 2-Methylnaphthalin gewachsen waren. Eine aminosäuresequenzbasierte Homologiesuche dieser putativen Naphthalincarboxylase zeigte 48% Ähnlichkeit mit der anaeroben Benzolcarboxylase einer eisenreduzierenden,

benzolabbauenden Kultur (BF) und 45% Ähnlichkeit zur Alpha-Untereinheit der Phenylphosphatcarboxylase von *Aromatoleum aromaticum* EbN1. In näherer Umgebung auf dem Genom konnte eine zweite Beta-Untereinheit der putativen Naphthalincarboxylase identifiziert werden. Außerdem konnte gezeigt werden, dass diese bei Wachstum auf Naphthalin exprimiert ist. Ein weiterer überzeugender Hinweis für funktionelle und strukturelle Konsistenz der Untereinheiten von putativer Naphthalincarboxylase, Benzolcarboxylase und Phenylphosphatcarboxylase war, dass alle dieselbe Carboxylase korrelierte Proteindomain enthielten. Darüber hinaus wurden weitere offene Leserahmen (ORFs) gefunden, welche möglicherweise für eine 2-Naphthoate-CoA Ligase kodieren. Einer davon war exklusiv exprimiert bei Wachstum auf Naphthalin und 2-Naphthoesäure. Solch eine Naphthoate-CoA Ligase ist für anaeroben Naphthalinabbau obligat, da sie die Carboxylgruppe mit HS-CoA für den anschließenden Abbau des aromatischen Rings aktiviert.

Zusätzlichen Einblick in die metabolischen Möglichkeiten der polyzyklische aromatische Kohlenwasserstoff (PAK) abbauenden Kultur N47 wurde einerseits durch die Genomsequenzierung erreicht, andererseits durch das Abbilden der entsprechenden Proteome während des Wachstums auf den PAKs Naphthalin, 2-Methylnaphthalin und 2-Naphthoesäure auf die aus dem Genom vorhergesagten metabolischen Pfade. Das Sequenzieren, das Assembly und das taxonomische Binning brachten 17 Contigs des dominanten Deltaproteobakteriums der Kultur hervor. Das so entstandene Metagenom deckt den Großteil des gesamten Genoms ab, legt man die Abschätzung durch das Vorhandensein der üblichen Cluster von orthologen Gruppen (COGs) zu Grunde. N47 besitzt die Gene für potentielles Wachstum auf D-Mannose, D-Fruktose, D-Galaktose,  $\alpha$ -D-Glukose-1P, Stärke, Glykogen, Peptidoglykan und außerdem die Möglichkeit für Buttersäuregärung. Im Widerspruch zu den vorhandenen Genen zur Nitratammonifikation, wuchs N47 nicht mit  $\text{NO}_3^-$  als terminalem Elektronenakzeptor. Darüber hinaus ist N47 das erste Bakterium, das sowohl einen kompletten TCA Zyklus als auch den reductiven acetyl-CoA-Weg enthält. Trotzdem ist nicht bekannt ob die Stoffwechselwege für heterotrophes oder autotrophes Wachstum in N47 genutzt werden. Die Befähigung zur Genomevolution des Metagenoms spiegelte sich in dem prozentual signifikant hohen Anteil von repetitiven Sequenzen und Transposase korrelierten Protein Domänen wieder. Für die vielen unikalen, putativen Gene mit unbekannter Funktion im Metagenom von N47 wurde angenommen, dass diese Anwärter für bisher unbekannte Reaktionen in Stoffwechselwegen sind.



## Table of contents

Summary .....	i
Zusammenfassung .....	iii
<b>1. General Introduction .....</b>	<b>1</b>
1.1 Aromatic hydrocarbons .....	2
1.2 Anaerobic microbial aromatic hydrocarbon degradation .....	2
1.3 Microbial anaerobic naphthalene degradation .....	4
1.4 Genome sequences of aromatic hydrocarbon degraders .....	5
1.5 Study of aromatic hydrocarbon degradation by isotope fractionation .....	6
1.6 Highly enriched, sulphate-reducing, naphthalene-degrading culture N47 .....	7
1.7 Objectives .....	7
1.8 References .....	8
<b>2. C and H stable isotope fractionation during strictly anaerobic naphthalene and benzene degradation: mechanistic implications and potential to assess natural attenuation .....</b>	<b>17</b>
2.1 Introduction .....	18
2.2 Material and Methods .....	20
2.2.1 Cultivation Conditions .....	20
2.2.2 Analytical Methods .....	21
2.2.3 Quantification of isotope fractionation .....	21
2.3 Results .....	23
2.3.1 Carbon isotope fractionation during anaerobic benzene and naphthalene degradation .....	23
2.3.2 Hydrogen isotope fractionation during anaerobic benzene and naphthalene degradation .....	24
2.3.3 Two-dimensional isotope fractionation investigation .....	26
2.4 Discussion .....	27
2.4.1 Hydrogen and carbon isotope fractionation to assess natural attenuation .....	27

2.4.2 Comparison of dual-isotope fractionation .....	29
2.5 References .....	32

### **3. Identification of new potential enzymes involved in anaerobic naphthalene**

#### **degradation by the sulphate-reducing enrichment culture N47 ..... 37**

3.1 Introduction .....	38
3.2 Material and Methods.....	40
3.2.1 Growth conditions for the enrichment culture N47.....	40
3.2.2 Terminal restriction fragment length polymorphism (T-RFLP).....	40
3.2.3 Sodium dodecyl sulfate-polyacrylamide gel electrophoresis (SDS PAGE) .....	40
3.2.4 Linear quadrupole ion trap-Orbitrap (LTQ Orbitrap XL) mass spectrometry (MS) with nano-electrospray ionization (ESI) .....	41
3.2.4.1 Tryptic cleavage.....	41
3.2.4.2 MS analysis and data processing .....	41
3.2.4.3 Criteria for identification .....	42
3.2.5 Two-dimensional gel electrophoresis (2-DGE).....	42
3.2.6 Matrix-assisted laser desorption ionization-time of flight mass spectrometry (MALDI-TOF-MS) .....	43
3.2.6.1 Tryptic cleavage.....	43
3.2.6.2 MS analysis and data processing .....	43
3.2.6.3 Criteria for identification .....	44
3.2.7 Operon Prediction in N47.....	44
2.3 Results and discussion.....	45
2.3.1 Culture composition.....	45
2.3.2 Shotgun proteome analysis of naphthalene- and 2-methylnaphthalene- grown N47 cells .....	45
2.3.3 Proteome analysis using 2-DGE.....	46
2.3.4 Verification of putative candidates by homology studies.....	48
2.3.5 Domain-based enzyme comparison.....	50
2.3.6 2-Naphthoate-CoA-ligase .....	53
3.4 Conclusion.....	55
3.5 References .....	55

<b>4. Genomic insights in the metabolic potential of the polycyclic aromatic hydrocarbon degrading sulphate-reducing culture N47.....</b>	<b>59</b>
4.1 Introduction .....	60
4.2 Material and Methods.....	62
4.2.1 Cultivation of the enrichment culture N47 .....	62
4.2.2 Sequencing and annotation.....	62
4.2.3 Taxonomic binning for classification of contigs.....	62
4.2.4 Completeness estimation of genomic sequence .....	63
4.2.5 Number of genes with homologous in other bacteria.....	63
4.2.6 Unique genes based on taxonomic levels.....	63
4.2.7 Gene duplications within the metagenome.....	64
4.2.8 Repetitive sequences covering the metagenome .....	64
4.2.9 Domain representation and frequency of occurrence .....	64
4.2.10 Determination of protein expression .....	64
4.2.11 Tryptic cleavage of protein bands .....	65
4.2.12 MS/MS scan of tryptic peptides .....	66
4.2.13 MS data analysis.....	66
4.2.14 Gene visualization by metabolic pathway colouring.....	67
4.3 Results and Discussion.....	67
4.3.1 Origin of contigs.....	67
4.3.2 Completeness of metagenome .....	68
4.3.3 General genomic features in comparison to other genomes.....	68
4.3.4 Conservation of predicted proteome.....	70
4.3.5 Unique genes according to taxonomic constraints .....	70
4.3.6 Parologue genes in N47 .....	70
4.3.7 Repetitive sequences covering the N47 metagenome .....	71
4.3.8 Over- and underrepresented domains within N47.....	71
4.3.9 Identification of existing gene clusters and expression during growth on substrates .....	72
4.3.10 Genes for central catabolism and anabolism of nucleic acid, amino acids, sugars and lipids.....	72
4.3.11 Hydrocarbon metabolism.....	73
4.3.12 Butanoate fermentation.....	73
4.3.13 Mobility and signalling.....	74

4.3.14 Transport systems .....	74
4.3.15 Vitamins and antibiotics .....	75
4.3.16 Energy metabolism .....	75
4.4 References .....	79
<b>5. General Conclusion and Outlook.....</b>	<b>87</b>
5.1 Conclusion and Outlook .....	88
5.2 References .....	90
Supplementary material chapter 2 .....	I
Supplementary material chapter 4.....	V
Clarifications .....	XIV
Danksagung.....	XVI
Curriculum Vitae.....	XVIII



# **Widmung**

**meinem verstorbenem Opa Richard  
und meiner Familie**

*„Hoffen wir das Beste liebe Leser.“*  
(Richard Fleckenstein)



**1.**

## **General Introduction**

## **1.1 Aromatic hydrocarbons**

Aromatic compounds, such as lignin components, flavonoids, quinones, aromatic amino acids, or constituents of fossil fuels are the second most abundant class of organic compounds in nature [1]. A subgroup of those aromatic compounds, are aromatic hydrocarbons that consist of one or more benzene rings. Aromatic hydrocarbons are highly stable due to their delocalized electron system which is significantly greater than that of a hypothetical localized structure (e.g. Kekulé structure) [2]. Monoaromatic hydrocarbons, like for example benzene, toluene, ethylbenzene and the three xylene isomers, the so called BTEX compounds, contain only one aromatic ring. On the other hand, the polycyclic aromatic hydrocarbons (PAHs) possess at least two condensed aromatic rings, as for example naphthalene, anthracene, phenanthrene, benzo[a]pyrene or ovalene.

Oxic and anoxic environments such as aquifers, surface freshwater bodies, soils, and terrestrial and marine sediments are frequently impacted by aromatic hydrocarbons [3] because of crude oil spillage, fossil fuel combustion and gasoline leakage. Additionally, natural inputs like forest fire smoke and natural petroleum seepage lead to a release of aromatic hydrocarbons into the environment [3]. Contamination of groundwater ecosystems results in the depletion of oxygen and in the formation an anoxic contaminant plume.

In general, aromatic compounds are widely used and also produced in industry, because of the stability of their benzene ring system. This in turn is also the reason of the persistence of those compounds, when released to the environment. Together with their toxic and carcinogenic properties contamination by aromatic hydrocarbons pose a great risk to environment, animals and humans [4,5] and is of great social and scientific concern. As for example it has been shown naphthalene can cause destruction of red blood cells leading to haemolytic anaemia and may cause nausea, vomiting, diarrhoea, blood in the urine and a skin colour more yellow than usual [6]. Therefore natural degradation potential is of particular interest.

## **1.2 Anaerobic microbial aromatic hydrocarbon degradation**

It has been shown that microorganisms are of major importance maintaining the health of the biosphere [7]. Aerobic biodegradation of aromatic hydrocarbons is well known and has been studied for many years. In contrast the knowledge of anaerobic biodegradation of aromatic hydrocarbons developed only during the last two decades. As for example non-substituted

aromatic compounds were initially thought unlikely to be anaerobically degradable due to the lack of activating ring substituents such as the methyl group in toluene [8]. Nevertheless anaerobic benzene degradation has been shown under methanogenic [9-13], sulphate- [11,13-22], ferric iron- [23-27], and nitrate-reducing [13,28-30] conditions. As well it has been shown the anaerobic biodegradation of other monoaromatic hydrocarbons under various terminal electron acceptor conditions.

For the first time, Mihelic *et al.* demonstrated in microcosm studies that naphthalene and acenaphthene were degraded under nitrate-reducing conditions [31]. In further microcosm experiments diverse PAHs have been shown to be degraded anaerobically with various terminal electron acceptors, like nitrate [31-37], sulphate [34,36-40], ferric iron [41], manganese(IV) [36] and CO<sub>2</sub> [31] which has been reviewed by Meckenstock *et al.* [42]. However, isolation and cultivation was only possible for three sulphate-reducing enrichment cultures [39,43,44], three sulphate-reducing pure cultures [45,46] and one nitrate-reducing pure culture [47], capable to degrade naphthalene.

After more and more cultures capable of anaerobic aromatic hydrocarbon degradation have been cultivated, the pathways used by the bacteria for the catabolism of those compounds were investigated. For aromatic compounds containing a methyl side chain fumarate is added to the methyl group of the aromatic hydrocarbon to activate the C-H bond. For toluene this reaction is catalyzed by benzylsuccinate synthase and has been shown for the first time in *Thauera aromatica* [48]. This mechanism has also been shown for the degradation of m-xylene [49], p-xylene [50], ethylbenzene [51] and 2-methylnaphthalene [52,53]. Recently all genes and proteins involved in the anaerobic degradation of 2-methylnaphthalene by sulfate-reducing enrichment culture N47 have been described [53]. For alkylbenzenes containing two or more carbon atoms in the side chain another transformation mechanism is proposed as summarized in Carmona *et al.* [1]. Thus it is demonstrated/proposed that ethylbenzene is hydroxylated directly by ethylbenzene dehydrogenase to (S)-1-phenylethanol which is further transformed to acetophenone by a subsequent oxidation of the alkyl carbon adjacent to the ring catalyzed by (S)-1-phenylethanol dehydrogenase as reviewed.

For the more recalcitrant non-substituted aromatic hydrocarbons several initial reactions have been postulated so far. Regarding benzene, a direct methylation to toluene [54,55], a hydroxylation to phenol [9,18,56], or a direct carboxylation to benzoate [18,57,58] has been proposed. Very recently it could be shown by combining proteomic and genomic analyses, that in a highly enriched, iron-reducing culture, the initial step of benzene degradation is most likely a carboxylation [59]. The genes for a benzene carboxylase and a benzoate-CoA ligase

have been identified located adjacent in the genome and were expressed exclusively during growth on benzene. In the case of anaerobic naphthalene degradation on the one hand a methylation to 2-methylnaphthalene has been suggested [60] and on the other hand a carboxylation to 2-naphthoic acid has been hypothesized [43,46]. Phenanthrene, the next larger PAH, is meant to be carboxylated as well [43].

### **1.3 Microbial anaerobic naphthalene degradation**

The gene clusters involved in the anaerobic degradation of 2-methylnaphthalene were recently identified in a highly enriched, sulphate-reducing culture by combining proteomics and genomics [53]. Based on the detection of metabolites specific for the anaerobic 2-methylnaphthalene degradation pathway during growth on naphthalene as well as the measurement of enzyme activities of several reactions of the 2-methylnaphthalene degradation pathway in naphthalene-grown cells lead to the proposal that anaerobic naphthalene degradation proceeds via methylation to 2-methylnaphthalene [60]. A further support is that N47 cells adapted to growth on naphthalene utilize 2-methylnaphthalene without any induction phase [60].

On the other hand it has been shown that  $^{13}\text{C}$ -labelled bicarbonate from the buffer is incorporated into the carboxyl group of 2-naphthoic acid by a sulfidogenic consortium during anaerobic growth on naphthalene [43]. Furthermore comparative proteome analysis of marine, sulphate-reducing cultures NaphS2, NaphS3 and NaphS6 revealed a specific 2-methylnaphthalene-induced protein band, absent in naphthalene-grown cell proteome, which could be correlated to naphthyl-2-methyl-succinate synthase (Nms) [46]. Nms catalyzes fumarate addition to the methyl group of 2-methylnaphthalene forming naphthyl-2-methyl-succinate, analogue to the anaerobic toluene degradation. The growth of NaphS2 on  $\text{d}_8$ -labelled naphthalene and unlabelled 2-methylnaphthalene at the same time showed forming of high abundant deuterated 2-naphthoyl-CoA and comparatively very low portion of unlabeled naphthyl-2-methyl-succinate [46]. Additionally naphthalene-grown cells underwent an extended lag phase, when shifted to 2-methylnaphthalene [46]. This all supports the hypothesis of carboxylation of initial reaction mechanism during anaerobic naphthalene degradation.

## 1.4 Genome sequences of aromatic hydrocarbon degraders

Genome sequencing may provide a promising tool to obtain a better insight into anaerobic aromatic hydrocarbon degradation pathways. By identification of operons and their structure responsible for anaerobic aromatic hydrocarbon degradation this methodical approach offers insight into the physiological potential of the bacteria. The benefit of genome sequences is even higher, when combining it with other approaches as for example proteomic studies, because then on the one hand predicted open reading frames (ORFs) can be verified and on the other hand measured peptide sequences can be mapped to the genome to identify the complete enzyme. In the last years additional to the classical Sanger sequencing method, a new and faster method was developed, pyrosequencing. This allows for faster and cheaper automated sequencers, like 454-pyrosequencing, called next-generation sequencing.

Nevertheless even though presently it is the so called post-genomic era only four genomes of obligate anaerobes degrading aromatic compounds are sequenced and published. The photosynthetic alpha-proteobacterium *Rhodospseudomonas palustris* CGA009, which is capable of degrading lignin monomers, phenol (to 4-hydroxyphenylacetate), benzoate, 4-hydroxybenzoate and possesses additional five benzene ring cleavage pathways [61].

According to the 10 gene cluster identified, the denitrifying beta-proteobacterium *Aromatoleum aromaticum* EbN1 known to degrade toluene and ethylbenzene, should be as well able to grow on benzoate, p-cresol, phenol, 3-hydroxybenzoate, benzaldehyde, phenylacetate, benzylalcohol and phenylalanine [62]. Furthermore paralogous gene clusters have been found which indicate for a larger degradation spectrum than previously known [63].

*Dechloromonas aromatica* RCB [29] is a nitrate-reducing beta-proteobacterium able to catabolize benzene, toluene, ethylbenzene and all three xylene isomers [64]. Astonishingly its genome sequence contained none of the previously characterized enzymes for anaerobic aromatic degradation, which indicates for new pathways [65].

A genomic island of 300 kb length in the genome of the Fe(III)-reducing delta-proteobacterium *Geobacter metallireducens* GS-15 contains the enzymes for the degradation of phenol, p-cresol, 4-hydroxybenzaldehyde, 4-hydroxybenzoate, benzyl alcohol, benzaldehyde and benzoate, while the toluene degradation pathway is located in a separate region [66].

Up to now no genome of a bacterium capable to anaerobically degrade at least one PAH is publicly available.

## 1.5 Study of aromatic hydrocarbon degradation by isotope fractionation

Compound Specific Isotope Analysis (CSIA) became a common promising tool for the evaluation of aromatic hydrocarbon degradation over the last decade. Since mass balances are hard to establish in the subsurface, CSIA enables to determine natural attenuation of aromatic hydrocarbons in the environment [67-69]. If a significant enrichment of heavy isotopes can be measured over time or spatial direction this is a direct proof for biodegradation of the investigated substance [67], because non-destructive abiotic natural processes such as dispersion, sorption or volatilization generally do not entail significant isotope fractionation [70-73].

The intrinsic bioremediation potential of different contaminated sites was evaluated by measurement of the carbon as well as the hydrogen isotopic enrichment of benzene [19,74-76]. Furthermore it has been shown that it is possible to quantify the extent of biodegradation by changes in the isotope signature [77,78] based on references derived from batch experiments, allowing for a maximal possible degradation assessment in the field.

Furthermore it has been demonstrated, that CSIA enables for the appointment of degradation pathways to aromatic contaminants [79,80]. Nevertheless due to masking effects by biotic transformation processes preceding the (bio)chemical bond cleavage even the same biotransformation pathway may not always show the same isotope fractionation [81,82]. A circumvention of that problem is plotting the changes of the isotope ratio of one element relative to another, drawing so called dual isotope plots. These are much less affected by masking effects, because they compensated themselves in the dual isotope plots as both elements are masked to the same extent. Those dual isotope plots have been recently shown to be a robust tool to visually distinguish different reaction pathways for one compound [82-84]. For example regarding benzene, carbon and hydrogen isotope fractionation studies have been performed for anaerobic mechanistic elucidation using different terminal electron acceptors [13,77,84,85].

In contrast to the rather well investigated isotope fractionation patterns during anaerobic monoaromatic hydrocarbon degradation, naphthalene is the only PAH for which isotope fractionation during anaerobic degradation was measured [19]. However if the isotopic shift of carbon fractionation was too small to trace biodegradation in nature and no other element has been measured to draw conclusions about the initial reaction mechanism based on dual isotope plots.

## 1.6 Highly enriched, sulphate-reducing, naphthalene-degrading culture N47

The culture N47 was obtained from soil material from a contaminated aquifer near Stuttgart, Germany. It has been shown that the culture anaerobically oxidizes naphthalene, 2-methylnaphthalene, 1-naphthoic acid, 2-naphthoic acid, phenylacetic acid, benzoic acid, cyclohexanecarboxylic acid, and cyclohex-1-ene-carboxylic acid as sole carbon source with sulphate as terminal electron acceptor [44]. Over the years the culture has been more and more purified and today the culture consist of two major organisms. Using terminal restriction fragment length polymorphism (T-RFLP) analyses one was asserted to NCBI taxonomy [86] class level *Deltaproteobacteria* the other to *Spirochaetes*. Regarding T-RFLP fingerprints during growth on naphthalene and 2-methylnaphthalene it has been demonstrated that 513-bp T-RF assigned to *Deltaproteobacteria* is considerably dominating and the 207-bp T-RF belonging to members of *Spirochaetes* is minor [53]. 16S rRNA phylogeny of the major deltaproteobacterium revealed *Desulfobacterium cetonicum* [87] as next cultivated relative, but the sequence identity of 92.9% was very low, however. The 16S rRNA sequence identity to NaphS2 was 87% only [53].

## 1.7 Objectives

This thesis therefore aims at enlightening of anaerobic naphthalene degradation by further investigation of the initial reaction mechanism, regarding the physiological potential of an organism able to anaerobically degrade naphthalene, evaluate its physiology when grown on naphthalene and finally trace anaerobic naphthalene degradation in the environment qualitatively as well as quantitatively.

For this reason the genome of highly enriched sulphate-reducing naphthalene degrading organism N47 [44] was sequenced, assembled, annotated and screened for its physiological potential. Furthermore the proteome of N47 growing on naphthalene, 2-methylnaphthalene and 2-naphthoic acid was analysed by sodium dodecyl sulfate-polyacrylamide gel electrophoresis (SDS PAGE) coupled to linear quadrupole ion trap-Orbitrap (LTQ Orbitrap XL) mass spectrometry (MS) with nano-electrospray ionization (ESI) to get insight into its physiology.

These data were connected to proteome comparison of naphthalene- and 2-methylnaphthalene-grown N47 cells by two-dimensional gel electrophoresis (2-DGE) coupled

to matrix-assisted laser desorption ionization-time of flight mass spectrometry (MALDI-TOF-MS) for the identification of selected protein spots. This possibly enables for identifying enzymes involved in the initial reaction activation mechanism during anaerobic naphthalene degradation.

Furthermore, conclusions on the reaction mechanism could feasibly be strengthened by dual plots of carbon and hydrogen stable isotope fractionation measurements, as they potentially give insight into initial reaction activation mechanism. Therefore, stable isotope fractionation measurements of carbon and hydrogen during growth on naphthalene were compared for N47 and NaphS2 [45]. Additionally, these data were screened for their potential to serve as indicator to trace anaerobic naphthalene degradation in nature qualitatively and quantitatively, as well as the reliability.

This thesis contains the following three specific objectives:

- a) Annotation and metabolic potential analysis of the metagenome of the sulphate-reducing naphthalene-degrading highly enriched culture N47 and subsequently regarding its physiology by proteome analyses growing on naphthalene, 2-methylnaphthalene and 2-naphthoic acid.
- b) Searching for possible enzymes catalyzing the initial reaction of anaerobic naphthalene degradation using different proteomic techniques for comparison of naphthalene-grown and 2-methylnaphthalene-grown N47 cells.
- c) Screen stable isotope measurements (C and H) from different cultures to inference on the initial reaction mechanism, as well as investigate the potential of this technique to trace *in situ* naphthalene biodegradation.

## 1.8 References

1. Carmona M, Zamarro MT, Blazquez B, Durante-Rodriguez G, Juarez JF, Valderrama JA, Barragan MJL, Garcia JL, Diaz E: **Anaerobic catabolism of aromatic compounds: a genetic and genomic view**. *Microbiology and Molecular Biology Reviews* 2009, **73**:71-+.
2. McNaught AD, Wilkinson A: **Compendium of chemical terminology**. *International Union of Pure and Applied Chemistry (IUPAC)* 1997.
3. Foght J: **Anaerobic biodegradation of aromatic hydrocarbons: Pathways and prospects**. *Journal of Molecular Microbiology and Biotechnology* 2008, **15**:93-120.
4. (ATSDR) AFTSaDR: **Polycyclic aromatic hydrocarbons (PAHs)**. *Agency for Toxic Substances and Disease Registry - Division of Toxicology, Atlanta G.A.* 1996.

5. McLeod MP, Eltis LD: **Genomic insights into aerobic pathways for degradation of organic pollutants.** *E. Diaz (ed.), Microbial biodegradation: genomics and molecular biology* 2008, **Caister Academic Press, Norfolk, United Kingdom**:1 - 23.
6. (ATSDR) AFTSaDR: **Public health statement: Naphthalene, 1-methylnaphthalene, and 2-methylnaphthalene.** *Agency for Toxic Substances and Disease Registry - Division of Toxicology, Washington D.C.* 2005.
7. Dagley S: **Determinants of biodegradability.** *Q. Rev. Biophys.* 1978, **11**:577 - 602.
8. Evans WC, Fuchs G: **Anaerobic degradation of aromatic compounds.** *Annual Review of Microbiology* 1988, **42**:289-317.
9. Vogel TM, Grbic-Galic D: **Incorporation of oxygen from water into toluene and benzene during anaerobic fermentative transformation.** *Appl. Environ. Microbiol.* 1986, **52**:200-202.
10. Grbic-Galic D, Vogel TM: **Transformation of toluene and benzene by mixed methanogenic cultures.** *Appl. Environ. Microbiol.* 1987, **53**:254-260.
11. Kazumi J, Caldwell ME, Suflita JM, Lovley DR, Young LY: **Anaerobic degradation of benzene in diverse anoxic environments.** *Environmental Science & Technology* 1997, **31**:813-818.
12. Weiner JM, Lovley DR: **Rapid benzene degradation in methanogenic sediments from a petroleum-contaminated aquifer.** *Applied and Environmental Microbiology* 1998, **64**:1937-1939.
13. Mancini SA, Ulrich AC, Lacrampe-Couloume G, Sleep B, Edwards EA, Lollar BS: **Carbon and hydrogen isotopic fractionation during anaerobic biodegradation of benzene.** *Appl. Environ. Microbiol.* 2003, **69**:191-198.
14. Edwards EA, Grbic-Galic D: **Complete mineralization of benzene by aquifer microorganisms under strictly anaerobic conditions.** *Appl. Environ. Microbiol.* 1992, **58**:2663-2666.
15. Lovley DR, Coates JD, Woodward JC, Phillips EJP: **Benzene oxidation coupled to sulfate reduction.** *Appl. Environ. Microbiol.* 1995, **61**:953-958.
16. Phelps CD, Kazumi J, Young LY: **Anaerobic degradation of benzene in BTX mixtures dependent on sulfate reduction.** *FEMS Microbiology Letters* 1996, **145**:433-437.
17. Anderson RT, Lovley DR: **Anaerobic bioremediation of benzene under sulfate-reducing conditions in a petroleum-contaminated aquifer.** *Environmental Science & Technology* 2000, **34**:2261-2266.
18. Caldwell ME, Suflita JM: **Detection of phenol and benzoate as intermediates of anaerobic benzene biodegradation under different terminal electron-accepting conditions.** *Environmental Science & Technology* 2000, **34**:1216-1220.
19. Griebler C, Safinowski M, Vieth A, Richnow HH, Meckenstock RU: **Combined application of stable carbon isotope analysis and specific metabolites determination for assessing in situ degradation of aromatic hydrocarbons in a tar oil-contaminated aquifer.** *Environmental Science & Technology* 2004, **38**:617-631.
20. Kleinstaub S, Schleinitz KM, Breifeld J, Harms H, Richnow HH, Vogt C: **Molecular characterization of bacterial communities mineralizing benzene under sulfate-reducing conditions.** *Fems Microbiology Ecology* 2008, **66**:143-157.
21. Musat F, Widdel F: **Anaerobic degradation of benzene by a marine sulfate-reducing enrichment culture, and cell hybridization of the dominant phylotype.** *Environmental Microbiology* 2008, **10**:10-19.
22. Oka AR, Phelps CD, McGuinness LM, Mumford A, Young LY, Kerkhof LJ: **Identification of critical members in a sulfidogenic benzene-degrading consortium by DNA stable isotope probing.** *Applied and Environmental Microbiology* 2008, **74**:6476-6480.

23. Lovley DR, Woodward JC, Chapelle FH: **Stimulated anoxic biodegradation of aromatic hydrocarbons using Fe(III) ligands.** *Nature* 1994, **370**:128-131.
24. Lovley DR, Woodward JC, Chapelle FH: **Rapid anaerobic benzene oxidation with a variety of chelated Fe(III) forms.** *Applied and Environmental Microbiology* 1996, **62**:288-291.
25. Anderson RT, Rooney-Varga JN, Gaw CV, Lovley DR: **Anaerobic benzene oxidation in the Fe(III) reduction zone of petroleum contaminated aquifers.** *Environmental Science & Technology* 1998, **32**:1222-1229.
26. Caldwell ME, Tanner RS, Suflita JM: **Microbial metabolism of benzene and the oxidation of ferrous iron under anaerobic conditions: Implications for bioremediation.** *Anaerobe* 1999, **5**:595-603.
27. Kunapuli U, Lueders T, Meckenstock RU: **The use of stable isotope probing to identify key iron-reducing microorganisms involved in anaerobic benzene degradation.** *Isme Journal* 2007, **1**:643-653.
28. Burland SM, Edwards EA: **Anaerobic benzene biodegradation linked to nitrate reduction.** *Applied and Environmental Microbiology* 1999, **65**:529-533.
29. Coates JD, Chakraborty R, Lack JG, O'Connor SM, Cole KA, Bender KS, Achenbach LA: **Anaerobic benzene oxidation coupled to nitrate reduction in pure culture by two strains of *Dechloromonas*.** *Nature* 2001, **411**:1039-1043.
30. Kasai Y, Kodama Y, Takahata Y, Hoaki T, Watanabe K: **Degradative capacities and bioaugmentation potential of an anaerobic benzene-degrading bacterium strain DN11.** *Environmental Science & Technology* 2007, **41**:6222-6227.
31. Mihelcic JR, Luthy RG: **Degradation of polycyclic aromatic hydrocarbon compounds under various redox conditions in soil-water systems.** *Appl. Environ. Microbiol.* 1988, **54**:1182-1187.
32. Mihelcic JR, Luthy RG: **Microbial degradation of acenaphthene and naphthalene under denitrification conditions in soil-water systems.** *Appl. Environ. Microbiol.* 1988, **54**:1188-1198.
33. Al-Bashir B, Cseh T, Leduc R, Samson R: **Effect of soil/contaminant interactions on the biodegradation of naphthalene in flooded soil under denitrifying conditions.** *Applied Microbiology and Biotechnology* 1990, **34**:414-419.
34. Durant ND, Wilson LP, Bouwer EJ: **Microcosm studies of subsurface PAH-degrading bacteria from a former manufactured gas plant.** *Journal of Contaminant Hydrology* 1995, **17**:213-237.
35. Bregnard TPA, Hohener P, Haner A, Zeyer J: **Degradation of weathered diesel fuel by microorganisms from a contaminated aquifer in aerobic and anaerobic microcosms.** *Environmental Toxicology and Chemistry* 1996, **15**:299-307.
36. Langenhoff AAM, Zehnder AJB, Schraa G: **Behaviour of toluene, benzene and naphthalene under anaerobic conditions in sediment columns.** *Biodegradation* 1996, **7**:267-274.
37. Rockne KJ, Strand SE: **Biodegradation of bicyclic and polycyclic aromatic hydrocarbons in anaerobic enrichments.** *Environmental Science & Technology* 1998, **32**:3962-3967.
38. Coates JD, Anderson RT, Lovley DR: **Oxidation of polycyclic aromatic hydrocarbons under sulfate-reducing conditions.** *Applied and Environmental Microbiology* 1996, **62**:1099-1101.
39. Bedessem ME, SwobodaColberg NG, Colberg PJS: **Naphthalene mineralization coupled to sulfate reduction in aquifer-derived enrichments.** *Fems Microbiology Letters* 1997, **152**:213-218.

40. Coates JD, Woodward J, Allen J, Philp P, Lovley DR: **Anaerobic degradation of polycyclic aromatic hydrocarbons and alkanes in petroleum-contaminated marine harbor sediments.** *Applied and Environmental Microbiology* 1997, **63**:3589-3593.
41. Coates JD, Anderson RT, Woodward JC, Phillips EJP, Lovley DR: **Anaerobic hydrocarbon degradation in petroleum-contaminated harbor sediments under sulfate-reducing and artificially imposed iron-reducing conditions.** *Environmental Science & Technology* 1996, **30**:2784-2789.
42. Meckenstock RU, Safinowski M, Griebler C: **Anaerobic degradation of polycyclic aromatic hydrocarbons.** *Fems Microbiology Ecology* 2004, **49**:27-36.
43. Zhang XM, Young LY: **Carboxylation as an initial reaction in the anaerobic metabolism of naphthalene and phenanthrene by sulfidogenic consortia.** *Applied and Environmental Microbiology* 1997, **63**:4759-4764.
44. Meckenstock RU, Annweiler E, Michaelis W, Richnow HH, Schink B: **Anaerobic naphthalene degradation by a sulfate-reducing enrichment culture.** *Applied and Environmental Microbiology* 2000, **66**:2743-2747.
45. Galushko A, Minz D, Schink B, Widdel F: **Anaerobic degradation of naphthalene by a pure culture of a novel type of marine sulphate-reducing bacterium.** *Environmental Microbiology* 1999, **1**:415-420.
46. Musat F, Galushko A, Jacob J, Widdel F, Kube M, Reinhardt R, Wilkes H, Schink B, Rabus R: **Anaerobic degradation of naphthalene and 2-methylnaphthalene by strains of marine sulfate-reducing bacteria.** *Environmental Microbiology* 2009, **11**:209-219.
47. Rockne KJ, Chee-Sanford JC, Sanford RA, Hedlund BP, Staley JT, Strand SE: **Anaerobic naphthalene degradation by microbial pure cultures under nitrate-reducing conditions.** *Applied and Environmental Microbiology* 2000, **66**:1595-1601.
48. Biegert T, Fuchs G, Heider F: **Evidence that anaerobic oxidation of toluene in the denitrifying bacterium *Thauera aromatica* is initiated by formation of benzylsuccinate from toluene and fumarate.** *European Journal of Biochemistry* 1996, **238**:661-668.
49. Krieger CJ, Beller HR, Reinhard M, Spormann AM: **Initial reactions in anaerobic oxidation of m-xylene by the denitrifying bacterium *Azoarcus* sp strain T.** *Journal of Bacteriology* 1999, **181**:6403-6410.
50. Morasch B, Meckenstock RU: **Anaerobic degradation of p-xylene by a sulfate-reducing enrichment culture.** *Current Microbiology* 2005, **51**:127-130.
51. Kniemeyer O, Fischer T, Wilkes H, Glockner FO, Widdel F: **Anaerobic degradation of ethylbenzene by a new type of marine sulfate-reducing bacterium.** *Applied and Environmental Microbiology* 2003, **69**:760-768.
52. Annweiler E, Materna A, Safinowski M, Kappler A, Richnow HH, Michaelis W, Meckenstock RU: **Anaerobic degradation of 2-methylnaphthalene by a sulfate-reducing enrichment culture.** *Applied and Environmental Microbiology* 2000, **66**:5329-5333.
53. Selesi D, Jehmlich N, von Bergen M, Schmidt F, Rattei T, Tischler P, Lueders T, Meckenstock RU: **Combined genomic and proteomic approaches identify gene clusters involved in anaerobic 2-methylnaphthalene degradation in the sulfate-reducing enrichment culture N47.** *Journal of Bacteriology* 2010, **192**:295-306.
54. Coates JD, Chakraborty R, McInerney MJ: **Anaerobic benzene biodegradation--a new era.** *Research in Microbiology* 2002, **153**:621-628.
55. Ulrich AC, Beller HR, Edwards EA: **Metabolites detected during biodegradation of C-13(6)-benzene in nitrate-reducing and methanogenic enrichment cultures.** *Environmental Science & Technology* 2005, **39**:6681-6691.

56. Chakraborty R, Coates JD: **Hydroxylation and carboxylation-two crucial steps of anaerobic benzene degradation by *Dechloromonas* strain RCB.** *Applied and Environmental Microbiology* 2005, **71**:5427-5432.
57. Kunapuli U, Griebler C, Beller HR, Meckenstock RU: **Identification of intermediates formed during anaerobic benzene degradation by an iron-reducing enrichment culture.** *Environmental Microbiology* 2008, **10**:1703-1712.
58. Abu Laban N, Selesi D, Jobelius C, Meckenstock RU: **Anaerobic benzene degradation by Gram-positive sulfate-reducing bacteria.** *Fems Microbiology Ecology* 2009, **68**:300-311.
59. Abu Laban N, Selesi D, Rattei T, Tischler P, Meckenstock RU: **Identification of enzymes involved in anaerobic benzene degradation by a strictly anaerobic iron-reducing enrichment culture.** *Environmental Microbiology* 2010:in press.
60. Safinowski M, Meckenstock RU: **Methylation is the initial reaction in anaerobic naphthalene degradation by a sulfate-reducing enrichment culture.** *Environmental Microbiology* 2006, **8**:347-352.
61. Larimer FW, Chain P, Hauser L, Lamerdin J, Malfatti S, Do L, Land ML, Pelletier DA, Beatty JT, Lang AS, et al.: **Complete genome sequence of the metabolically versatile photosynthetic bacterium *Rhodospseudomonas palustris*.** *Nature Biotechnology* 2004, **22**:55-61.
62. Rabus R, Kube M, Heider J, Beck A, Heitmann K, Widdel F, Reinhardt R: **The genome sequence of an anaerobic aromatic-degrading denitrifying bacterium, strain EbN1.** *Archives of Microbiology* 2005, **183**:27-36.
63. Rabus R: **Functional genomics of an anaerobic aromatic-degrading denitrifying bacterium, strain EbN1.** *Applied Microbiology and Biotechnology* 2005, **68**:580-587.
64. Chakraborty R, O'Connor SM, Chan E, Coates JD: **Anaerobic degradation of benzene, toluene, ethylbenzene, and xylene compounds by *Dechloromonas* strain RCB.** *Applied and Environmental Microbiology* 2005, **71**:8649-8655.
65. Salinero KK, Keller K, Feil WS, Feil H, Trong S, Di Bartolo G, Lapidus A: **Metabolic analysis of the soil microbe *Dechloromonas aromatica* str. RCB: Indications of a surprisingly complex life-style and cryptic anaerobic pathways for aromatic degradation.** *Bmc Genomics* 2009, **10**.
66. Butler JE, He Q, Nevin KP, He ZL, Zhou JZ, Lovley DR: **Genomic and microarray analysis of aromatics degradation in *Geobacter metallireducens* and comparison to a *Geobacter* isolate from a contaminated field site.** *Bmc Genomics* 2007, **8**.
67. Lollar BS, Slater GF, Sleep B, Witt M, Klecka GM, Harkness M, Spivack J: **Stable carbon isotope evidence for intrinsic bioremediation of tetrachloroethene and trichloroethene at area 6, Dover Air Force Base.** *Environmental Science & Technology* 2001, **35**:261-269.
68. Meckenstock RU, Morasch B, Griebler C, Richnow HH: **Stable isotope fractionation analysis as a tool to monitor biodegradation in contaminated aquifers.** *Journal of Contaminant Hydrology* 2004, **75**:215-255.
69. Abe Y, Hunkeler D: **Does the Rayleigh equation apply to evaluate field isotope data in contaminant hydrogeology?** *Environmental Science & Technology* 2006, **40**:1588-1596.
70. Slater GF, Ahad JME, Lollar BS, Allen-King R, Sleep B: **Carbon isotope effects resulting from equilibrium sorption of dissolved VOCs.** *Analytical Chemistry* 2000, **72**:5669-5672.
71. Schuth C, Taubald H, Bolano N, Maciejczyk K: **Carbon and hydrogen isotope effects during sorption of organic contaminants on carbonaceous materials.** *Journal of Contaminant Hydrology* 2003, **64**:269-281.

72. Wang Y, Huang YS: **Hydrogen isotopic fractionation of petroleum hydrocarbons during vaporization: implications for assessing artificial and natural remediation of petroleum contamination.** *Applied Geochemistry* 2003, **18**:1641-1651.
73. Fischer A, Bauer J, Meckenstock RU, Stichler W, Griebler C, Maloszewski P, Kastner M, Richnow HH: **A multitracer test proving the reliability of Rayleigh equation-based approach for assessing biodegradation in a BTEX contaminated aquifer.** *Environmental Science & Technology* 2006, **40**:4245-4252.
74. Mancini SA, Lacrampe-Couloume G, Jonker H, Van Breukelen BM, Groen J, Volkering F, Lollar BS: **Hydrogen isotopic enrichment: An indicator of biodegradation at a petroleum hydrocarbon contaminated field site.** *Environmental Science & Technology* 2002, **36**:2464-2470.
75. Vieth A, Kastner M, Schirmer M, Weiss H, Godeke S, Meckenstock RU, Richnow HH: **Monitoring in situ biodegradation of benzene and toluene by stable carbon isotope fractionation.** *Environmental Toxicology and Chemistry* 2005, **24**:51-60.
76. Mak KS, Griebler C, Meckenstock RU, Liedl R, Peter A: **Combined application of conservative transport modelling and compound-specific carbon isotope analyses to assess in situ attenuation of benzene, toluene, and o-xylene.** *Journal of Contaminant Hydrology* 2006, **88**:306-320.
77. Fischer A, Theuerkorn K, Stelzer N, Gehre M, Thullner M, Richnow HH: **Applicability of stable isotope fractionation analysis for the characterization of benzene biodegradation in a BTEX-contaminated aquifer.** *Environmental Science & Technology* 2007, **41**:3689-3696.
78. Fischer A, Gehre M, Breitfeld J, Richnow HH, Vogt C: **Carbon and hydrogen isotope fractionation of benzene during biodegradation under sulfate-reducing conditions: a laboratory to field site approach.** *Rapid Communications in Mass Spectrometry* 2009, **23**:2439-2447.
79. Elsner M, Zwank L, Hunkeler D, Schwarzenbach RP: **A new concept linking observable stable isotope fractionation to transformation pathways of organic pollutants.** *Environmental Science & Technology* 2005, **39**:6896-6916.
80. Zwank L, Berg M, Elsner M, Schmidt TC, Schwarzenbach RP, Haderlein SB: **New evaluation scheme for two-dimensional isotope analysis to decipher biodegradation processes: Application to groundwater contamination by MTBE.** *Environmental Science & Technology* 2005, **39**:1018-1029.
81. Nijenhuis I, Andert J, Beck K, Kastner M, Diekert G, Richnow H-H: **Stable isotope fractionation of tetrachloroethene during reductive dechlorination by *Sulfurospirillum multivorans* and *Desulfitobacterium* sp. strain PCE-S and abiotic reactions with cyanocobalamin.** *Appl. Environ. Microbiol.* 2005, **71**:3413-3419.
82. Vogt C, Cyrus E, Herklotz I, Schlosser D, Bahr A, Herrmann S, Richnow HH, Fischer A: **Evaluation of toluene degradation pathways by two-dimensional stable isotope fractionation.** *Environmental Science & Technology* 2008, **42**:7793-7800.
83. Elsner M, McKelvie J, Lacrampe Couloume G, Sherwood Lollar B: **Insight into methyl tert-butyl ether (MTBE) stable isotope fractionation from abiotic reference experiments.** *Environmental Science & Technology* 2007, **41**:5693-5700.
84. Fischer A, Herklotz I, Herrmann S, Thullner M, Weelink SAB, Stams AJM, Schlomann M, Richnow HH, Vogt C: **Combined carbon and hydrogen isotope fractionation investigations for elucidating benzene biodegradation pathways.** *Environmental Science & Technology* 2008, **42**:4356-4363.
85. Mancini SA, Devine CE, Elsner M, Nandi ME, Ulrich AC, Edwards EA, Lollar BS: **Isotopic evidence suggests different initial reaction mechanisms for anaerobic benzene biodegradation.** *Environmental Science & Technology* 2008, **42**:8290-8296.

86. Sayers EW, Barrett T, Benson DA, Bryant SH, Canese K, Chetvernin V, Church DM, DiCuccio M, Edgar R, Federhen S, et al.: **Database resources of the National Center for Biotechnology Information**. *Nucl. Acids Res.* 2009, **37**:D5-15.
87. Galushko AS, Rozanova EP: ***Desulfobacterium cetonicum* sp. nov.: a sulfate-reducing bacterium which oxidizes fatty acids and ketones**. *Mikrobiologiya* 1991, **60**:102 - 107.





**2.**

**C and H stable isotope fractionation during strictly anaerobic naphthalene and benzene degradation: mechanistic implications and potential to assess natural attenuation**

Franz D. Bergmann, Nidal Abu Laban, Armin Meyer,  
Martin Elsner, Rainer U. Meckenstock

submitted to

*Environmental Science and Technology*

## 2.1 Introduction

Polycyclic aromatic hydrocarbons (PAHs) and monoaromatic hydrocarbons such as BTEX compounds (benzene, toluene, ethylbenzene and xylene) are among the most abundant organic pollutants in contaminated aquifers [1,2]. A number of reports showed degradation of nonsubstituted mono- and polycyclic aromatic hydrocarbons (namely benzene, naphthalene, phenanthrene, biphenyl) with nitrate [3-5], iron [6-8], or sulphate-reducing [9-16] and methanogenic cultures [17-19]. In this context, two research questions are of particular relevance. On the one hand, there is a need of methods which can directly prove in situ degradation of aromatic compounds in contaminated aquifers. On the other hand, there is great scientific interest in the elucidation of the initial activation mechanism of non-substituted aromatic hydrocarbons. For the sulphate-reducing benzene-degrading highly enriched Gram positive culture BPL, evidence for carboxylation as initial activation mechanism has been given by substrate utilization, co-metabolism tests and metabolite screening [20]. Likewise, for the iron-reducing benzene-degrading highly enriched Gram positive culture BF, proteomic and genomic analyses suggested a direct carboxylation of benzene to benzoate as first degradation step [21]. Carboxylation [11] or methylation [22] as initial biodegradation steps are two proposed alternatives for anaerobic naphthalene degradation by the culture N47. For the sulphate-reducing naphthalene-degrading pure culture NaphS2 it was possible to exclude methylation as mechanism [16], however, no direct proof for carboxylation was obtained so far.

Compound Specific Isotope Analysis (CSIA) is receiving increasing attention as an innovative approach to address both research gaps: to determine the natural attenuation of organic pollutants in the environment [23-25], as well as to appoint degradation pathways of organic contaminants [26,27]. Stable isotope ratios from single organic compounds are determined in environmental samples by gas chromatography - isotope ratio mass spectrometry (GC-IRMS). The outcome is expressed in  $\delta$ -notation as difference in per mill compared to an international reference standard according to equation 2.1 [28].  $R = {}^h\text{E}/{}^l\text{E}$  is the stable isotope ratio for element E where h indicates the heavy and l the light isotope (e.g.  ${}^{13}\text{C}/{}^{12}\text{C}$  and  ${}^2\text{H}/{}^1\text{H}$ ).

$$\text{Equation 2.1: } \delta^h E = \left( \frac{R_{\text{sample}} - R_{\text{reference}}}{R_{\text{reference}}} \right)$$

Non-destructive natural attenuation processes such as dispersion, sorption or volatilization frequently do not entail significant isotope fractionation [29-32]. In contrast, chemical

reactions and biotransformations are involving the formation or breaking of bonds and are therefore generally associated with isotope effects meaning that the light isotopomers (e.g.,  $^{12}\text{C}$ ,  $^1\text{H}$ ) typically react faster than the heavy isotopomers (e.g.,  $^{13}\text{C}$ ,  $^2\text{H}$ ). The resulting enrichment of heavy isotopes in the remaining substrate allows tracing reactions by isotopic shifts, even without the need of metabolite detection. This offers the possibility of assessing biodegradation at contaminated sites by analyzing the isotopic composition of contaminants in field samples, either at one point over time or spatially resolved along the flow direction of a plume. If a significant enrichment of heavy isotopes is measurable this gives direct indication that biodegradation of the investigated substance is occurring [23] or can even be used to quantify the extent of biodegradation.

Nevertheless, interpretations can be complicated by the fact that even the same biotransformation pathway may not always show the same isotope fractionation in different organisms [33,34]. The reason is that biotic transformation processes are composed of many steps that precede the (bio)chemical bond cleavage, for example uptake of substrate, transport to reactive sites or formation of enzyme-substrate complexes [35,36]. If the back reaction of a preceding step is much slower than the actual reaction of interest, then almost every substrate molecule which reaches the reactive enzymatic site will immediately be converted regardless of its isotopic composition [26]. Consequently, the isotope enrichment that can be observed in aqueous solution becomes smaller. This effect is termed masking or commitment to catalysis meaning that observable isotope fractionation does no longer represent the intrinsic KIE (kinetic isotope effect) of the (bio)chemical transformation but that a smaller apparent kinetic isotope effect (AKIE) is obtained instead.

This problem may be circumvented in dual isotope plots by plotting the changes of the isotope ratio of one element relative to another. The dual isotope plots are much less affected by masking compared to pure isotope effects, because preceding steps are generally non-fractionating and therefore mask the KIE of both elements to the same extent. Two-dimensional isotope plots were recently shown to be a robust tool to discern different reaction pathways for the same compound [34,37,38].

Previous applications of CSIA to characterize non-substituted aromatics degradation have mainly been concerned with benzene. Measurement of carbon as well as hydrogen isotopic enrichment allowed evaluating the intrinsic bioremediation potential at different contaminated sites [39-42]. They were used to calculate the extent of benzene biodegradation by changes in the isotope signature [43,44].

Isotope fractionation (C and H) studies of benzene have also been performed for mechanistic elucidation, with aerobic and anaerobic cultures using different electron acceptors [38,43,45,46]. Pronounced shifts in the hydrogen isotopic composition were interpreted as evidence that anaerobic benzene degradation likely involves a C-H bond cleavage [38,45,46]. Several authors proposed a general picture where nitrate-reducing bacteria show a smaller slope in the  $\delta^2\text{H}$  versus  $\delta^{13}\text{C}$  dual isotope plot ( $\Lambda = 12-16$ ) compared to methanogens and sulphate-reducers ( $\Lambda = 22-28$ ) [46]. Different dual isotope slopes of benzene are therefore thought to hold promise for distinguishing different initial mechanisms of degradation, even though the real reaction chemistry and the enzymes involved are actually not known.

Contrasting with this insight on benzene degradation, no such dual isotope analyses have been performed for naphthalene or larger PAHs yet. Carbon isotope fractionation measured in one study showed an isotope shift of less than 1‰ [40], which is too small to trace biodegradation in nature. Hydrogen isotope data for anaerobic degradation of naphthalene and higher PAHs have been missing so far.

This study therefore investigates the potential of isotope analyses of carbon and hydrogen (i) to better assess naphthalene degradation at contaminated sites and (ii) to probe for different initial reaction mechanisms in anaerobic naphthalene and benzene degradation.

## **2.2 Material and Methods**

### **2.2.1 Cultivation Conditions**

Benzene-degrading cultures BF and BPL [20,47] and naphthalene-degrading cultures N47 and NaphS2 [12,14] were cultivated as described previously. Stable isotope fractionation experiments were performed with 11 bottles filled with 750 ml medium, 250 ml  $\text{CO}_2/\text{N}_2$  (20:80 v/v) headspace and sealed with Viton rubber stoppers (Maag Technik, Dübendorf, Switzerland). For culture BF, medium was spiked with 200  $\mu\text{M}$  (final concentration) benzene (Sigma-Aldrich, Steinheim, Germany) and with 500  $\mu\text{M}$  for culture BPL. Naphthalene (Sigma-Aldrich, Steinheim, Germany) was added as a solid crystal to roughly 120  $\mu\text{M}$  for N47 and 180  $\mu\text{M}$  for NaphS2. Bottles were shaken for at least 3 weeks at 150 rpm to achieve complete dissolution of naphthalene. Per culture, 5 bottles were inoculated with 10% (v/v) grown culture, two of them were autoclaved three times on subsequent days and served as sterile controls. All culture bottles were incubated at 30°C in the dark. Control experiments did not show any degradation or isotope fractionation (data not shown).

### 2.2.2 Analytical Methods

Benzene concentrations were analyzed from the headspace of fresh 3 ml sample by GC-MS as described by Abu Laban et al [20]. For measuring the concentration of naphthalene, 1 ml of sample were withdrawn, added to 1 ml cyclohexane (Sigma-Aldrich, Seelze, Germany) in a 2 ml Supelco vial (Supelco, Bellefonte, PA) closed with a Teflon coated cap and the mixture was vortexed for 2 minutes. After 30 minutes – when the two phases had separated again – 500 µl of the cyclohexane phase were taken to which 50 µl of 1250 µM toluene (Sigma-Aldrich, Seelze, Germany) in cyclohexane was added as internal standard. 1 µl of the mixture was injected for concentration analysis by GC/MS (GC: Trace-DSQ, MS: Thermo Finnigan; San Jose, California, USA) equipped with a fused-silica capillary column DB-5 (30 m length (L), 0.25 mm inner diameter (ID), 0.25 mm film thickness (T); Agilent, Palo Alto, USA). The GC/MS operation mode for measurements is given in the supplementary material. The concentration of naphthalene in water was calculated assuming complete extraction into the organic phase. The uncertainty for benzene and naphthalene concentration measurements was less than 5%.

For benzene, samples of 4-15 mL (depending on the benzene concentration) were periodically taken from culture bottles, transferred into Supelco vials with Teflon coated caps and stored at -20°C prior to analysis by gas chromatograph-isotope ratio mass spectrometry (GC-IRMS). For naphthalene, sample volumes were 6 ml for carbon isotope analysis and 15 – 120 ml for hydrogen isotope analysis depending on naphthalene concentrations (larger volumes in the end). Samples were immediately frozen at -20°C until analysis by GC-IRMS according to Elsner *et al.* [48]. Compound specific isotope ratios were measured as given in detail in the supplementary material.

### 2.2.3 Quantification of isotope fractionation

Isotope fractionation is expressed by the isotope enrichment factor  $\epsilon$  which links the changes in isotope ratios (given by  $R/R_0$ ) to the progress of the reaction (given by  $f$ , the fraction of substrate remaining) according to the Rayleigh equation (equation 2.2).

$$\text{Equation 2.2: } \ln \frac{R_t}{R_0} = \ln \left( \frac{1 + \delta^h E_t}{1 + \delta^h E_0} \right) = \epsilon * \ln f$$

$R_0$  is the isotope ratio of heavy to light isotopes at the starting point of the reaction, whereas  $R_t$  is the isotope ratio at a given sampling point at time  $t$  of the reaction. The isotopic signature for the element  $E$  at time points zero and  $t$  is given as  $\delta^h E_0$  and  $\delta^h E_t$ .  $\frac{c_t}{c_0} = f$  is the

fraction of the remaining compound at time t, where ct is its concentration remaining assuming that it is only affected by degradation.

Determination of isotope fractionation may also allow the identification of reaction mechanisms and degradation pathways [26,27]. The isotope enrichment factor  $\epsilon$  is a measure for the isotopic enrichment as average over all positions of an element in a molecule. It is caused by the kinetic isotope effect (KIE) in the reacting bond which is often indicative of a prevailing transformation mechanism. To this end, “dilution” by non-reacting atoms in a molecule, which show no or little isotope fractionation, diminish the  $\epsilon$  value if a compound contains more atoms of the same element. However, by the proposed corrections of Elsner *et al.* [26] such bulk enrichment factors can nonetheless be linked to the underlying transformation pathway [26,49]. This is particularly the case if concurring transformation pathways involve different chemical reactions and concern different elements [37,50]

For benzene, the isotope fractionation of carbon and hydrogen, as expressed by enrichment factors  $\epsilon$ , were obtained by linear regression according to the Rayleigh equation (equation 2.2). The evaluation of the apparent kinetic isotope effect (AKIE) was done as described by Elsner *et al.* [26]. Secondary isotope effects have been neglected during calculations. The carbon isotope measurements have been evaluated according to equation 2.3, giving a reasonable approximation:

$$\text{Equation 2.3: } \epsilon_{\text{reactive\_position}} \approx \frac{n}{x} * \epsilon_{\text{bulk}}$$

where n corresponds to the total positions of the atom and x is the number of reactive positions in the molecule; for carbon and hydrogen in benzene, n = 6 and x = 6 meaning that  $\epsilon_{\text{bulk}} = \epsilon_{\text{reactive\_position}}$ .

The evaluation for hydrogen isotope data have been done according to a modified Rayleigh equation, allowing for calculation of position specific enrichment factors as formerly described [37] (equation 2.4).

$$\text{Equation 2.4: } \ln \frac{R_{\text{reactive\_position}}}{R_{0,\text{reactive\_position}}} = \ln \left( \frac{1 + \delta^h E_0 + \frac{n}{x} * \Delta \delta^h E_{\text{bulk}}}{1 + \delta^h E_0} \right) = \epsilon_{\text{reactive\_position}} * \ln f$$

Here, n is the total number of atoms of a given element in the molecule and x is the number of atoms located in reactive positions. In the case of benzene n = 6 and x = 6 for both hydrogen and carbon meaning that all atoms are potentially reactive. In the case of naphthalene metabolites are only formed with substituents in 2-position. The other positions can therefore

be considered as non-reactive meaning that  $n = 10$  and  $x = 4$  for carbon, whereas  $n = 8$  and  $x = 4$  for hydrogen.

## 2.3 Results

### 2.3.1 Carbon isotope fractionation during anaerobic benzene and naphthalene degradation

Anaerobic benzene degradation using an iron- and a sulfate-reducing culture (BF and BPL) produced significant enrichment of carbon stable isotope  $\delta^{13}\text{C}$  values in the remaining benzene from  $-26\text{‰}$  to  $-20\text{‰}$  in both cultures (figure 2.1). Evaluation according to equation 2.3 gives carbon enrichment factors  $\epsilon_C$  of  $-3.0 \pm 0.5\text{‰}$  and  $-2.5 \pm 0.2\text{‰}$ , respectively. The corresponding apparent kinetic carbon isotope effects (AKIE<sub>C</sub>) were  $1.018 \pm 0.004$  and  $1.015 \pm 0.002$ .

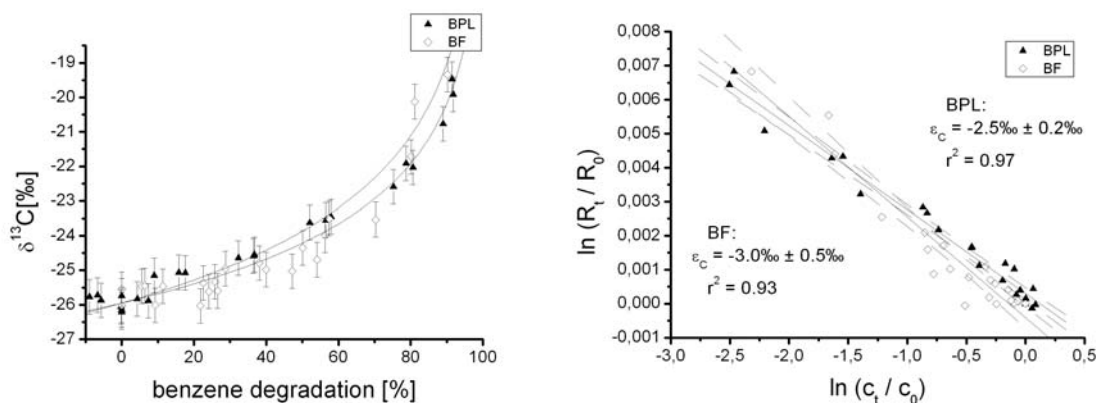


Figure 2.1: Plots of carbon isotope values versus benzene consumption in the iron- and sulfate-reducing cultures. Left panel: Correlation between benzene concentration and  $\delta^{13}\text{C}$ . Right panel: Logarithmic plot according to the Rayleigh equation (equation 2.2) for changes in  $\delta^{13}\text{C}$  and benzene concentrations. The solid line represents the respective linear regression and the dashed lines the 95% confidence intervals. The precision of carbon isotope measurements was better than  $0.5\text{‰}$  as indicated by the error bars.

A significant enrichment of  $^{13}\text{C}$  stable isotopes during the anaerobic degradation of naphthalene by the sulfate-reducing cultures N47 and NaphS2 was observed. Both showed shifts to more positive  $\delta^{13}\text{C}$  values, from  $-25.6\text{‰}$  to  $-21.5\text{‰}$  for N47 and from  $-25.6\text{‰}$  to  $-24.5\text{‰}$  for NaphS2 (figure 2.2). For NaphS2, however, changes in isotope ratios were so small that the overall difference of  $1.1\text{‰}$  was hardly significant considering the analytical uncertainty of the method as depicted by the error bars of  $\pm 0.5\text{‰}$  (figure 2.2). The enrichment

factors for carbon were  $-2.0‰ \pm 0.4‰$  for N47 and  $-0.3‰ \pm 0.1‰$  for NaphS2 (figure 2.2), whereas position specific enrichment factors  $\epsilon_C$  reactive\_position were  $-5.0‰ \pm 1.0‰$  for N47 and  $-0.7‰ \pm 0.3‰$  for NaphS2 (figure 2.2). The corresponding  $AKIE_C$  calculated was  $1.020 \pm 0.004$  for N47 and  $1.003 \pm 0.001$  for NaphS2.

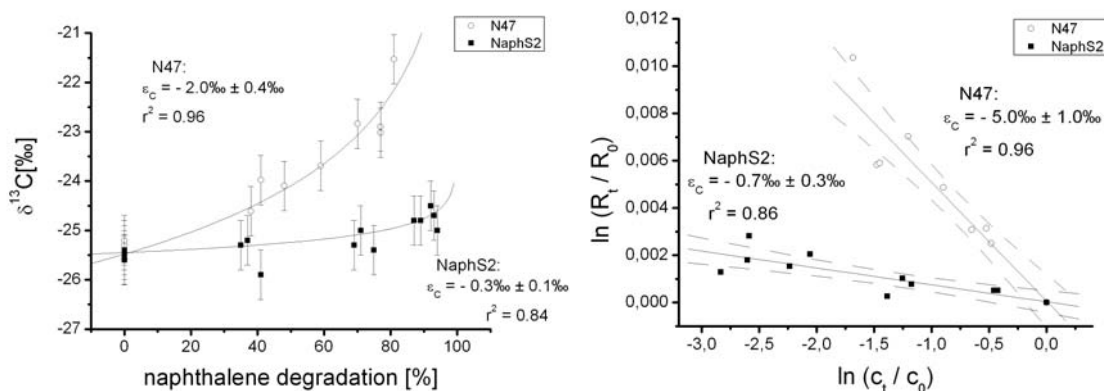


Figure 2.2: Carbon isotope fractionation during naphthalene degradation in batch systems by cultures N47 and NaphS2. Left panel: Correlation between naphthalene concentration and  $\delta^{13}C$ , including  $\epsilon_C$  calculated according to the Rayleigh equation (equation 2.2). Right panel: Logarithmic plot according to the modified Rayleigh equation (equation 2.4) for changes in  $\delta^{13}C$  and naphthalene concentrations. The solid line represents the respective linear regression and the dashed lines the 95% confidence intervals. The precision of carbon isotope measurements was better than 0.5‰ as indicated by the error bars.

### 2.3.2 Hydrogen isotope fractionation during anaerobic benzene and naphthalene degradation

Benzene became strongly enriched in  $^2H$  during degradation by the cultures BF and BPL, showing differences of hydrogen isotopic ratios ( $\Delta\delta^2H = \delta^2H_t - \delta^2H_0$ ) up to 116‰ (BF) and 122‰ (BPL) during the time course of benzene degradation (figure 2.3). In the autoclaved controls, no enrichment of the  $^2H$  was observed in both cultures as indicated by changes of  $\Delta\delta^2H$  that were within the analytical uncertainty of the methods (0‰ to -3.5‰). Calculated  $\epsilon_H$  and  $AKIE_H$  were statistically identical for both cultures ( $-56 \pm 8‰$  and  $-55 \pm 4‰$ ;  $1.510 \pm 0.113$  and  $1.492 \pm 0.056$ , respectively) (figure 2.3).

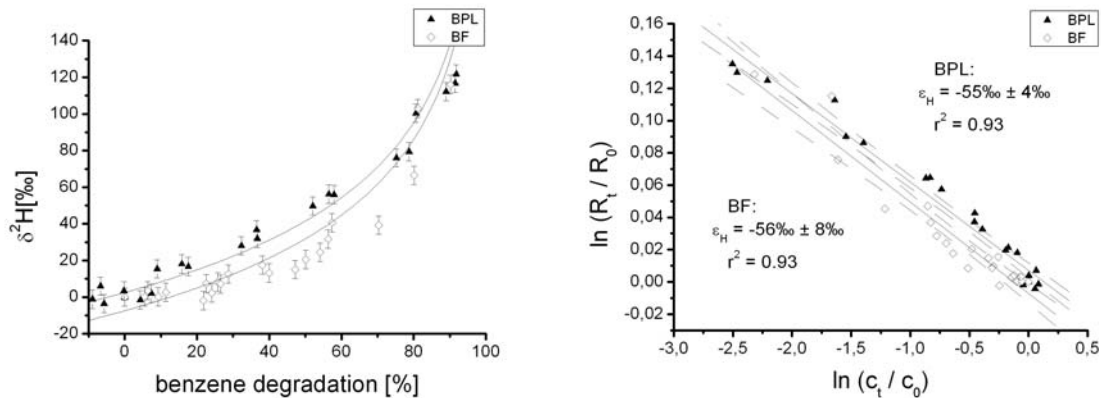


Figure 2.3: Plots of hydrogen isotope composition versus the residual concentration during benzene consumption in the iron- and sulfate-reducing cultures. Left panel: Correlation between benzene concentration and  $\delta^2\text{H}$ . Right panel: Logarithmic plot according to the Rayleigh equation (equation 2.2) for changes in  $\delta^2\text{H}$  and benzene concentrations. The solid line represents the respective linear regression and the dashed lines the 95% confidence intervals. The precision of hydrogen isotope measurements was better than 5‰ as indicated by the error bars.

Naphthalene became strongly enriched in  $^2\text{H}$  during degradation, contrasting with the relatively small changes in carbon isotope ratios. The hydrogen isotopic values shifted from -2‰ to 134‰ for N47 and from -3‰ to 120‰ for NaphS2 (figure 2.4). No significant enrichment of  $^2\text{H}$  could be observed in the control bottles. Isotope ratios in the beginning were slightly negative, because they were normalized according to the control bottles at time point zero, but are consistent within the analytical uncertainty of 5‰. Enrichment factors  $\epsilon_H$  calculated according to the Rayleigh equation (equation 2.2) were  $-59\text{‰} \pm 8\text{‰}$  for N47 and  $-43\text{‰} \pm 6\text{‰}$  for NaphS2 (figure 2.4), whereas position specific enrichment factors  $\epsilon_{H_{\text{reactive\_position}}}$  obtained from the Rayleigh equation after correcting the raw data for the effect of non-reacting positions (equation 2.4) were  $-100\text{‰} \pm 15\text{‰}$  for N47 and  $-73\text{‰} \pm 11\text{‰}$  for NaphS2 (figure 2.4).  $\text{AKIE}_H$  calculated were (with lower and upper 95% confidence boundaries): 1.67 (1.49 to 1.82) for N47 and 1.41 (1.32 to 1.49) for NaphS2.

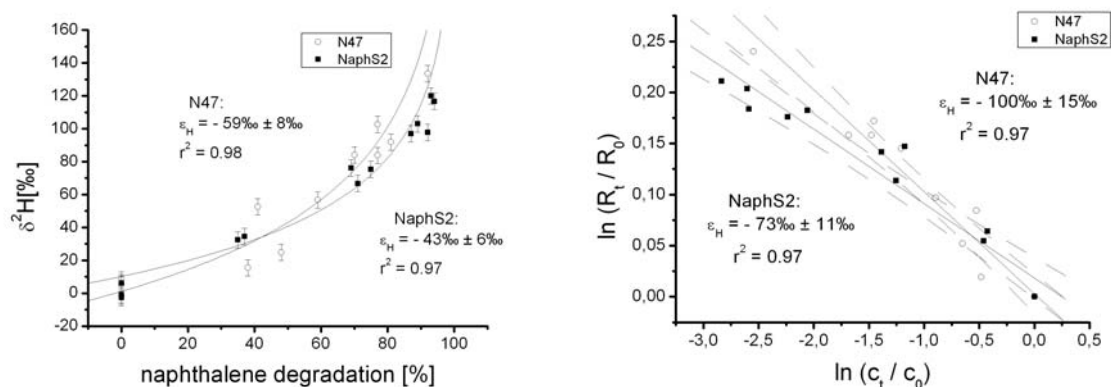


Figure 2.4: Plots of hydrogen isotope composition versus residual concentration during naphthalene degradation by cultures N47 and NaphS2. Left panel: Correlation between naphthalene concentration and  $\delta^2\text{H}$ , including  $\epsilon_{\text{H}}$  calculated according to the Rayleigh equation (equation 2.2). Right panel: Logarithmic plot according to the modified Rayleigh equation (equation 2.4) for changes in  $\delta^2\text{H}$  and naphthalene concentrations. The solid line represents the respective linear regression and the dashed lines the 95% confidence intervals. The precision of hydrogen isotope measurements was better than 5‰ as indicated by error bars.

### 2.3.3 Two-dimensional isotope fractionation investigation

Since the enrichment factors for a specific transformation reaction can significantly differ due to the influence of preceding non-fractionating steps such as membrane-transport, we plotted the dual isotope fractionation of carbon versus hydrogen ( $\Delta\delta^{13}\text{C} = \delta_{\text{t}}^{13}\text{C} - \delta_0^{13}\text{C}$ ,  $\Delta\delta^2\text{H} = \delta_{\text{t}}^2\text{H} - \delta_0^2\text{H}$ ) to decrease the variability. When the data were plotted for the iron- and sulfate-reducing culture, the observed slopes were statistically not distinguishable (figure 2.5), giving  $\Lambda$  values for the iron- and sulfate-reducing cultures of  $17 \pm 1$  and  $20 \pm 2$ , respectively.

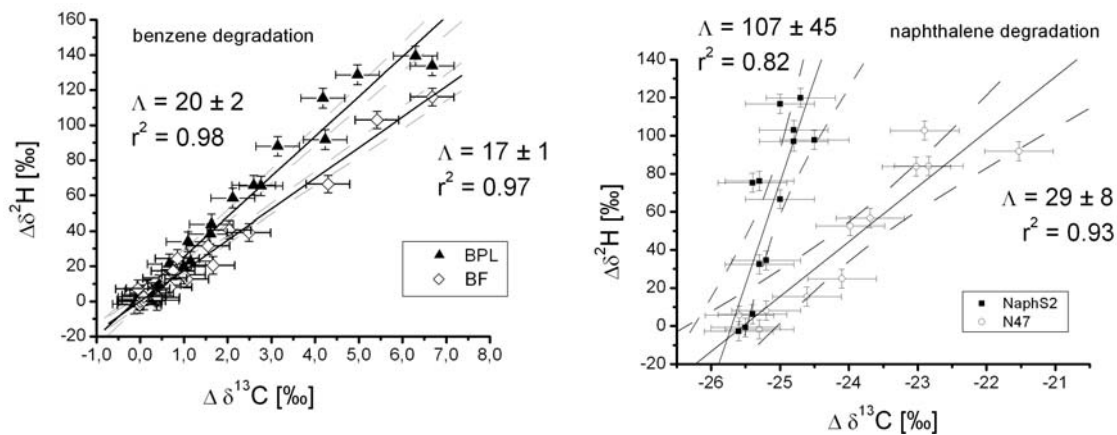


Figure 2.5: Dual isotope plots of  $\Delta\delta^2\text{H}$  versus  $\Delta\delta^{13}\text{C}$  for anaerobic benzene biodegradation in the iron-reducing BF (open diamonds) and sulfate-reducing BPL (solid triangles) cultures on the left and for anaerobic naphthalene degradation during sulfate reduction in N47 (open circles) and NaphS2 (closed squares) on the right hand side representing triplicate batch experiments of each tested culture. The slopes of the solid linear regression lines give the  $\Lambda$  values and the dashed lines represent the corresponding 95% confidence intervals. Error bars display the accuracy of  $\delta^{13}\text{C}$  and  $\delta^2\text{H}$  measurements, which were always better than  $\pm 0.5\text{‰}$  and  $\pm 5\text{‰}$ , respectively.

This study reports also for the first time both carbon and hydrogen isotope fractionation during anaerobic naphthalene degradation. However, the slopes  $\Lambda$  for N47 ( $29 \pm 8$ ) and for NaphS2 ( $107 \pm 45$ ) (figure 2.5), were significantly different on the 95% confidence level.

## 2.4 Discussion

### 2.4.1 Hydrogen and carbon isotope fractionation to assess natural attenuation

For benzene-degradation by the iron- and the sulfate-reducing cultures, the observed  $\epsilon_C$  and  $AKIE_C$  values (figure 2.1 and 2.3) fall into the range of data previously reported from nitrate- and sulfate-reducing mixed cultures, but are significantly greater than those measured for methanogenic-mixed cultures [38,45,46]. On the other hand, the obtained  $\epsilon_C$  values are within the range ( $-2.6\text{‰} \pm 0.8\text{‰}$  to  $-3.5\text{‰} \pm 0.3\text{‰}$ ) reported for aerobic cultures using monooxygenase reactions (e.g. *Alicyclophilus denitrificans* strain BC, *Burkholderia* sp.) [38,51]. The values of  $\epsilon_H$  and  $AKIE_H$  fall into the range of some previously reported methanogenic, sulfate- and nitrate-reducing mixed cultures. At the same time they are significantly smaller than those of one sulfate-reducing mixed culture and significantly greater than those of other nitrate-reducing and methanogenic mixed cultures [38,45,46]. One possible reason for this new picture could be that the degradation mechanism itself differs in Gram-positive compared to Gram-negative bacteria. A second cause for the difference could be the lacking outer membrane of Gram-positive bacteria and therefore a significantly smaller masking of the isotope effects.

The carbon isotopic enrichment factors determined for naphthalene degradation (figure 2.2) are in the range of formerly published values for culture N47 ( $\epsilon = -1.1\text{‰} \pm 0.4\text{‰}$ ) [40]. These ranges are very small, but they are surprisingly significant different assuming that anaerobic naphthalene degradation in cultures N47 and NaphS2 proceeds by similar biochemical reactions. This indicates two probable shortcomings for assessing in situ degradation of naphthalene by stable isotope fractionation analysis: Due to the low carbon isotope fractionation it is likely that the observed isotope shifts in contaminated aquifers are below significance level of 2‰ [24,52] even when the extent of biodegradation reaches 60 – 90 % (data not shown). This would exclude even a qualitative assessment of biodegradation in the field. For quantitative assessment, there is the risk that effective degradation is overestimated if the  $\epsilon$  of NaphS2 is assumed for calculations, or that it is underestimated if that of N47 is used [24,52].

The observed hydrogen isotope fractionation resolves the two shortcomings of the low and variable carbon isotope fractionation, however. The hydrogen isotope shift of 135‰ (N47) and 120‰ (NaphS2) are more than 20-fold larger than the instrument uncertainty of  $\pm 5\text{‰}$ . For this reason the measurement of hydrogen fractionation bears great potential to be used as reliable indicator for qualitatively assessing in situ biodegradation of naphthalene.

Furthermore, the difference in overall isotope shifts between the two strains is noticeably smaller for hydrogen (11‰) than for carbon (75‰), resulting in more consistent  $\epsilon$  values (figures 2.2 and 2.4). This allows for a consistent quantification of naphthalene degradation in the environment under anaerobic, especially sulfate-reducing conditions [52]. Calculating the difference in the resulting extent of biodegradation at a total fractionation of e.g. 52‰ was maximal 12%. This leads to the conclusion that measuring hydrogen stable isotope fractionation of naphthalene in the field might lead to reliable quantification of biodegradation. Furthermore, already minor extents of biodegradation (25 – 50%) will lead to sufficient strong isotope shifts that could be easily detected with CSIA. Hydrogen isotope measurements could therefore be conducted in a relatively small but sufficient concentration window between the maximum solubility of naphthalene in water (32 mg/l = 251  $\mu$ M) [53] and the analytical detection limit for precise compound-specific hydrogen isotope analysis of naphthalene, which has been lowered by special extraction methods (5 – 10  $\mu$ g/l = 0.04 – 0.08  $\mu$ M) [54].

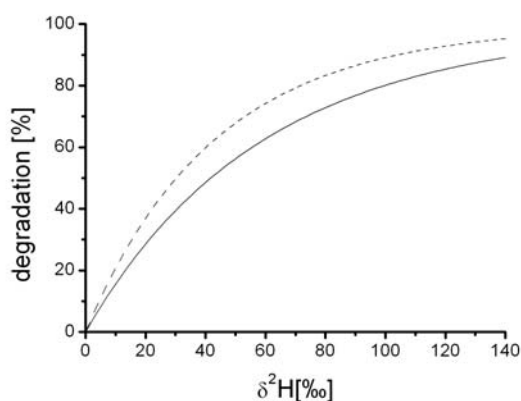


Figure 2.6: Estimation of the range of calculated biodegradation when quantifying naphthalene degradation in the field based on  $\epsilon$  values derived from cultures N47 ( $\epsilon = -100\text{‰} \pm 15\text{‰}$ , solid line) or NaphS2 ( $\epsilon = -73\text{‰} \pm 11\text{‰}$ , dashed line) for hydrogen.

It is common agreement for field sites that observed changes in carbon isotope ratios start to become sufficiently accurate and relevant when they are larger than 2 ‰ and 1 ‰ at minimum as this is the double value of the measurement uncertainty [24,52]. Transferring this to hydrogen isotope analysis, a minimum fractionation of 10 ‰ would be necessary. Nevertheless, we propose 15 ‰ change in hydrogen isotope ratio as a sufficient threshold for significance.

Based on the strong hydrogen isotope fractionation observed for naphthalene, one could conclude that compound-specific hydrogen isotope analysis could also be applied to larger

PAHs to sensitively detect anaerobic biodegradation, and maybe even for quantification. Specifically, one would expect even smaller carbon isotope fractionation, because the number of carbon atoms becomes larger with increasing molecular mass. In contrast, hydrogen fractionation would be expected to be similar, since the number of hydrogen atoms increases only to a minimal extent with the number of rings in polyaromatic hydrocarbons so that the intrinsic isotope effect is hardly diluted (e.g. 10 hydrogen atoms in fluorene, C<sub>13</sub>H<sub>10</sub>, and 10 hydrogen atoms in phenanthrene, C<sub>14</sub>H<sub>10</sub>). However, with increasing number of aromatic rings the maximal solubility of PAHs in water decreases to e.g. 0.002 g/l for fluorene, 0.001 g/l for phenanthrene and much less for substances with more aromatic rings [53]. Tracing and quantifying biodegradation of PAHs by measurement of hydrogen isotope fractionation becomes therefore a balance between water solubility of the compound versus the detection limit of CSIA.

#### 2.4.2 Comparison of dual-isotope fractionation

Figure 2.5 showed that there is remarkable agreement between the dual isotope slopes of the benzene-degrading cultures BF ( $\Lambda = 17 \pm 1$ ) and BPL ( $\Lambda = 20 \pm 2$ ), as well as the naphthalene-degrading culture N47 that is corrected for the number of atoms ( $\Lambda^* = 23 \pm 6$ , s. material and methods). According to the present state of the art this would give circumstantial evidence that all three cultures were using the same initial reaction mechanism, most likely carboxylation [20,21]. In contrast, the significantly different dual isotope slope for the naphthalene-degrading culture NaphS2 ( $\Lambda^* = 86 \pm 36$ ) would imply that this culture was using a different initial degradation step.

However, there are several lines of evidence which suggest that such an interpretation must be undertaken with caution. Until now, there has been the consistent picture that during anaerobic benzene degradation, nitrate-reducing cultures showed significantly smaller dual isotope slopes  $\Lambda$  ( $\sim 10 - 20$ ) compared to sulfate-reducing cultures or methanogens ( $\sim 30$ ) [38,45,46]. This picture is now changed by the results of this study for the sulfate-reducing culture BPL ( $\Lambda = 20 \pm 2$ ), which on the one hand closes the gap between nitrate- and sulfate-reducing bacteria and on the other hand widens up the range of  $\Lambda$  for sulfate-reducing benzene-degrading bacteria ( $\sim 20 - 30$ ). The observed  $\Lambda$  of the iron-reducing culture BF also falls in the range of values previously exclusively reported for nitrate-reducing bacteria. Based on  $\Lambda$  factors, it is therefore not possible to distinguish benzene degradation by nitrate-reducing organisms from sulphate-reducing organisms or iron-reducing cultures. Possible interpretations of the new set of dual isotope fractionation factors are that: i) either two

different initial transformation mechanisms may be active in sulfate reducers, or ii) dual isotope slopes may be more variable for the same benzene transformation mechanism than previously thought.

The same two interpretations would be possible for the two naphthalene degrading strains studied here which gave rise to such significantly different dual isotope slopes ( $\Lambda^* = 23 \pm 6$  versus  $\Lambda^* = 86 \pm 36$ ). If the second explanation is invoked meaning that NaphS2 and N47 are assumed to use the same initial reaction mechanism, the question is raised how the wide difference of the slopes in the dual isotope plots can be explained. Focussing on the AKIEs for hydrogen (1.67 ranging from 1.49 to 1.82) for N47 and 1.41 ranging from 1.32 to 1.49) for NaphS2), they were on the one hand big enough suggesting that breakage of a C-H bond is at least partly rate-determining. Contrasting, they were at the same time small enough that also another reaction step could at least partly rate-determining, too.

The first and most obvious explanation is that in N47 and NaphS2 two different enzyme mechanisms may be responsible for the initial reaction step. This can be further divided into three scenarios: First, there are two completely different initial reaction mechanisms, second, the same mechanism is catalyzed by two different enzymes causing the different  $\Lambda$ , third, the different slopes result from a shift in kinetics of two subsequent transformation steps of the same transformation mechanism where in one culture the first of these two steps is limiting and in the other culture the second step. Such a variation in dual isotope slopes for the same mechanism was recently demonstrated for degradation of isoproturon [55]. For this latter explanation again two more scenarios are possible; one is that the different  $\Lambda$ 's are caused by the same enzyme catalyzing the same reaction, but with slightly different kinetics. For example, a conformational change of the same enzyme could mean that in one conformation the substrate is not fitting equally well into the active site and therefore the rate of the first step differs relative to the second. The second, less likely scenario, is that the two subsequent steps take place in two separate enzymes.

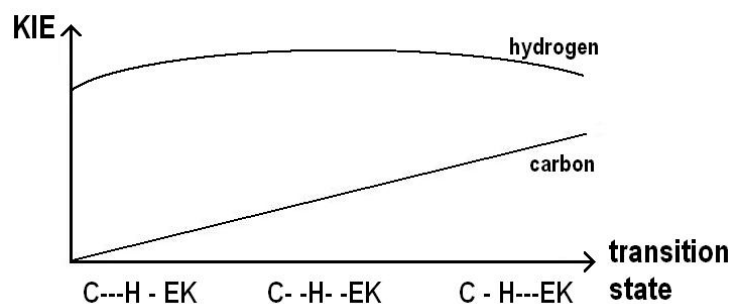


Figure 2.7: The KIE curve for hydrogen and carbon given for the three feasible transition states of a C-H bond and the enzyme complex (EK) of a (bio)chemical reaction.

A further explanation for different  $\Lambda$  values would be that the same (bio)chemical reaction occurs in the same type of enzyme, but with a somewhat different transition state. In particular, for hydrogen transfer three different scenarios can be thought of: i, an early transition state, where the H atom is still close to the aromatic compound (C---H - EK), ii, a symmetric one, where the H atom is halfway between the aromatic compound and the enzyme (C- -H- -EK), or iii, a late one where the H atom is already close to the enzyme (C - H---EK). Hydrogen isotope effects have been conceptualized to become maximal for symmetric transition states (for a treatment of the underlying theory see e.g. [56]). This leads to bell shaped curves like in figure 2.7. In contrast, carbon isotope effects are thought to gradually increase towards late transition states where changes in bonding are greatest compared to the original reactant [57]. Therefore, when considering changes in kinetic isotope effects in dependence on transition state structures, different trends are expected for hydrogen and carbon. Indeed, examples of enzymatic transformations are reported where trends of carbon and hydrogen isotope effects were opposite to each other [58]. Dual isotope slopes of hydrogen versus carbon may therefore differ even for the same reaction, depending on the exact location of the transition state.

Nevertheless, dual isotope plots can be a valuable tool to basically trace for different reaction mechanisms. This study, however, suggests to be careful with interpretations, if carbon and hydrogen atoms are involved in the rate-limiting bond-breaking step and furthermore, optionally different subsequent reaction steps are proceeding, sharing all similar activation energies. This emphasized the need for a mechanistic understanding of the underlying biochemistry to put differences in dual isotope slopes on a firm basis such as in the case of MTBE [27,37], nitrobenzene [50], isoproturon [55,59] or atrazine [60] degradation. Finally, the observed differences in dual isotope slopes did not necessarily rule out a common initial mechanism between the strains Naph2 and N47 and the anaerobic benzene degraders.

## 2.5 References

1. EPA US: **Carcinogenic Effects of Benzene: An Update.** *US Environmental Protection Agency* 1998, **National Center for Environmental Assessment**:97.
2. Van Hamme JD, Singh A, Ward OP: **Recent advances in petroleum microbiology.** *Microbiology and Molecular Biology Reviews* 2003, **67**:503-+.
3. Mihelcic JR, Luthy RG: **Degradation of polycyclic aromatic hydrocarbon compounds under various redox conditions in soil-water systems.** *Appl. Environ. Microbiol.* 1988, **54**:1182-1187.
4. Burland SM, Edwards EA: **Anaerobic Benzene Biodegradation Linked to Nitrate Reduction.** *Appl. Environ. Microbiol.* 1999, **65**:529-533.
5. Rockne KJ, Chee-Sanford JC, Sanford RA, Hedlund BP, Staley JT, Strand SE: **Anaerobic Naphthalene Degradation by Microbial Pure Cultures under Nitrate-Reducing Conditions.** *Appl. Environ. Microbiol.* 2000, **66**:1595-1601.
6. Anderson RT, Rooney-Varga JN, Gaw CV, Lovley DR: **Anaerobic benzene oxidation in the Fe(III) reduction zone of petroleum contaminated aquifers.** *Environ Sci Technol* 1998, **32**:1222-1229.
7. Anderson RT, Lovley DR: **Naphthalene and Benzene Degradation under Fe(III)-Reducing Conditions in Petroleum-Contaminated Aquifers.** *Biorem J* 1999, **3**:121 - 135.
8. Caldwell ME, Tanner RS, Suflita JM: **Microbial metabolism of benzene and the oxidation of ferrous iron under anaerobic conditions: Implications for bioremediation.** *Anaerobe* 1999, **5**:595-603.
9. Lovley DR, Coates JD, Woodward JC, Phillips EJP: **Benzene Oxidation Coupled to Sulfate Reduction.** *Appl. Environ. Microbiol.* 1995, **61**:953-958.
10. Craig DP, Junko K, Lily YY: **Anaerobic degradation of benzene in BTX mixtures dependent on sulfate reduction.** *FEMS Microbiol Lett* 1996, **145**:433-437.
11. Zhang X, Young LY: **Carboxylation as an initial reaction in the anaerobic metabolism of naphthalene and phenanthrene by sulfidogenic consortia.** *Appl. Environ. Microbiol.* 1997, **63**:4759-4764.
12. Galushko A, Minz D, Schink B, Widdel F: **Anaerobic degradation of naphthalene by a pure culture of a novel type of marine sulphate-reducing bacterium.** *Environmental Microbiology* 1999, **1**:415-420.
13. Anderson RT, Lovley DR: **Anaerobic bioremediation of benzene under sulfate-reducing conditions in a petroleum-contaminated aquifer.** *Environ Sci Technol* 2000, **34**:2261-2266.
14. Meckenstock RU, Annweiler E, Michaelis W, Richnow HH, Schink B: **Anaerobic Naphthalene Degradation by a Sulfate-Reducing Enrichment Culture.** *Appl. Environ. Microbiol.* 2000, **66**:2743-2747.
15. Musat F, Widdel F: **Anaerobic degradation of benzene by a marine sulfate-reducing enrichment culture, and cell hybridization of the dominant phylotype.** *Environmental Microbiology* 2008, **10**:10-19.
16. Musat F, Galushko A, Jacob J, Widdel F, Kube M, Reinhardt R, Wilkes H, Schink B, Rabus R: **Anaerobic degradation of naphthalene and 2-methylnaphthalene by strains of marine sulfate-reducing bacteria.** *Environmental Microbiology* 2009, **11**:209-219.
17. Grbic-Galic D, Vogel TM: **Transformation of toluene and benzene by mixed methanogenic cultures.** *Appl. Environ. Microbiol.* 1987, **53**:254-260.

18. Weiner JM, Lovley DR: **Rapid Benzene Degradation in Methanogenic Sediments from a Petroleum-Contaminated Aquifer.** *Appl. Environ. Microbiol.* 1998, **64**:1937-1939.
19. Chang W, Um Y, Holoman TRP: **Polycyclic aromatic hydrocarbon (PAH) degradation coupled to methanogenesis.** *Biotechnology Letters* 2006, **28**:425-430.
20. Abu Laban N, Selesi D, Jobelius C, Meckenstock RU: **Anaerobic benzene degradation by Gram-positive sulfate-reducing bacteria.** *Fems Microbiology Ecology* 2009, **68**:300-311.
21. Abu Laban N, Selesi D, Rattei T, Tischler P, Meckenstock RU: **Identification of enzymes involved in anaerobic benzene degradation by a strictly anaerobic iron-reducing enrichment culture.** *Environmental Microbiology* 2010:in press.
22. Safinowski M, Meckenstock RU: **Methylation is the initial reaction in anaerobic naphthalene degradation by a sulfate-reducing enrichment culture.** *Environmental Microbiology* 2006, **8**:347-352.
23. Lollar BS, Slater GF, Sleep B, Witt M, Klecka GM, Harkness M, Spivaack J: **Stable carbon isotope evidence for intrinsic bioremediation of tetrachloroethene and trichloroethene at area 6, Dover Air Force Base.** *Environ Sci Technol* 2001, **35**:261-269.
24. Meckenstock RU, Morasch B, Griebler C, Richnow HH: **Stable isotope fractionation analysis as a tool to monitor biodegradation in contaminated aquifers.** *Journal of Contaminant Hydrology* 2004, **75**:215-255.
25. Abe Y, Hunkeler D: **Does the Rayleigh equation apply to evaluate field isotope data in contaminant hydrogeology?** *Environ Sci Technol* 2006, **40**:1588-1596.
26. Elsner M, Zwank L, Hunkeler D, Schwarzenbach RP: **A new concept linking observable stable isotope fractionation to transformation pathways of organic pollutants.** *Environ Sci Technol* 2005, **39**:6896-6916.
27. Zwank L, Berg M, Elsner M, Schmidt TC, Schwarzenbach RP, Haderlein SB: **New evaluation scheme for two-dimensional isotope analysis to decipher biodegradation processes: Application to groundwater contamination by MTBE.** *Environ Sci Technol* 2005, **39**:1018-1029.
28. Clark IF, P: *Environmental isotopes in hydrogeology.* New York; 1997.
29. Slater GF, Ahad JME, Lollar BS, Allen-King R, Sleep B: **Carbon isotope effects resulting from equilibrium sorption of dissolved VOCs.** *Analytical Chemistry* 2000, **72**:5669-5672.
30. Schuth C, Taubald H, Bolano N, Maciejczyk K: **Carbon and hydrogen isotope effects during sorption of organic contaminants on carbonaceous materials.** *Journal of Contaminant Hydrology* 2003, **64**:269-281.
31. Wang Y, Huang YS: **Hydrogen isotopic fractionation of petroleum hydrocarbons during vaporization: implications for assessing artificial and natural remediation of petroleum contamination.** *Applied Geochemistry* 2003, **18**:1641-1651.
32. Fischer A, Bauer J, Meckenstock RU, Stichler W, Griebler C, Maloszewski P, Kastner M, Richnow HH: **A multitracer test proving the reliability of Rayleigh equation-based approach for assessing biodegradation in a BTEX contaminated aquifer.** *Environ Sci Technol* 2006, **40**:4245-4252.
33. Nijenhuis I, Andert J, Beck K, Kastner M, Diekert G, Richnow H-H: **Stable Isotope Fractionation of Tetrachloroethene during Reductive Dechlorination by *Sulfurospirillum multivorans* and *Desulfitobacterium* sp. Strain PCE-S and Abiotic Reactions with Cyanocobalamin.** *Appl. Environ. Microbiol.* 2005, **71**:3413-3419.

34. Vogt C, Cyrus E, Herklotz I, Schlosser D, Bahr A, Herrmann S, Richnow HH, Fischer A: **Evaluation of Toluene Degradation Pathways by Two-Dimensional Stable Isotope Fractionation.** *Environ Sci Technol* 2008, **42**:7793-7800.
35. Northrop DB: **The Expression of Isotope Effects on Enzyme-Catalyzed Reactions.** *Annu Rev Biochem* 1981, **50**:103-131.
36. Kampara M, Thullner M, Richnow HH, Harms H, Wick LY: **Impact of bioavailability restrictions on microbially induced stable isotope fractionation. 2. Experimental evidence.** *Environ Sci Technol* 2008, **42**:6552-6558.
37. Elsner M, McKelvie J, Lacrampe Couloume G, Sherwood Lollar B: **Insight into Methyl tert-Butyl Ether (MTBE) Stable Isotope Fractionation from Abiotic Reference Experiments.** *Environ Sci Technol* 2007, **41**:5693-5700.
38. Fischer A, Herklotz I, Herrmann S, Thullner M, Weelink SAB, Stams AJM, Schlomann M, Richnow HH, Vogt C: **Combined carbon and hydrogen isotope fractionation investigations for elucidating benzene biodegradation pathways.** *Environ Sci Technol* 2008, **42**:4356-4363.
39. Mancini SA, Lacrampe-Couloume G, Jonker H, Van Breukelen BM, Groen J, Volkering F, Lollar BS: **Hydrogen isotopic enrichment: An indicator of biodegradation at a petroleum hydrocarbon contaminated field site.** *Environ Sci Technol* 2002, **36**:2464-2470.
40. Griebler C, Safinowski M, Vieth A, Richnow HH, Meckenstock RU: **Combined application of stable carbon isotope analysis and specific metabolites determination for assessing in situ degradation of aromatic hydrocarbons in a tar oil-contaminated aquifer.** *Environ Sci Technol* 2004, **38**:617-631.
41. Vieth A, Kastner M, Schirmer M, Weiss H, Godeke S, Meckenstock RU, Richnow HH: **Monitoring in situ biodegradation of benzene and toluene by stable carbon isotope fractionation.** *Environmental Toxicology and Chemistry* 2005, **24**:51-60.
42. Mak KS, Griebler C, Meckenstock RU, Liedl R, Peter A: **Combined application of conservative transport modelling and compound-specific carbon isotope analyses to assess in situ attenuation of benzene, toluene, and o-xylene.** *Journal of Contaminant Hydrology* 2006, **88**:306-320.
43. Fischer A, Theuerkorn K, Stelzer N, Gehre M, Thullner M, Richnow HH: **Applicability of stable isotope fractionation analysis for the characterization of benzene biodegradation in a BTEX-contaminated aquifer.** *Environ Sci Technol* 2007, **41**:3689-3696.
44. Fischer A, Gehre M, Breitfeld J, Richnow HH, Vogt C: **Carbon and hydrogen isotope fractionation of benzene during biodegradation under sulfate-reducing conditions: a laboratory to field site approach.** *Rapid Commun Mass Sp* 2009, **23**:2439-2447.
45. Mancini SA, Ulrich AC, Lacrampe-Couloume G, Sleep B, Edwards EA, Lollar BS: **Carbon and Hydrogen Isotopic Fractionation during Anaerobic Biodegradation of Benzene.** *Appl. Environ. Microbiol.* 2003, **69**:191-198.
46. Mancini SA, Devine CE, Elsner M, Nandi ME, Ulrich AC, Edwards EA, Lollar BS: **Isotopic Evidence Suggests Different Initial Reaction Mechanisms for Anaerobic Benzene Biodegradation.** *Environ Sci Technol* 2008, **42**:8290-8296.
47. Kunapuli U, Lueders T, Meckenstock RU: **The use of stable isotope probing to identify key iron-reducing microorganisms involved in anaerobic benzene degradation.** *Isme Journal* 2007, **1**:643-653.
48. Elsner M, Couloume GL, Lollar BS: **Freezing to preserve groundwater samples and improve headspace quantification limits of water-soluble organic contaminants for carbon isotope analysis.** *Analytical Chemistry* 2006, **78**:7528-7534.

49. Schmidt T, Zwank L, Elsner M, Berg M, Meckenstock R, Haderlein S: **Compound-specific stable isotope analysis of organic contaminants in natural environments: a critical review of the state of the art, prospects, and future challenges.** *Anal Bioanal Chem* 2004, **378**:283-300.
50. Hofstetter TB, Schwarzenbach RP, Bernasconi SM: **Assessing Transformation Processes of Organic Compounds Using Stable Isotope Fractionation.** *Environ Sci Technol* 2008, **42**:7737-7743.
51. Hunkeler D, Anderson N, Aravena R, Bernasconi SM, Butler BJ: **Hydrogen and carbon isotope fractionation during aerobic biodegradation of benzene.** *Environ Sci Technol* 2001, **35**:3462-3467.
52. EPA US: **A Guide for Assessing Biodegradation and Source Identification of Organic Ground Water Contaminants using Compound Specific Isotope Analysis (CSIA).** *US Environmental Protection Agency* 2008, **Office of Research and Development.**
53. Schwarzenbach RP, Gschwend PM, Imboden DM: *Environmental Organic Chemistry.* Hoboken, New Jersey: John Wiley & Sons, Inc.; 2003.
54. Wang Y, Huang Y, Huckins JN, Petty JD: **Compound-Specific Carbon and Hydrogen Isotope Analysis of Sub-Parts per Billion Level Waterborne Petroleum Hydrocarbons.** *Environmental Science & Technology* 2004, **38**:3689-3697.
55. Penning H, Cramer CJ, Elsner M: **Rate-Dependent Carbon and Nitrogen Kinetic Isotope Fractionation in Hydrolysis of Isoproturon.** *Environ Sci Technol* 2008, **42**:7764-7771.
56. Sühnel J, Schowen RL: **Theoretical Basis for Primary and Secondary Hydrogen Isotope Effects.** *CRC Press* 1991, **Paul Cook, Enzyme Mechanism from Isotope Effects.**
57. Huskey WP: **Origins and Interpretations of Heavy-Atom Isotope Effects.** *CRC Press* 1991, **Paul Cook, Enzyme Mechanism from Isotope Effects.**
58. Scharshmidt M, Fisher MA, Cleland WW: *Biochemistry* 1984, **23**:547.
59. Penning H, Sorensen SR, Meyer AH, Aamand J, Elsner M: **C, N, and H Isotope Fractionation of the Herbicide Isoproturon Reflects Different Microbial Transformation Pathways.** *Environmental Science & Technology* 2010, **44**:2372-2378.
60. Meyer AH, Penning H, Elsner M: **C and N Isotope Fractionation Suggests Similar Mechanisms of Microbial Atrazine Transformation Despite Involvement of Different Enzymes (AtzA and TrzN).** *Environmental Science & Technology* 2009, **43**:8079-8085.



### 3.

## **Identification of new potential enzymes involved in anaerobic naphthalene degradation by the sulphate-reducing enrichment culture N47**

Franz D. Bergmann, Draženka Selesi, Rainer U. Meckenstock

submitted to

*Archives of Microbiology*

### 3.1 Introduction

Naphthalene is the smallest polycyclic aromatic hydrocarbon and it exhibits a low chemical reactivity due to its aromatic  $10\pi$  electron system. Since several decades, aerobic naphthalene degradation has been extensively studied and the initial reactions by oxygenase enzymes have been described in detail [1]. In contrast, the biochemical mechanism of anaerobic naphthalene degradation with alternative electron acceptors like sulphate or nitrate has not yet been adequately elucidated although several nitrate- and sulphate-reducing pure and highly enriched microbial cultures are available [2-6]. However, in the absence of molecular oxygen totally different and new biochemical reactions must be used by the microorganisms to activate the non-substituted aromatic ring structure of naphthalene.

Two different biochemical activation reactions have been proposed for naphthalene degradation under anoxic conditions namely methylation of naphthalene to 2-methylnaphthalene [7,8] and direct carboxylation to 2-naphthoic acid [2,6]. The proposal of the methylation reaction was based on metabolite analyses of culture supernatants of the sulfate-reducing culture N47 during growth on deuterated  $D_8$ -naphthalene. Here, deuterated  $D_7$ -naphthyl-2-methyl-succinate and  $D_7$ -naphthyl-2-methylene-succinate were identified which are specific metabolites of the anaerobic 2-methylnaphthalene degradation pathway [8]. Other metabolites identified in culture N47 were e.g. 2-naphthoic acid [4]. Moreover, enzymatic activities of several reactions of the 2-methylnaphthalene degradation pathway were measured in naphthalene-grown cells i.e. naphthyl-2-methyl-succinate synthase, naphthyl-2-methyl-succinyl-CoA transferase and naphthyl-2-methenyl-succinyl-CoA dehydrogenase [8,9]. Naphthyl-2-methyl-succinate synthase (Nms) catalyzes fumarate addition to the methyl group leading to the formation of naphthyl-2-methyl-succinate [7]. Nms is a glycyl radical enzyme analogous to the benzylsuccinate synthase (Bss) involved in anaerobic toluene degradation [10,11]. The enzyme and metabolite studies supported a methylation of naphthalene to 2-methylnaphthalene and the subsequent degradation via the 2-methylnaphthalene pathway to the central metabolite 2-naphthoyl-CoA for the sulphate-reducing culture N47. The utilization of 2-methylnaphthalene of naphthalene-adapted N47 cells without induction phase further supported methylation as possible activation reaction [8]. Recently, the complete gene cluster of 2-methylnaphthalene degradation and its expression in 2-methylnaphthalene-grown N47 cells were described [12].

The second putative anaerobic degradation mechanism of naphthalene activation was for the first time proposed by Zhang and Young who observed the incorporation of  $^{13}C$ -labeled

bicarbonate from the buffer into the carboxyl group of 2-naphthoic acid [2]. This finding was interpreted as a carboxylation as the initial activation reaction of naphthalene. A similar incorporation of  $^{13}\text{C}$  from the bicarbonate buffer into the carboxyl group was shown for culture N47 [4]. Comparative proteome analysis after electrophoretic separation of the cell extracts from sulphate-reducing cultures NaphS2, NaphS3 and NaphS6 growing on naphthalene and methylnaphthalene revealed Nms synthase as a specific 2-methylnaphthalene-induced protein band that was apparently absent in naphthalene-grown cells [6]. During simultaneous growth of culture NaphS2 on  $\text{D}_8$ -labeled naphthalene and unlabeled 2-methylnaphthalene a high abundance of deuterated 2-naphthoyl-CoA and a comparatively very low portion of unlabeled naphthyl-2-methyl-succinate were formed during growth [6]. These results rather supported a direct carboxylation of naphthalene instead of methylation. The additional formation of trace amounts of labelled naphthyl-2-methyl-succinate during this experiment was explained by reverse reactions of the 2-methylnaphthalene degradation pathway starting from 2-naphthoyl-CoA [6]. In contrast to the results of Safinowski and Meckenstock, the exposure of naphthalene-grown cells to 2-methylnaphthalene resulted in an extended lag phase [6]. So far, the activity of a putative carboxylating enzyme could not be measured in crude cell extracts.

Both putative pathways have in common that 2-naphthoyl-CoA is the central intermediate compound. 2-Naphthoyl-CoA is subjected to ring reduction by a putative 2-naphthoyl-CoA reductase whose gene sequence has been recently deduced from the genome sequence of culture N47 [12].

Here, we performed a proteomic study to identify enzymes involved in the initial activation reaction of anaerobic naphthalene degradation. In a differential expression study with naphthalene, 2-methylnaphthalene, and 2-naphthoic acid as growth substrates, the whole proteomes of naphthalene-grown N47 cells were screened for the presence of proteins of anaerobic aromatic hydrocarbon degradation. In combination with the genome sequence information, we were able to identify several genes coding for a putative carboxylating enzyme in naphthalene-grown N47 cultures.

## **3.2 Material and Methods**

### **3.2.1 Growth conditions for the enrichment culture N47**

The sulphate-reducing culture N47 was enriched from a former coal gasification site and cultivated as reported previously [9]. The substrates naphthalene and 2-methylnaphthalene were added as 1.5% solutions in 2,2,4,4,6,8,8-heptamethylnonane (Sigma-Aldrich, Steinheim, Germany) to the cultivation bottles after autoclaving (1 ml/50 ml medium). 2-naphthoic acid was provided as solid crystals to the bottles before autoclaving to reach a final concentration of 600  $\mu$ M. Inoculum of the enrichment culture N47 was added to the growth media in 1:10 dilutions. Substrate utilization was monitored by colorimetric measurement of sulphide production [13].

### **3.2.2 Terminal restriction fragment length polymorphism (T-RFLP)**

To assure that on both substrates the composition of the enrichment culture was identical, a sample was taken from every bottle for analysis of terminal restriction fragment length polymorphism (T-RFLP). Samples were washed 3 times with 0.5x PBS (phosphate buffered saline). DNA extraction was done with FastDNA<sup>®</sup> SPIN Kit for Soil purchased from MP Biomedicals (Illkirch, France) following the delivered manual. In the first step, instead of 978  $\mu$ l sodium phosphate buffer, only 878  $\mu$ l were used. Additionally, 100  $\mu$ l 10mM potassium citrate was added, to get rid of the iron(II)sulphide, produced during growth. T-RFLP analysis of bacterial 16S rRNA gene amplicons was done as described elsewhere [14] using primers Ba27f-FAM and 907r [15,16] and digestion by restriction enzyme *MspI* (Fermentas, St. Leon-Rot, Germany). Primary electropherogram evaluation was performed using GeneMapper 5.1 software (Applied Biosystems).

### **3.2.3 Sodium dodecyl sulfate-polyacrylamide gel electrophoresis (SDS PAGE)**

For whole proteome analysis, triplicate cultures of N47 grown on naphthalene or 2-methylnaphthalene were harvested when 3.5 mM sulphide accumulated, 2-naphthoic acid grown cells at 2.5 mM sulphide concentration. Cell harvesting, protein purification, and SDS PAGE of the 800 ml sample were performed as described elsewhere [12]. The visualization of protein bands in SDS PAGE was done by Coomassie brilliant blue staining [17].

### **3.2.4 Linear quadrupole ion trap-Orbitrap (LTQ Orbitrap XL) mass spectrometry (MS) with nano-electrospray ionization (ESI)**

#### 3.2.4.1 Tryptic cleavage

Every lane of the gels was cut into 10 slices using a scalpel. Subsequently, each was washed for 10 min with 200  $\mu$ l H<sub>2</sub>O. The destaining was done by washing the slices thrice with 200  $\mu$ l 60% acetonitrile (ACN) for 15 min and 10 min with 200  $\mu$ l H<sub>2</sub>O. For protein reduction and alkylation 100  $\mu$ l 5mM dithiothreitol (DTT) was added and incubated for 15 min at 60°C. Then, the DTT solution was removed, 100  $\mu$ l 25mM iodacetamide was added and incubated for 15 min in the dark. Subsequently, the slice was washed with 200  $\mu$ l H<sub>2</sub>O for 5 min. The next three washing steps were all done for 15 min and with a volume of 200  $\mu$ l in the order: 100% ACN, 50mM ammonium bicarbonate, and 40% ACN. As next washing step, 200  $\mu$ l 100% ACN were used for 5 min. The supernatant was discarded and the resting gel pieces were air dried. The gel slices were overlaid with 0.01  $\mu$ g/ $\mu$ l trypsin in 50mM ammonium bicarbonate. After 10 min, 25mM ammonium bicarbonate solution was added to completely cover the slices with liquid. The digestion proceeded over night at 37°C. Then, 1-2  $\mu$ l 0.5% trifluoroacetic acid (TFA) was added and shaken for 15 min. 50-100  $\mu$ l 50% ACN and 0.1% TFA were added and shaken for 15 min. Afterwards 50-100  $\mu$ l 99.9% ACN together with 0.1% TFA were added and shaken for 15 min. The samples were completely dried in a speed vac. The samples were redissolved in 2% ACN / 0.5% TFA immediately before the analysis.

#### 3.2.4.2 MS analysis and data processing

The digested peptides were separated by reversed phase chromatography (PepMap, 15 cm x 75  $\mu$ m ID, 3  $\mu$ m/100Å pore size, LC Packings) operated on a nano-HPLC (high performance liquid chromatography) (Ultimate 3000, Dionex) with a nonlinear 120 min gradient using 2% acetonitrile in 0.1% formic acid in water (A) and 0.1% formic acid in 98% acetonitrile (B) as eluents with a flow rate of 250 nl/min. The gradient settings were subsequently: 0-90 min: 2-30 % B, 90-105 min: 31-99% B, 106-115 min: Stay at 99% B. The nano-LC was connected to a linear quadrupole ion trap-Orbitrap (LTQ Orbitrap XL) mass spectrometer (ThermoFisher, Bremen, Germany) equipped with a nano-ESI (electrospray ionization) source. The mass spectrometer (MS) was operated in the data-dependent mode to automatically switch between Orbitrap-MS and LTQ-MS/MS acquisition. Survey full scan MS spectra (from m/z 300 to 1500) were acquired in the Orbitrap with resolution  $R = 60,000$  at m/z 400 (after accumulation to a target of 1,000,000 charges in the LTQ). The method used allowed

sequential isolation of the ten most intense ions, depending on signal intensity, for fragmentation on the linear ion trap using collision-induced dissociation at a target value of 100,000 ions. High resolution MS scans in the orbitrap and MS/MS scans in the linear ion trap were performed in parallel. Target peptides already selected for MS/MS were dynamically excluded for 30 sec. General mass spectrometry conditions were: electrospray voltage, 1.25-1.4 kV; no sheath and auxiliary gas flow. Ion selection threshold was 500 counts for MS/MS, and an activation Q-value of 0.25 and activation time of 30 ms were also applied for MS/MS.

All MS/MS samples were analyzed using Mascot (Matrix Science (Version: 2.2.06)). Mascot was set up to search the N47 Database (Number of residues: 1353040, Number of sequences: 5244) assuming the digestion enzyme trypsin and with a fragment ion mass tolerance of 1 Da and a parent ion tolerance of 10 PPM. Iodoacetamide derivative of cysteine as stable modification and oxidation of methionine, deamidation of arginine and glutamine as well as hydroxyl modification of lysine, arginine and histidines as variable modifications were specified in Sequest and Mascot as variable modifications.

#### 3.2.4.3 Criteria for identification

Scaffold (version Scaffold\_2\_02\_03, Proteome Software Inc., Portland, Oregon) was used to validate MS/MS based peptide and protein identifications. Peptide identifications were accepted if they could be established at greater than 80.0% probability as specified by the Peptide Prophet algorithm [18]. Protein identifications were accepted if they could be established at greater than 95 % probability and contained at least 2 identified peptides. Protein probabilities were assigned by the Protein Prophet algorithm [19]. Proteins that contained similar peptides and could not be differentiated based on MS/MS analysis alone were grouped to satisfy the principles of parsimony.

Nevertheless, it is a great challenge to identify all expressed proteins due to multiple reasons. For example the large number of genes encoded in organisms, the dynamic range of proteins is very large and often beyond the intrinsic limitation of instrument sensitivity and furthermore posttranslational modifications further increasing protein complexity [20].

#### **3.2.5 Two-dimensional gel electrophoresis (2-DGE)**

For comparative proteome analysis of naphthalene- and 2-methylnaphthalene-grown N47 cultures, cells from 1 l cultures were harvested, and proteins were extracted and quantified as mentioned above. Aliquots of triplicate samples containing 50 µg proteins were separated in

the first dimension by isoelectric focusing (IEF) and in the second dimension by SDS-polyacrylamide gel electrophoresis (SDS-PAGE). IEF was performed using 18 cm immobilized nonlinear pH gradient strips (pH 3-10; GE Healthcare Europe GmbH, Freiburg, Germany). The strips were rehydrated for 16 h at room temperature in the presence of lysis buffer in an Immobiline DryStrip reswelling tray (GE Healthcare). The strips were placed in a Manifold tray on the Ettan IPGphor II unit (GE Healthcare) and covered with DryStrip cover fluid (GE Healthcare). Voltage was increased stepwise from 150 to 8,000 V over 5.5 h and held at this value for 2 h resulting in 32 kVh. Prior to the second dimension, strips were equilibrated in buffer containing 6 M urea, 2% SDS, 30% glycerol, 100 mM Tris, pH 8.8, 0.01% bromophenol blue, reduced with 60 mM 1,4-dithioerythritol and subsequently alkylated with 220 mM iodoacetamide. The stripes were immediately applied on top of a 12% SDS-PAGE and electrophoresis was carried out at 50 V for 30 min and then increased to 90 V until the bromophenol blue dye migrated to the bottom of the gel. The proteins were visualized by silver staining [21], scanned and analysed using Proteomweaver 2-D Analysis Software (Bio-Rad Laboratories, Hercules, USA).

### **3.2.6 Matrix-assisted laser desorption ionization-time of flight mass spectrometry (MALDI-TOF-MS)**

#### 3.2.6.1 Tryptic cleavage

Protein spots from 2D-gels were manually cut out, destained and washed with buffer containing 50 mM  $\text{NH}_4\text{HCO}_3$  in 30% ACN and equilibrated in 10 mM  $\text{NH}_4\text{HCO}_3$  prior to proteolytic digestion. Gel pieces were shrunk with 100% v/v ACN and rehydrated in 10 mM  $\text{NH}_4\text{HCO}_3$ . This treatment was repeated, followed by the addition of 0.1-0.2  $\mu\text{g}$  of modified trypsin (SIGMA) per piece. Digestion was carried out overnight at 37°C. The supernatant was collected and combined with the eluates of subsequent elution steps with 80% v/v ACN, 1% v/v TFA. The combined eluates were dried in a SpeedVac centrifuge. The dry samples were dissolved in 20  $\mu\text{l}$  50% v/v ACN, 0.1% v/v TFA for the subsequent MALDI preparation. Therefore, 0.5  $\mu\text{l}$  of a 1:1 mixture of sample and a matrix solution consisting of 5 mg/ml CHCA (Bruker, Bremen, Germany) were spotted on a MALDI target.

#### 3.2.6.2 MS analysis and data processing

Mass spectra were acquired using a Proteomics Analyzer 4700 (MALDI-TOF/TOF) mass spectrometer (Applied Biosystems, Framingham, USA). Measurements were performed with

a 355 nm Nb:YAG laser in positive reflector mode with a 20 kV acceleration voltage. For each MS and MS/MS spectrum 3000 shots were accumulated. For each spot on a MALDI plate the eight most intense peptides were selected for additional MS/MS analysis. The acquired MS/MS spectra were searched against the UniRef100 databases (updated April 2009) using an in-house version of Mascot with the following parameters: As taxon we chose human and as enzyme trypsin. We set carbamidomethylation as fixed modification and oxidized methionine as variable modifications.

### 3.2.6.3 Criteria for identification

The GPS Explorer 2 software reports two different scores: The Mascot best ion score, the highest score of a single peptide, and a total ion score, the sum of all peptide scores of one protein. The significance level for a peptide score is usually higher than 20 and for a protein score higher than 50-60. Because different database searches have different Mascot significance levels due to different databases sizes and different numbers of masses submitted for a search, scores cannot be compared directly. For this reason, the software calculates a confidence interval from Mascot protein scores or ion scores, and the Mascot significance level for each search is defined as the 95% confidence level. Therefore, the total ion score confidence level is a reliable and comparable parameter for the significance of a database search.

### **3.2.7 Operon Prediction in N47**

The sequencing, assembly and annotation of the N47 metagenome was described elsewhere and resulted in 17 contigs [Bergmann F., Selesi D., Weinmaier T., Tischler P., Rattei T., Meckenstock R.U., unpublished]. Operon Finding Software (OFS) [22] was used to predict the operons of N47. OFS is based on information about conserved neighbourhood. To gain this information, genomes to BLAST [23] against are needed. For operon prediction in the *Gammaproteobacteria Escherichia coli* K12, the parameter  $\beta$  was chosen in a way that no Gammaproteobacterium (NCBI taxonomyid 1236) was included in the set of informant genomes [22]. Thus, for the N47 genome a set of informant genomes was chosen that did not contain *Deltaproteobacteria* (NCBI taxonomyid 28221). All genomes of publicly available bacteria from RefSeq [24] (July 2009) have been used as informant genomes except those from *Deltaproteobacteria*.

## 2.3 Results and discussion

### 2.3.1 Culture composition

For differential expression experiments with the enrichment culture N47 it was essential to assure that the microbial composition was not changing when growing on different substrates. Therefore, T-RFLP analysis was done for every grown culture. All T-RFLP fingerprints showed a dominant 513-bp T-RF assigned to *Deltaproteobacteria* and a minor 207-bp T-RF belonging to members of *Spirochaetes* (data not shown). This agrees with the picture given earlier by Selesi *et al* [12]. As the culture composition did not change, we could directly assign differences in protein expression to the utilization of naphthalene, 2-methylnaphthalene, or 2-naphthoic acid as growth substrate.

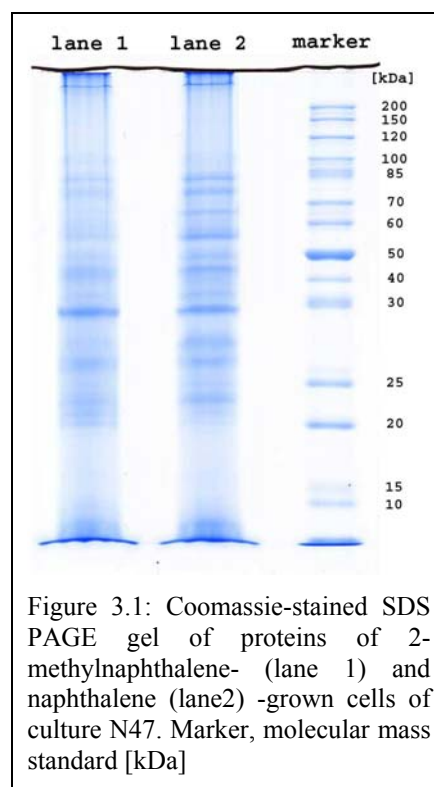


Figure 3.1: Coomassie-stained SDS PAGE gel of proteins of 2-methylnaphthalene- (lane 1) and naphthalene (lane2) -grown cells of culture N47. Marker, molecular mass standard [kDa]

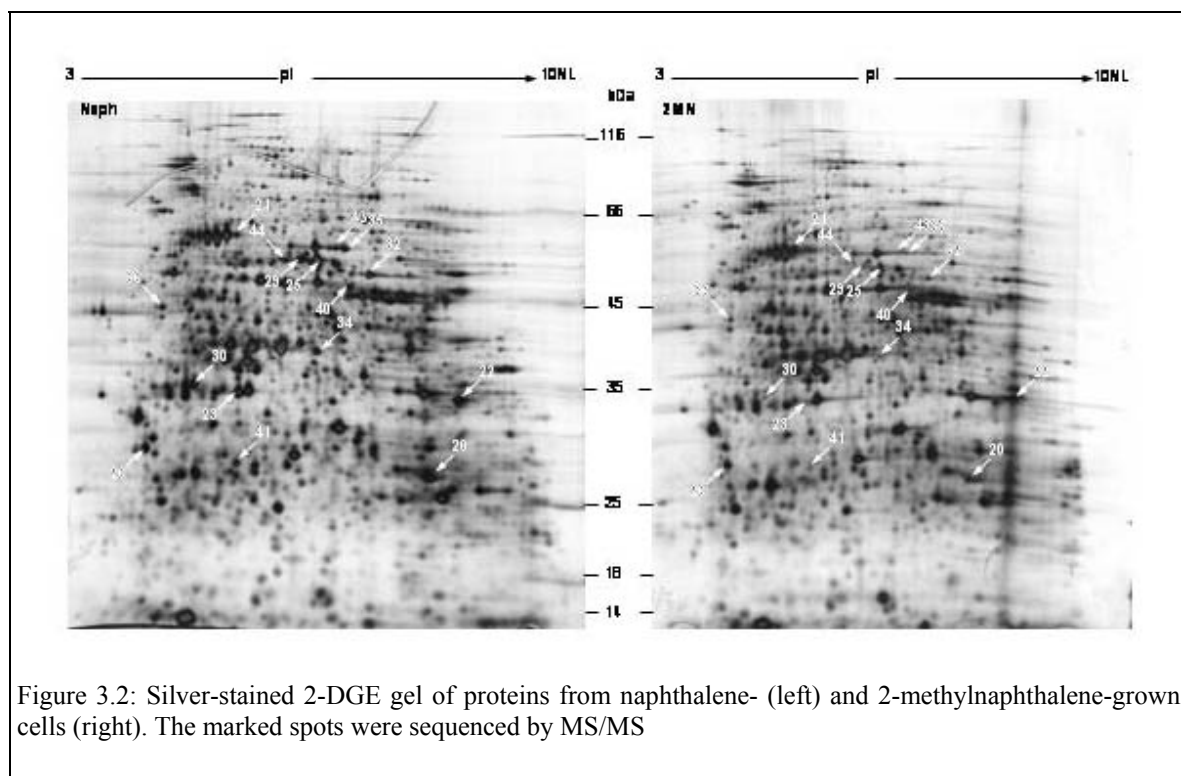
### 2.3.2 Shotgun proteome analysis of naphthalene- and 2-methylnaphthalene-grown N47 cells

Comparing the bands for naphthalene and 2-methylnaphthalene of the Coomassie-stained one-dimensional SDS PAGE, no significant difference was visible (figure 3.1). However, the MS/MS peptide sequencing identified 854 proteins when growing on naphthalene as sole carbon source and 782 proteins with 2-methylnaphthalene. 689 proteins were identified in both lanes, whereas 165 unique proteins were exclusively detected with naphthalene and 93 with 2-methylnaphthalene.

Nevertheless, the detection of proteins meant to be exclusive for a certain substrate has to be treated with caution. As already mentioned in the material and methods section, if a protein could not be detected this does not necessarily imply that it is not expressed upon growth [20]. Moreover, there is a certain loss during protein purification. However, none of the proteins exclusively detected in cells grown with either naphthalene or 2-methylnaphthalene as substrate could be related to aromatic hydrocarbon degradation. For some proteins a potential function in aromatics degradation could not be excluded completely because they did not show the slightest homology to known proteins and their function could not be assigned, therefore.

For both substrates naphthalene and 2-methylnaphthalene, all enzymes for the complete anaerobic 2-methylnaphthalene degradation pathway [12] were expressed, which agrees with earlier results [8] and might also support the methylation hypothesis for the initial reaction step of anaerobic naphthalene degradation.

In contrast to this study, the protein pattern in SDS gels showed a strong band when the marine strain NaphS2 was anaerobically grown on naphthalene as compared to 2-methylnaphthalene [6]. Peptide sequencing of this band, which was only present for 2-methylnaphthalene grown cells, showed a 50% sequence similarity to benzylsuccinate synthase, the toluene activating enzyme [6]. Therefore, methylation as initial reaction mechanism for anaerobic degradation of naphthalene by NaphS2 was excluded by the authors. However, the respective part of the SDS gel for the naphthalene-grown cells was not analyzed by MS/MS. Therefore, it could not be excluded, that the enzyme is expressed during growth on naphthalene in minor amounts as well, invisible on the gel.



### 2.3.3 Proteome analysis using 2-DGE

To quantitatively compare proteomic differences in expression levels during growth on naphthalene and 2-methylnaphthalene we employed two-dimensional gel electrophoresis (2-DGE). For both substrates, the protein patterns showed more than 900 spots, sharing similarities in distribution and intensity (figure 3.2). A closer inspection revealed 19 spots exclusively expressed with naphthalene and 65 proteins which were up-regulated with

naphthalene compared to 2-methylnaphthalene as growth substrate. Even though there are a number of limitations, it is commonly accepted that a two-fold change or larger is sufficient to state significant differences in expression [25]. Among the exclusively expressed or up-regulated proteins with naphthalene as growth substrate, potential candidate enzymes for the initial step in anaerobic naphthalene degradation should be present.

However, it was only possible to identify 3 of the exclusively expressed spots by MALDI-TOF-MS/MS and assign them to the genome sequence: 164667\_163711\_-\_selsg002p03 (spot nr. 1), 7009\_6038\_-\_sellg003n09 (spot nr. 7) and 104821\_108153+\_selsg002p03 (spot nr. 11). These sequences indicated homology to a hypothetical cytosolic protein, putative uncharacterized protein and an ATPase (AAA+ superfamily)-like protein. Nonetheless, from neither of the identified protein sequences a conclusion could be drawn on a potential role in naphthalene degradation.

Therefore 18 randomly chosen spots of the up-regulated proteins of naphthalene-grown cultures were sequenced which resulted in the identification of 8 distinct proteins (table 3.1). The determined sequence of spot nr 28, which matched ORF 163516\_164325+\_contig00524 and spot nr 37, which matched ORF 199830\_200120\_selgw57b, had both homology to hypothetical proteins only.

ORF 67369\_66557\_-\_selsg002p03 was retrieved when sequencing spot nr 20. This was identified as enoyl-CoA hydratase, as the alignment with the best BLAST hit resulted in 47% identity with an e-value of 3E-63 and 95% sequence coverage with the sequence of *Thermosinus carboxydivorans* Nor1. Enoyl-CoA hydratase is known to hydrate the double bond between the alpha and beta carbon atom of acyl-CoA, essential in fatty acid metabolism. Furthermore, it has been shown that an enoyl-CoA hydratase is leading to the hydrolytic aromatic ring cleavage in anaerobic benzoate degradation [26,27]. Sequenced spot nr 36 matched ORF 65327\_64020\_-\_selsg002p03, which is coding for the beta-subunit of 2-naphthoyl-CoA reductase, identified by Selesi *et al.* [12]. Additionally the delta-subunit of 2-naphthoyl-CoA reductase (ORF 63225\_62320\_-\_selsg002p03) was hit by the sequence of spot nr 22.

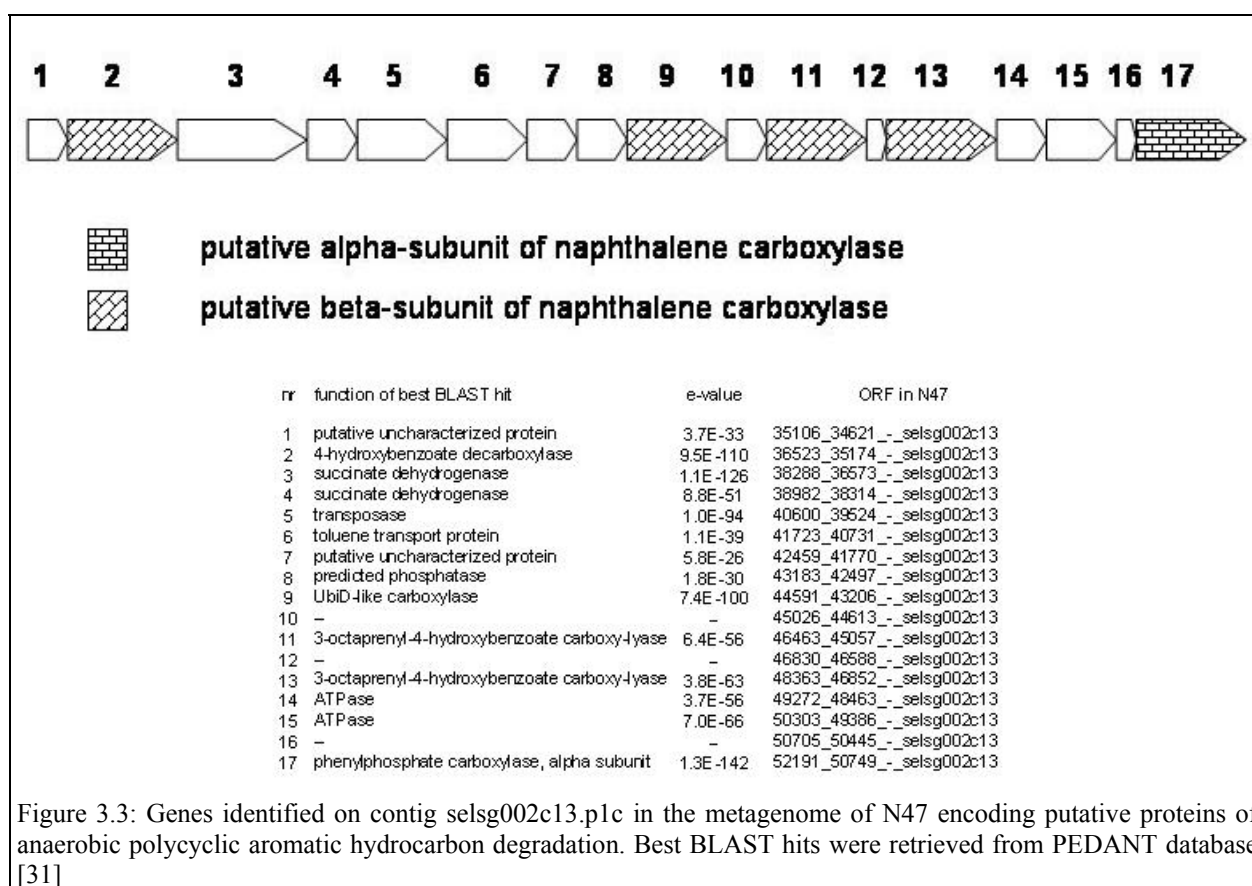
The sequences of spots nr 30, 35, and 41 matched an identical ORF (46463\_45057\_-\_selsg002c13), which had 29% identity with an e-value of 2E-41 and 90% sequence coverage to 3-octaprenyl-4-hydroxybenzoate carboxylase of *Halorhodospira halophila* SL1 based on amino acid sequence alignment. The same enzyme was also hit with an e-value of 2E-48 and 30% identity by ORF 48363\_46852\_-\_selsg002c13, which was matched by the sequenced spots nr 21 and 43. Spot nr 23 and 26 were assigned to ORF 50303\_49386\_selsg002c13,

which showed homology to an ATPase-like protein with 38% identity and an e-value of  $2E-51$ . Another six sequenced spots (25, 29, 32, 34, 40 and 44) hit the same ORF 52191\_50749\_-\_selsg002c13, with amino acid sequence homology to alpha-subunit of phenylphosphate carboxylase with 45% identity and e-value of  $1E-115$ , which is sufficient to assign functional and structural properties to the enzyme.

### **2.3.4 Verification of putative candidates by homology studies**

A further BLAST [28] comparison on amino acid level of ORF 52191\_50749\_-\_selsg002c13 of N47 (putative carboxylase alpha-subunit) to recently discovered anaerobic benzene carboxylase of the iron-reducing benzene-degrading culture BF [29] resulted in 48% identity, an e-value of  $1.4E-130$  and covered nearly 99% of the N47 ORF length. However, the function of anaerobic benzene carboxylase was deduced from sequence homology to the enzyme phenylphosphate carboxylase [29,30]. Phenylphosphate carboxylase catalyzes the carboxylation of phenylphosphate to 4-hydroxybenzoate during anaerobic phenol degradation [30]. The putative carboxylase ORF 52191\_50749\_-\_selsg002c13 of N47 showed 45% protein sequence identity and an e-value of  $1.4E-114$  when blasting it against the alpha-subunit of phenylphosphate carboxylase of *A. aromaticum* EbN1 which was also the best hit when blasting the N47 sequence against all non-redundant peptide sequence databases. The calculated molecular masses as well as the poly peptide chain length of the putative N47 carboxylase and the phenylphosphate carboxylase of strain EbN1 were in the same range (53992 Da (EbN1) vs 53226 Da (N47) and 485 aa's (EbN1) vs 481 aa's (N47)). As the alignment values were sufficient for functional and structural consistency, we conclude that ORF 52191\_50749\_-\_selsg002c13 codes for the putative alpha-subunit of an anaerobic naphthalene carboxylase.

In addition to a putative carboxylase alpha-subunit, we identified four ORFs for a putative beta-subunit on the same contig selsg002C13.p1c: 48363\_46852\_-\_selsg002c13, 36523\_35174\_-\_selsg002c13, 46463\_45057\_-\_selsg002c13 and 44591\_43206\_-\_selsg002c13. These ORFs are located in relative neighbourhood to the putative alpha-subunit on the genome and exhibit significant homology to the gene of the phenylphosphate carboxylase beta-subunit (*ppcB*) of *A. aromaticum* EbN1 (figure 3.3). Putative *ppcA* and *ppcB* (except 36523\_35174\_-\_selsg002c13) genes for naphthalene carboxylase are expressed on both substrates naphthalene and 2-methylnaphthalene. Furthermore, the operon prediction result showed that they were meant to be part of the same operon.



Notably, similar to anaerobic benzene carboxylase we could not identify an ORF on the N47 genome which might be similar to the *ppcC* or *ppcD* genes coding for the two other subunits (gamma and delta) of phenylphosphate carboxylase (table 3.2). In anaerobic phenol degradation, the gamma-subunit catalyzes the phosphatase reaction of phenolphosphate [30]. Similar to anaerobic benzene carboxylation, such a phosphatase reaction would not make sense for carboxylation of naphthalene because there is simply no activated phosphate bound to the molecule. Furthermore, this finding excludes that the putative carboxylase protein which is expressed during growth on naphthalene (52191\_50749\_-\_selsg002c13) might be involved in degradation of phenol or other phenolic compounds because here the gamma- and delta-subunits would be needed.

This is further supported when growing culture N47 on phenol. The T-RFLP analysis of the microbial community showed that the dominant 513-bp T-RF (assigned to *Deltaproteobacteria*) for the naphthalene-grown culture became much smaller and the formerly marginal 207-bp T-RF (belonging to members of *Spirochaetes*) became dominant for the phenol-grown culture (data not shown). This indicates that the phenol degradation was performed by the spirochaetal members of the culture and not by the sulphate-reducing deltaproteobacteria.

### 2.3.5 Domain-based enzyme comparison

Distinct units of molecular protein evolution are called domains and are usually connected to particular aspects of molecular function, as for example catalysis or binding, representing discrete units of three-dimensional structure [32]. Therefore, it can be taken as strong hint for functional and structural similarity if two proteins are sharing the same domain and therefore strengthen the results of sequence similarity searches. The domains mentioned in the following were retrieved from InterPro database which integrates predictive models or 'signatures' representing protein domains [33].

The domain IPR002830 is carboxylase related (derived from UbiD gene relation) and has the three direct related children IPR014095: Phenylphosphate carboxylase, alpha subunit, IPR014096: Phenylphosphate carboxylase, beta subunit and IPR022390: Menaquinone biosynthesis decarboxylase, SCO4490 family. UbiD codes for 3-octaprenyl-4-hydroxybenzoate decarboxylase catalyzing the conversion of 3-octaprenyl-4-hydroxybenzoate to 2-octaprenyl phenol in the ubiquinone biosynthetic pathway [34]. Furthermore, three ORFs similar to UbiD have been shown to be phenol-induced and were proposed for carboxylation of phenylphosphate during anaerobic phenol degradation [35].

All ORFs given in table 3.2 contained the IPR002830 domain according to automatic annotation of PEDANT database [31], which further supported a putative carboxylase function, especially for the two putative subunits (alpha: ORF 52161\_50749\_-\_selsg002c13 and beta: ORF 48363\_46852\_-\_selsg002c13). This domain has also been found in the alpha- and beta-subunit of phenylphosphate carboxylase of *A. aromaticum* EbN1, but not in the gamma- and delta-subunit. Furthermore, the alpha- and beta-subunit of an anaerobic benzene carboxylase of culture BF [29] contained this domain.

spot nr.	regulation factor	ORF in N47	protein match	function
20	2.69	67369_66557_-_selsg002p03	enoyl-CoA hydratase	anaerobic benzoate degradation
36	2.07	65327_64020_-_selsg002p03	2-naphthoyl-CoA reductase, beta subunit	anaerobic 2-methylnaphthalene degradation
22	4.68	63225_62320_-_selsg002p03	2-naphthoyl-CoA reductase, delta subunit	anaerobic 2-methylnaphthalene degradation
41	2.17	46463_45057_-_selsg002c13	3-octaprenyl-4-hydroxybenzoate carboxylase	anaerobic phenol degradation
30	3.41	46463_45057_-_selsg002c13	3-octaprenyl-4-hydroxybenzoate carboxylase	anaerobic phenol degradation
35	4.86	46463_45057_-_selsg002c13	3-octaprenyl-4-hydroxybenzoate carboxylase	anaerobic phenol degradation
43	2.06	48363_46852_-_selsg002c13	3-octaprenyl-4-hydroxybenzoate carboxylase	anaerobic phenol degradation
21	2.30	48363_46852_-_selsg002c13	3-octaprenyl-4-hydroxybenzoate carboxylase	anaerobic phenol degradation
23	3.51	50303_49386_-_selsg002c13	ATPase	cell division and chromosome partitioning
26	5.75	50303_49386_-_selsg002c13	ATPase	cell division and chromosome partitioning
25	2.48	52191_50749_-_selsg002c13	phenylphosphate carboxylase, alpha subunit	anaerobic phenol degradation
29	5.50	52191_50749_-_selsg002c13	phenylphosphate carboxylase, alpha subunit	anaerobic phenol degradation
32	2.68	52191_50749_-_selsg002c13	phenylphosphate carboxylase, alpha subunit	anaerobic phenol degradation
34	5.08	52191_50749_-_selsg002c13	phenylphosphate carboxylase, alpha subunit	anaerobic phenol degradation
40	2.41	52191_50749_-_selsg002c13	phenylphosphate carboxylase, alpha subunit	anaerobic phenol degradation
44	3.71	52191_50749_-_selsg002c13	phenylphosphate carboxylase, alpha subunit	anaerobic phenol degradation
28	2.11	163516_164325+_contig00524	hypothetical protein	
37	3.14	199830_200120+_selgw57b	hypothetical protein	

Table 3.1: ORFs of N47 identified by MS/MS sequencing of selected overexpressed proteins of 2-DGE (figure 3.2). The up-regulation on naphthalene compared to 2-methylnaphthalene is given in the regulation factor column and the best enzyme match and corresponding function was retrieved from PEDANT database [31]

gene EbN1	ORF in N47	e-value	identity	IPR002830	Naph	2MN	2NA
ppcB	52191_50749_-_selsg002c13	2.2E-54	34%	yes	yes	yes	yes
ppcB	48363_46852_-_selsg002c13	2.3E-39	30%	yes	yes	yes	yes
ppcB	36523_35174_-_selsg002c13	1.8E-35	27%	yes	no	no	no
ppcB	46463_45057_-_selsg002c13	1.1E-31	28%	yes	yes	yes	yes
ppcB	44591_43206_-_selsg002c13	1.6E-31	26%	yes	yes	yes	yes
ppcC	--	--	--	--	--	--	--
ppcD	--	--	--	--	--	--	--

Table 3.2: Homologues of *ppcBCD* of *A. aromaticum* EbN1 on contig selsg002C13.p1c of N47 with an e-value better than 1E-20. IPR002830 displays if enzyme contains the carboxylase-related InterPro domain. Expression of ORFs is indicated for growth on the substrate naphthalene (Naph), 2-methylnaphthalene (2MN), and 2-naphthoic acid (2NA).

### 2.3.6 2-Naphthoate-CoA-ligase

In contrast to the anaerobic benzene carboxylation gene cluster of culture BF where a putative benzoate-CoA-ligase is located directly downstream of the carboxylase genes on the genome, no putative 2-naphthoate-CoA-ligase gene could be identified in the genomic neighbourhood of the proposed N47 naphthalene carboxylase genes. However, we have been able to measure a specific 2-naphthoate-CoA-ligase activity in N47 cell extracts (data not shown). The amino acid sequence of benzoate-CoA ligase of *Rhodopseudomonas palustris* [36] containing IPR011957 was blasted against the N47 genome to identify putative candidates. None of the retrieved ORFs contained IPR011957, but some contained IPR020845 (table 3.3), which has InterPro relationships to 9 other ligase-related InterPro domains.

However, one of the ORFs given in table 3 is probably the 2-naphthoate-CoA-ligase needed for anaerobic naphthalene degradation, even if not located in the same operon as the carboxylase, neither on the same contig. The most promising ORF for a putative 2-naphthoate-CoA-ligase is 106353\_104638\_-\_selgw20\_gw20b, because it is expressed exclusively on naphthalene and 2-naphthoic acid according to the one dimensional SDS-PAGE proteomic approach. Similar to growth on naphthalene during growth on 2-naphthoic acid an activation of the carboxyl group to the coenzyme A thioester 2-naphthoyl-CoA would be essential. Nevertheless, also ORFs 338094\_587879\_-\_selgw50\_gw25b and 564377\_562347\_-\_selgw50\_gw25b are possible candidates, as both were expressed in cells grown on all three tested substrates. However, there was no information about possible up-regulation available because the respective spots could not be identified in the 2D gels. Therefore a specific 2-naphthoate-CoA-ligase could not be identified yet.

ORF	e-value	identity	IPR020845	Naph	2MN	2NA
589435_587879_-_selgw50_gw25b	1.1E-45	29%	yes	no	no	no
323109_321535_-_selh_gw24b_gw46b	7.5E-35	24%	yes	no	no	no
267595_269115+_sel041e02	1.0E-32	23%	yes	no	no	no
338094_336481_-_selgw50_gw25b	1.4E-31	25%	no	yes	yes	yes
507810_509261+_selsg002p03	8.7E-29	24%	yes	no	no	no
564377_562347_-_selgw50_gw25b	2.4E-21	23%	yes	yes	yes	yes
106353_104638_-_selgw20_gw20b	6.7E-19	22%	no	yes	no	yes
686472_685252_-_selsg002p03	1.8E-14	25%	no	no	no	no
36074_33483_-_sel041c11 <sup>*)</sup>	3.0E-11	22%	no	no	no	no

<sup>\*)</sup> additionally contains: IPR009081, IPR002123, IPR006162, IPR006163

Table 3.3: ORFs in the N47 genome homologue to benzoate-CoA ligase of *R. palustris* according to BLAST with an e-value cutoff of E-10. IPR020845 contains the ligase-specific AMP-binding domain. Expression of ORFs is indicated for growth on the substrate naphthalene (Naph), 2-methylnaphthalene (2MN), and 2-naphthoic acid (2NA).

### 3.4 Conclusion

Until now two hypotheses for the initial step in anaerobic naphthalene degradation are discussed. On the one hand, a methylation of naphthalene to 2-methylnaphthalene was proposed [4,8]. The 2-methylnaphthalene would then be further degraded by the recently described 2-methylnaphthalene degradation pathway [7,9,12]. On the other hand, a direct carboxylation of naphthalene to 2-naphthoic acid was suggested [2,6].

Based on the results presented here we conclude that in anaerobic degradation, naphthalene is activated by a carboxylase reaction producing 2-naphthoic acid. This conclusion is based on i. the specific up-regulation of a carboxylase related polypeptide during growth on naphthalene as compared to 2-methylnaphthalene, ii. a striking similarity of the sequence and the gene structure to the genes encoding anaerobic benzene carboxylase which catalysis a chemically similar reaction, and iii. the absence of gamma- and delta-subunits of the putative naphthalene carboxylase which distinguishes this enzyme from phenylphosphate carboxylase, the closest related enzyme where the two subunits gamma and delta are needed for the phosphatase reaction.

The similarity of the carboxylase enzymes for the non-substituted aromatic hydrocarbons naphthalene and benzene suggest a new class of carboxylases catalysing this novel reaction. The anaerobic activation of non-substituted aromatic hydrocarbons presents an unprecedented reaction in biochemistry which remains open to be elucidated in detail.

### 3.5 References

1. Habe H, Omori T: **Genetics of polycyclic aromatic hydrocarbon metabolism in diverse aerobic bacteria.** *Biosci Biotech Bioch* 2003, **67**:225-243.
2. Zhang XM, Young LY: **Carboxylation as an initial reaction in the anaerobic metabolism of naphthalene and phenanthrene by sulfidogenic consortia.** *Appl Environ Microb* 1997, **63**:4759-4764.
3. Galushko A, Minz D, Schink B, Widdel F: **Anaerobic degradation of naphthalene by a pure culture of a novel type of marine sulphate-reducing bacterium.** *Environ Microbiol* 1999, **1**:415-420.
4. Meckenstock RU, Annweiler E, Michaelis W, Richnow HH, Schink B: **Anaerobic naphthalene degradation by a sulfate-reducing enrichment culture.** *Appl Environ Microb* 2000, **66**:2743-2747.
5. Rockne KJ, Chee-Sanford JC, Sanford RA, Hedlund BP, Staley JT, Strand SE: **Anaerobic naphthalene degradation by microbial pure cultures under nitrate-reducing conditions.** *Appl Environ Microb* 2000, **66**:1595-1601.

6. Musat F, Galushko A, Jacob J, Widdel F, Kube M, Reinhardt R, Wilkes H, Schink B, Rabus R: **Anaerobic degradation of naphthalene and 2-methylnaphthalene by strains of marine sulfate-reducing bacteria.** *Environ Microbiol* 2009, **11**:209-219.
7. Annweiler E, Materna A, Safinowski M, Kappler A, Richnow HH, Michaelis W, Meckenstock RU: **Anaerobic degradation of 2-methylnaphthalene by a sulfate-reducing enrichment culture.** *Appl Environ Microb* 2000, **66**:5329-5333.
8. Safinowski M, Meckenstock RU: **Methylation is the initial reaction in anaerobic naphthalene degradation by a sulfate-reducing enrichment culture.** *Environ Microbiol* 2006, **8**:347-352.
9. Safinowski M, Meckenstock RU: **Enzymatic reactions in anaerobic 2-methylnaphthalene degradation by the sulphate-reducing enrichment culture N 47.** *FEMS Microbiol Lett* 2004, **240**:99-104.
10. Leuthner B, Leutwein C, Schulz H, Hörth P, Haehnel W, Schiltz E, Schägger H, Heider J: **Biochemical and genetic characterization of benzylsuccinate synthase from *Thauera aromatica*: a new glycyl radical enzyme catalysing the first step in anaerobic toluene metabolism.** *Mol Microbiol* 1998, **28**:615-628.
11. Krieger CJ, Roseboom W, Albracht SPJ, Spormann AM: **A stable organic free radical in anaerobic benzylsuccinate synthase of *Azoarcus* sp strain T.** *J Biol Chem* 2001, **276**:12924-12927.
12. Selesi D, Jehmlich N, von Bergen M, Schmidt F, Rattei T, Tischler P, Lueders T, Meckenstock RU: **Combined genomic and proteomic approaches identify gene clusters involved in anaerobic 2-methylnaphthalene degradation in the sulfate-reducing enrichment culture N47.** *J Bacteriol* 2010, **192**:295-306.
13. Cline JD: **Spectrophotometric determination of hydrogen sulfide in natural waters.** *Limnol Oceanogr* 1969, **14**:454 - 458.
14. Lueders T, Kindler R, Miltner A, Friedrich MW, Kaestner M: **Identification of bacterial micropredators distinctively active in a soil microbial food web.** *Appl Environ Microb* 2006, **72**:5342-5348.
15. Weisburg WG, Barns SM, Pelletier DA, Lane DJ: **16S ribosomal DNA amplification for phylogenetic study.** *J Bacteriol* 1991, **173**:697-703.
16. Muyzer G, Teske A, Wirsen C, Jannasch H: **Phylogenetic relationships of *Thiomicrospira* species and their identification in deep-sea hydrothermal vent samples by denaturing gradient gel electrophoresis of 16S rDNA fragments.** *Arch Microbiol* 1995, **164**:165-172.
17. Zehr BD, Savin TJ, Hall RE: **A one-step, low background Coomassie staining procedure for polyacrylamide gels.** *Anal Biochem* 1989, **182**:157-159.
18. Keller A, Nesvizhskii AI, Kolker E, Aebersold R: **Empirical statistical model to estimate the accuracy of peptide identifications made by MS/MS and database search.** *Anal Chem* 2002, **74**:5383-5392.
19. Nesvizhskii AI, Keller A, Kolker E, Aebersold R: **A statistical model for identifying proteins by tandem mass spectrometry.** *Anal Chem* 2003, **75**:4646-4658.
20. Wu LF, Han DK: **Overcoming the dynamic range problem in mass spectrometry-based shotgun proteomics.** *Expert Rev Proteomic* 2006, **3**:611-619.
21. Rappsilber J, Siniosoglou S, Hurt EC, Mann M: **A generic strategy to analyze the spatial organization of multi-protein complexes by cross-linking and mass spectrometry.** *Analytical Chemistry* 2000, **72**:267-275.
22. Westover BP, Buhler JD, Sonnenburg JL, Gordon JI: **Operon prediction without a training set.** *Bioinformatics* 2005, **21**:880-888.
23. Altschul SF, Gish W, Miller W, Myers EW, Lipman DJ: **Basic local alignment search tool.** *J Mol Biol* 1990, **215**:403-410.

24. Pruitt KD, Tatusova T, Maglott DR: **NCBI reference sequences (RefSeq): a curated non-redundant sequence database of genomes, transcripts and proteins.** *Nucleic Acids Res* 2007, **35**:D61-D65.
25. Ting L, Cowley MJ, Hoon SL, Guilhaus M, Raftery MJ, Cavicchioli R: **Normalization and statistical analysis of quantitative proteomics data generated by metabolic labeling.** *Mol Cell Proteomics* 2009, **8**:2227-2242.
26. Boll M, Fuchs G, Heider J: **Anaerobic oxidation of aromatic compounds and hydrocarbons.** *Curr Opin Chem Biol* 2002, **6**:604-611.
27. Rabus R, Kube M, Heider J, Beck A, Heitmann K, Widdel F, Reinhardt R: **The genome sequence of an anaerobic aromatic-degrading denitrifying bacterium, strain EbN1.** *Arch Microbiol* 2005, **183**:27-36.
28. Altschul SF, Madden TL, Schaffer AA, Zhang J, Zhang Z, Miller W, Lipman DJ: **Gapped BLAST and PSI-BLAST: a new generation of protein database search programs.** *Nucleic Acids Res* 1997, **25**:3389-3402.
29. Abu Laban N, Selesi D, Rattei T, Tischler P, Meckenstock RU: **Identification of enzymes involved in anaerobic benzene degradation by a strictly anaerobic iron-reducing enrichment culture.** *Environ Microbiol* 2010:in press.
30. Schuhle K, Fuchs G: **Phenylphosphate carboxylase: a new C-C lyase involved in anaerobic in phenol metabolism in *Thauera aromatica*.** *J Bacteriol* 2004, **186**:4556-4567.
31. Walter MC, Rattei T, Arnold R, Guldener U, Munsterkotter M, Nenova K, Kastenmuller G, Tischler P, Wolling A, Volz A, et al.: **PEDANT covers all complete RefSeq genomes.** *Nucleic Acids Res* 2009, **37**:D408-D411.
32. Marchler-Bauer A, Anderson JB, Cherukuri PF, DeWeese-Scott C, Geer LY, Gwadz M, He S, Hurwitz DI, Jackson JD, Ke Z, et al.: **CDD: a conserved domain database for protein classification.** *Nucleic Acids Res* 2005, **33**:D192-196.
33. Hunter S, Apweiler R, Attwood TK, Bairoch A, Bateman A, Binns D, Bork P, Das U, Daugherty L, Duquenne L, et al.: **InterPro: the integrative protein signature database.** *Nucleic Acids Res* 2009, **37**:D211-215.
34. Zeng H, Snavely I, Zamorano P, Javor GT: **Low ubiquinone content in *Escherichia coli* causes thiol hypersensitivity.** *J Bacteriol* 1998, **180**:3681-3685.
35. Breinig S, Schiltz E, Fuchs G: **Genes involved in anaerobic metabolism of phenol in the bacterium *Thauera aromatica*.** *J Bacteriol* 2000, **182**:5849-5863.
36. Gibson J, Dispensa M, Fogg GC, Evans DT, Harwood CS: **4-Hydroxybenzoate-coenzyme A ligase from *Rhodospseudomonas palustris*: purification, gene sequence, and role in anaerobic degradation.** *J Bacteriol* 1994, **176**:634-641.



## 4.

# **Genomic insights in the metabolic potential of the polycyclic aromatic hydrocarbon degrading sulphate-reducing culture N47**

Franz D. Bergmann, Draženka Selesi, Thomas Weinmaier,  
Patrick Tischler, Thomas Rattei, Rainer U. Meckenstock

submitted to

*Environmental Microbiology*

## 4.1 Introduction

Aromatic hydrocarbons are frequently released into the environment via accidental spills, leaking storage tanks, former gas plants or disposal of organic chemicals. Due to their high chemical stability these compounds may persist for decades and centuries [1]. BTEX compounds (benzene, toluene, ethylbenzene and xylene) and polycyclic aromatic hydrocarbons (PAHs) are considered to be among the most prevalent groundwater pollutants. Due to their relatively high solubility and mobility, they are endangering the quality of drinking water supplies and representing a significant environmental threat [2,3]. The aerobic degradation of aromatic hydrocarbons was studied for decades and the individual metabolic pathways including initial hydroxylation steps and ring cleavage by oxygenase enzymes are well-known [4]. However, in water-saturated sediments such as aquifers organic contamination readily leads to the depletion of dissolved oxygen and anaerobic biodegradation contributes almost exclusively to natural attenuation [5]. For this reason, the elucidation and understanding of anaerobic degradation pathways and the metabolic degradation potential of anaerobic bacteria is of great relevance. Insights have been achieved only during the last decade and a number of novel biochemical reactions have been discovered that can activate aromatic hydrocarbons in the absence of molecular oxygen [3,6-11].

Deeper insights into degradation pathways as well as into the general physiological potential of microbes can be gained by determining genome sequences as basis for further investigations. Among other things the genome allows for operon prediction and therefore identification of potential candidates of yet unknown genes which are able to close the gaps in not yet fully known pathways.

Among aromatic hydrocarbon degrading microbes, the genomes of a few BTEX degraders and the photosynthetic alpha-proteobacterium *Rhodospseudomonas palustris* CGA009 anaerobically degrading lignin monomers, phenol (to 4-hydroxyphenylacetate), benzoate, 4-hydroxybenzoate (*bad* and *hba* genes found) and additionally possessing five benzene ring cleavage pathways [12] have been sequenced and published [13-16].

In the denitrifying beta-proteobacterium *Aromatoleum aromaticum* EbN1 degrading toluene and ethylbenzene [17] 10 gene cluster have been found which enable anaerobic growth on the aromatics: Ethylbenzene, toluene, benzoate, p-cresol, phenol, 3-hydroxybenzoate, benzaldehyde, phenylacetate, benzylalcohol and phenylalanine. During degradation they all converge to the central intermediate benzoyl-CoA except 3-hydroxybenzoate [17].

Furthermore, an operon-like structure has been identified coding for the proteins suggested to be involved in anaerobic p-ethylphenol degradation [18]. Additionally, paralogous gene clusters have been found indicating that the degradation spectrum is even larger than previously known [14]. The substrate-dependent regulation of toluene and ethylbenzene degradation genes has been shown [19] and it has been probed for growth condition dependent regulation by defining degradation pathway-specific subproteomes [20]. In 2008, a regulation mechanism for the *bzd* genes involved in anaerobic benzoate catabolism has been shown [21].

The sequence of the nitrate-reducing beta-proteobacterium *Dechloromonas aromatica* RCB [22] degrading benzene, toluene, ethylbenzene and all three xylene isomers [23] has been sequenced as well [16]. Surprisingly, the *D. aromatica* RCB genome did not contain genes previously characterized for anaerobic aromatics degradation [16].

The genome of the Fe(III)-reducing delta-proteobacterium *Geobacter metallireducens* GS-15 contains a 300 kb island containing the enzymes for degradation of phenol, p-cresol, 4-hydroxybenzaldehyde, 4-hydroxybenzoate, benzyl alcohol, benzaldehyde and benzoate, while toluene degradation enzymes are encoded in a separate region [15]. A constraint-based modeling approach was applied to the genome to provide physiological and ecological insights in the metabolism [24]. Features of metabolism, physiology, and gene regulation of *G. metallireducens* GS-15 differed strongly to other *Geobacteraceae* [25]. Recently, a two-component system has been identified in *G. metallireducens* GS-15, which is involved in transcriptional regulation of the initial step of benzoate degradation [26].

For the highly enriched delta-proteobacterial, sulfate-reducing culture N47 it has already been shown that it is able to anaerobically degrade naphthalene, 2-methylnaphthalene, and 2-naphthoic acid [27]. Combined genome sequencing and liquid chromatography-tandem mass spectrometry-based shotgun proteome analyses were performed to identify gene clusters involved in 2-methylnaphthalene degradation [28] displaying the potential of a combined proteomic and genomic approach.

In this study, the metagenome of the major organism (> 95%) of enrichment culture N47 is annotated and analyzed, representing the first published genome sequence of a sulfate-reducing, PAH-degrading bacterium. The set of genes revealed from this delta-proteobacterium of the *Desulfobacteraceae* serves as basis to predict metabolic pathways present in N47 and determine the theoretical physiological potential and the physiology when actually grown on PAHs. Subsequently the proteome of N47 when grown on different substrates (naphthalene, 2-methylnaphthalene, 2-naphthoic acid) was analyzed by liquid

chromatography electrospray ionization mass spectrometry mass spectrometry (LC-ESI MS/MS) and matched to the metagenome. This revealed expressed genes and active metabolic pathways during anaerobic growth on PAHs.

## **4.2 Material and Methods**

### **4.2.1 Cultivation of the enrichment culture N47**

The sulfate-reducing culture N47 was cultivated in freshwater medium as described previously [29]. 1 ml of a 1.5% solution of naphthalene in a carrier phase 2,2,4,4,6,8,8-heptamethylnonane (Sigma-Aldrich, Steinheim, Germany) was added as substrate per 50 ml medium into the cultivation bottles after autoclaving. Cultures were inoculated in 1:10 dilutions and utilization of substrate was monitored by colorimetric measurement of sulfide [30].

### **4.2.2 Sequencing and annotation**

The genomic DNA was isolated from a 400 ml naphthalene-grown culture using the Wizard genomic DNA purification kit by following the manufacturer's protocol (Promega, Madison, WI). Whole metagenome information was obtained by the combination of 454-pyrosequencing and Sanger sequencing of plasmid libraries by Roche GmbH (Penzberg, Germany) and AGOWA GmbH (Berlin, Germany). A manual check of the automated assembly has been done resulting in 18 contigs and subsequently the automated annotation was performed using PEDANT [31]. For more detailed information see [28]. All metagenomic sequence data from this study were deposited at GenBank [32] under accession numbers XXX.

### **4.2.3 Taxonomic binning for classification of contigs**

As no pure culture has been sequenced, it had to be assured that each of the 18 contigs achieved belongs to N47. For this reason the distribution of the bidirectional best hit (BBH) of every gene for every contig separately was evaluated according to their taxonomy. Single, misleading best hits according to their taxonomy caused by for example horizontal gene transfer (HGT) were of minor statistical relevance, as the taxonomy of all best hits for one contig were simultaneously evaluated (table 4.1).

For every gene of every contig, the NCBI taxonomy [33] of the best BLAST hit [34] was retrieved from the SIMAP database [35] with an e-value cutoff of  $1e-10$ . This cutoff was chosen as it is a compromise between selectivity and sensitivity of the retrieved proteins. Subsequently, every gene was asserted to one of the following seven categories (1) *Spirochaetes*, (2) *Alphaproteobacteria*, (3) *Betaproteobacteria*, (4) *delta/epsilon subdivisions*, (5) *Gammaproteobacteria*, (6) *Zetaproteobacteria*, and (7) Others (containing all taxa not fitting in one of the first 6 categories) based on the class level of NCBI taxonomy of the best BLAST hit and evaluated for all genes of one contig at once, separately for every contig. If less than 1% of the genes of a contig were asserted to *Spirochaetes*, the contig was assigned to the N47 metagenome.

#### **4.2.4 Completeness estimation of genomic sequence**

To assess the completeness of the N47 metagenome, taxonomic markers consisting of the 53 most universal bacterial clusters of orthologous groups (COGs) in the eggNOG database [36] have been searched in the contigs. To predict COG assignments for the N47 proteome, it has been scanned for the best bidirectional hits (BBHs) to the 50 COGs of *Pelobacter carbinolicus* DSM2380, the closest relative of N47 in the eggNOG database. The e-value cutoff was set to  $1e-10$  and at least 50% of the length of both, query and hit protein, had to be involved in the alignment.

#### **4.2.5 Number of genes with homologous in other bacteria**

For calculating the percentage of genes of N47 showing homology with known proteins the similarities in all sequences belonging to bacteria (NCBI taxonomy id 2) were searched within UniProtKB (October 2009) [37] using SIMAP with varying e-value cutoffs of  $1e-02$ ,  $1e-03$ , and  $1e-10$  to compare different sensitivities regarding the number of homologues. The same analysis was performed against UniProtKB/Swiss-Prot (October 2009). The threshold for a functional and structural consistency was assumed to be 40% identity and used to detect conservation. For both analyses the ratio of alignment length to sequence length for each of the proteins had to be  $\geq 0.5$  and the matching sequences had to have  $\geq 40.0\%$  identity.

#### **4.2.6 Unique genes based on taxonomic levels**

In this case, a gene is meant to be unique if no orthologue gene can be found within proteomes of a given NCBI taxonomy level, in this case subphylum (*delta/epsilon subdivisions*) and class (*Deltaproteobacteria*). The e-value ( $1e-04$ ) cutoff was chosen to

increase the sensitivity of the build COGs and the inparalogmergescorefactor (1.5) was set to assure the inparalogue is more similar to the protein of the same organism than to its BBH to exclude wrong proteins in the clusters. All proteins of N47 not member in any of the calculated COGs were meant to be unique.

#### **4.2.7 Gene duplications within the metagenome**

In N47, the paralogues with functional equivalence have been identified by searching the best BLAST match for each protein against the whole proteome excluding the query protein itself. Afterwards a single linkage clustering was applied. The sequence similarity criteria two proteins have to fulfil for establishing a link between them were: (i) the alignment had an e-value  $\leq 1e-10$ , (ii) the ratio of alignment length to sequence length of each protein was  $\geq 0.5$ , and (iii) the sequences had  $\geq 40\%$  local identity.

#### **4.2.8 Repetitive sequences covering the metagenome**

The repeat detection in N47 was done by using the software REPuter [38]. All exact maximal repeats were searched using the parameters -f for forward repeats, -p for palindromes, -r for reverse repeats, and -c for complement repeats. Examples for the different repetition types can be found at: <http://bibiserv.techfak.uni-bielefeld.de/reputer/manual.html>. The length parameter -l was set to 100 nucleotides for the first run and 500 for the second run.

#### **4.2.9 Domain representation and frequency of occurrence**

All protein domains were predicted by InterProScan [39]. N47 has been checked for remarkable over- and underrepresented domains. This was done by counting the number of occurrence of every domain in the predicted N47 proteome and comparing them to the number of occurrences of the domains in the conserved proteomes of different taxonomic levels: *Proteobacteria* (NCBI taxonomy id 1224, level: phylum), *delta/epsilon subdivisions* (NCBI taxonomy id 68525, level: subphylum), and *Deltaproteobacteria* (NCBI taxonomy id 28221, level: class). Subsequently, this information was used to perform a two-tailed Fisher's Exact Test with Bonferroni correction for multiple testing. Domains with a p-value  $\leq 0.01$  were presumed to be significantly enriched or depleted.

#### **4.2.10 Determination of protein expression**

To get an overview about actually expressed genes and active metabolic pathways N47 was grown on 3 different substrates for several generations. Therefore N47 was inoculated and

cultivated with 1.5% solutions of naphthalene and 2-methylnaphthalene as mentioned above. 2-naphthoic acid was provided as solid crystals to a total theoretical concentration of 600  $\mu\text{M}$  before autoclaving to the bottles.

Proteins were harvested in an active growth phase as determined by increasing sulfide concentrations [30]. Growing on naphthalene, N47 cells were harvested at a sulfide concentration of 3.5 mM; for 2-methylnaphthalene at 3.5 mM and for 2-naphthoic acid on 2.5 mM. For naphthalene and 2-methylnaphthalene grown cells, biological triplicates were sampled and duplicates for 2-naphthoic acid grown cultures. As the respectively measured proteomes were mapped to the deltaproteobacterial metagenome no assurance by terminal restriction fragment length polymorphism (T-RFLP) analysis that the same culture is dominant on every substrate was necessary. Cell harvesting, protein purification, sodium dodecyl sulfate-polyacrylamide gel electrophoresis (SDS PAGE) of the 800 ml sample was done as described elsewhere [28]. Visualization of protein bands was done by Coomassie brilliant blue staining [40].

#### **4.2.11 Tryptic cleavage of protein bands**

Every lane of the gels was divided into 10 fractions using a scalpel and subsequently each was washed for 10 minutes with 200  $\mu\text{l}$   $\text{H}_2\text{O}$ . The destaining was done by washing the fractions 3 times with 200  $\mu\text{l}$  60% acetonitrile (ACN) for 15 minutes and 10 minutes with 200  $\mu\text{l}$   $\text{H}_2\text{O}$ . For protein reduction and alkylation, 100  $\mu\text{l}$  5mM dithiothreitol (DTT) was added and incubated for 15 minutes at 60°C. Then, the DTT solution was removed. 100  $\mu\text{l}$  25mM iodacetamide was added and incubated for 15 minutes in the dark. Subsequently it was washed with 200  $\mu\text{l}$   $\text{H}_2\text{O}$  for 5 minutes. The next three washing steps were all done for 15 minutes and a volume of 200  $\mu\text{l}$  in the order: 100% ACN, 50mM ammoniumbicarbonate, and 40% ACN. A last washing step was performed with 200  $\mu\text{l}$  100% ACN for 5 minutes. The supernatant was discarded and the resting gel pieces were air dried. The gel slices were overlaid with 3  $\mu\text{l}$  of 0.01  $\mu\text{g}/\mu\text{l}$  trypsin in 50mM ammoniumbicarbonate. After 10 minutes, 25mM ammoniumbicarbonate solution was added to completely cover the spots with liquid. The digestion proceeded over night at 37°C. Addition of 1-2  $\mu\text{l}$  0.5% trifluoroacetic acid (TFA) and a 15 minutes shake was followed by addition of 50-100  $\mu\text{l}$  50% ACN, 0.1% TFA, and 15 minutes shaking. Subsequently addition of 50-100  $\mu\text{l}$  99.9% ACN, 0.1% TFA, and a 15 minutes shake precipitated the peptides. The samples were completely dried in a speed vac. The samples were redissolved in 2% ACN / 0.5% TFA immediately right the analysis.

#### **4.2.12 MS/MS scan of tryptic peptides**

The digested peptides were separated by reversed phase chromatography (PepMap, 15 cm x 75 µm ID, 3 µm/100Å pore size, LC Packings) operated on a nano-HPLC (high performance liquid chromatography) (Ultimate 3000, Dionex) with a nonlinear 120 min gradient using 2% acetonitrile in 0.1% formic acid in water (A) and 0.1% formic acid in 98% acetonitrile (B) as eluents with a flow rate of 250 nl/min. The gradient settings were subsequently: 0-90 min: 2-30 % B, 90-105 min: 31-99% B, 106-115 min: Stay at 99% B. The nano-LC was connected to a linear quadrupole ion trap-Orbitrap (LTQ Orbitrap XL) mass spectrometer (ThermoFisher, Bremen, Germany) equipped with a nano-ESI (electrospray ionization) source. The mass spectrometer (MS) was operated in the data-dependent mode to automatically switch between Orbitrap-MS and LTQ-MS/MS acquisition. Survey full scan MS spectra (from m/z 300 to 1500) were acquired in the Orbitrap with resolution  $R = 60,000$  at m/z 400 (after accumulation to a target of 1,000,000 charges in the LTQ). The method used allowed sequential isolation of the ten most abundant ions, depending on signal intensity, for fragmentation on the linear ion trap using collision-induced dissociation at a target value of 100,000 ions. High resolution MS scans in the orbitrap and MS/MS scans in the linear ion trap were performed in parallel. Target peptides already selected for MS/MS were dynamically excluded for 30 seconds. General mass spectrometry conditions were: electrospray voltage, 1.25-1.4 kV; no sheath and auxiliary gas flow. Ion selection threshold was 500 counts for MS/MS, and an activation Q-value of 0.25 and activation time of 30 ms were also applied for MS/MS.

#### **4.2.13 MS data analysis**

All MS/MS samples were analyzed using Mascot (Matrix Science (Version: 2.2.06)). Mascot was set up to search the N47 Database (Number of residues: 1353040, Number of sequences: 5244) assuming the digestion enzyme trypsin and with a fragment ion mass tolerance of 1 Da and a parent ion tolerance of 10 PPM. Iodoacetamide derivative of cysteine as stable modification and oxidation of methionine, deamidation of arginine, and glutamine as well as hydroxyl modification of lysine, arginine, and histidines as variable modifications were specified in Sequest and Mascot as variable modifications.

Scaffold (version Scaffold\_2\_02\_03, Proteome Software Inc., Portland, Oregon) was used to validate MS/MS based peptide and protein identifications. Peptide identifications were accepted if they could be established at greater than 80.0% probability as specified by the Peptide Prophet algorithm [41]. Protein identifications were accepted if they could be

established at greater than 95.0% probability and contained at least 2 identified peptides. Protein probabilities were assigned by the Protein Prophet algorithm [42]. Proteins containing similar peptides which could not be differentiated based on MS/MS analysis alone were grouped to satisfy the principles of parsimony.

Nevertheless, it is a great challenge to identify all expressed proteins due to multiple reasons. For example the large number of genes encoded in organisms, the dynamic range of proteins is very large and often beyond the intrinsic limitation of instrument sensitivity and furthermore posttranslational modifications further increasing protein complexity [43].

#### **4.2.14 Gene visualization by metabolic pathway colouring**

The expressed and unexpressed genes of N47 were subsequently visualized by colouring the pathways of KEGG PATHWAY database [44] according to the different substrates. As KEGG PATHWAY database does not offer multicolour, an in-house tool was used to stain the maps with different colours for each substrate (see supplementary material). For the KEGG orthologous (KO) group assignment, the best hit was searched using BLAST with an e-value cutoff of  $1e-10$  and at least 50% of the length of both query and hit protein had to be involved in the alignment. Afterwards the corresponding square(s) to the KO hit in the associated KEGG PATHWAY map(s) were coloured.

It occurred that an enzyme for a single reaction was found only in cells grown on two of the three substrates naphthalene, 2-methylnaphthalene, and 2-naphthoic acid. As there is always a certain loss during extraction and purification of the proteins as well as during the peptide sequencing process, which is in general more probable than that an enzyme is not expressed on a certain substrate, such a reaction was assumed to be present with all three substrates. The completeness of pathways was judged by manual inspection regarding if all pathway-specific key enzymes are present, as there are no thresholds and tools to cover that problem.

### **4.3 Results and Discussion**

#### **4.3.1 Origin of contigs**

The DNA for sequencing the metagenome of the sulfate-reducing naphthalene degrader N47 was derived from a highly enriched culture consisting mainly of the candidate Deltaproteobacterium N47 and a minor portion of an unclassified Spirochaete [28]. Therefore, it had to be clarified whether all assembled contigs (table 4.1) belong to N47. As described in

material and methods the NCBI taxonomy for the best BLAST hit was evaluated for all genes on every contig. For contigs 1-17 it was estimated that 35% - 70% of the hits belonged to the *delta/epsilon subdivisions* and should therefore belong to N47. From the rest, 2% - 23% matched to the other classes of *Proteobacteria*, a minor part in the created category Others, and a negligible number belonging to the class *Spirochaetes*. The percentage of genes per category is given in table 2. Noticeable, contig sellg003N09.q1c does not fit the general picture. No gene of contig sellg003N09.q1c had its best hit in the phylum *Proteobacteria*, but 18.2% hit the phylum *Spirochaetes*. In this contig, two orders of magnitude more genes expose similarity to genes of the taxon *Spirochaetes* than in all other contigs. For this reason, we considered contig sellg003N09.q1c not to be part of the N47 metagenome and excluded it from further analysis. Furthermore, this contig was the second shortest of the 18 contigs of the metagenome and significantly shorter than the bigger ones (table 4.1). Contig sellg003N09.q1c had a significantly different GC content (table 4.1). The remaining 17 contigs summed up to 4,678,763 bp in total, had an average GC content of 40.7%, contained 5231 predicted genes, and 48 predicted genetic elements.

#### **4.3.2 Completeness of metagenome**

We then analysed the content of essential genes on the remaining 17 contigs in order to assess if the obtained sequences cover the majority of the N47 genome. The reference strain taken for the comparison, *Pelobacter carbinolicus* DSM2380, has 59 sequences for the 53 chosen COGs in the eggNOG database (table S4.1). Homologues for 52 COG sequences were found in N47. This led to the conclusion that the sequence of the genome of N47 is nearly complete, as according to the found COGs approximately 98% of the sequence is covered.

#### **4.3.3 General genomic features in comparison to other genomes**

As expected, dotplot calculations [45] of the genomic sequence to detect structural similarities between N47 and other bacteria did not show reasonable result, because the nearest taxonomic neighbour of N47, *Desulfatibacillum alkenivorans* AK-01 had a 16S rRNA identity of 91% only.

nr	contig	length [bp]	%GC	% genes	% genes	% genes	% genes	% genes	% genes	% genes
				matching	matching	matching	matching	matching	matching	matching
				spirochaetes	$\alpha$ -proteobact.	$\beta$ -proteobact.	$\delta/\epsilon$ subdivision	$\gamma$ -proteobact.	$\zeta$ -proteobact.	other taxa
1	contig00524	521779	40.1	0.0	1.3	1.1	66.1	5.1	0.2	26.1
2	contig03913	34823	42.8	0.0	0.0	0.0	59.1	18.2	0.0	22.7
3	Sel010e01.p1c	390633	41.3	0.0	0.3	4.2	58.7	6.1	0.3	30.3
4	Sel041c11.q1c	144009	40.4	0.8	2.3	1.5	55.6	3.8	0.0	36.1
5	Sel041e02.p1c	741192	40.4	0.2	0.6	2.5	66.9	4.7	0.0	25.1
6	Sel049c06.q1c	57786	41.8	0.0	0.0	6.3	45.8	14.6	0.0	33.3
7	Selgw20_gw20b	153293	41.2	0.0	2.4	4.8	47.2	9.6	0.0	36.0
8	Selgw47_gw25b	56628	43.7	0.0	0.0	2.6	61.5	5.1	0.0	30.8
9	Selgw50_gw25b	625935	40.8	0.2	2.6	3.7	67.2	3.7	0.0	22.7
10	Selgw57b	243987	41.2	0.5	0.5	1.4	60.9	9.3	0.0	27.4
11	SelH_gw24b_gw46b	383688	39.6	0.9	0.6	0.9	64.7	5.9	0.0	26.9
12	sellg005M05.q1c	44314	41.8	0.0	0.0	0.0	55.9	5.9	0.0	38.2
13	selsg002C13.p1c	81709	42.7	0.0	0.0	13.2	35.8	9.4	0.0	41.5
14	selsg002P03.q1c	1026095	40.4	0.2	1.4	3.6	59.1	4.8	0.1	30.7
15	selsg003L05.q1c	9368	39.5	0.0	0.0	0.0	40.0	10.0	0.0	50.0
16	selsg004L10.q1c	123464	43.8	0.0	2.0	4.9	51.0	1.0	0.0	41.2
17	selsg008G07.p1c	40060	41.7	0.0	0.0	0.0	35.3	2.9	0.0	61.8
	sum (1 - 17)	4678763	40.7	0.2	1.2	2.9	61.4	5.4	0.1	28.8
18	sellg003N09.q1c	11859	55.4	18.2	0.0	0.0	0.0	0.0	0.0	81.8

Table 4.1: Length and GC content of the assembled contigs. According to the taxonomic binning done for the created groups of the subphylum level, the first 17 were assigned to N47, contig nr 18 to the Spirochaete.

#### **4.3.4 Conservation of predicted proteome**

To see if predicted N47 proteins share conservation among known bacterial proteins, which is also an indicator for the correctness of their prediction, sequences were compared to known ones in the database (table S4.2). Applying the most restrictive of the given e-values ( $1e-10$ ) to UniProt Knowledgebase, 81% of the predicted proteins shared significant homology to other bacterial proteins. 19% of the genes had no significant homologues which could be either due to wrong gene prediction or these are candidates for novel proteins.

#### **4.3.5 Unique genes according to taxonomic constraints**

Unique genes are found in almost every novel genome of microorganisms. Unique genes are of special interest, because they are meant to be responsible for specific adaptations of bacteria to their evolutionary niche. They are not member of COGs calculated for the requested taxonomic level. The number of unique genes per proteome varied depending on the chosen taxonomic level (tables S4.3 and S4.4). Regarding the NCBI taxonomy level *delta/epsilon subdivisions* of *Proteobacteria*, N47 had 1867 unique genes, which is about 4.5 times more than the average of 417 per organism (table S4.3). Compared to the NCBI taxonomy level *Deltaproteobacteria* only, N47 had even 1949 unique genes, compared to a higher average of 695 per organism, which is roughly 3 times more than the average *deltaproteobacterium* (table S4.4). There are two possible reasons for such a surprising amount of novel genes. First the conservation of the genes might have been too low to match the strict criteria for the BBH to be asserted to a COG. Second, N47 might possess many unique proteins probably catalyzing specific reactions related to its natural habitat.

#### **4.3.6 Parologue genes in N47**

N47 has 1375 parologue proteins which were distributed in 360 different clusters (table S4.5). This means 26.3 % of all predicted proteins were paralogues. Comparing this value to all other genomes of *Deltaproteobacteria* sequenced so far it was significantly larger than the maximum of 23.6 % found so far for *Sorangium cellulosum* 'So ce 56' [46] and 2/3 bigger than the average of 16.0 % (already including N47). Widening the field of comparison to the subphylum level *delta/epsilon subdivision*, the hitherto maximum is equal (26.3 %), but the average (including N47) drops to 11.6 %, which makes the percentage of parologue proteins in N47 even more outstanding. An explanation for such a high number could be found in the likewise significantly enriched number of proteins containing at least one transposase domain as shown in the section about over- and underrepresented domains. The benefit is highlighted

in the corresponding paragraph. A second explanation would be haplotypes, which cannot be excluded here.

#### **4.3.7 Repetitive sequences covering the N47 metagenome**

Recombination events challenge the stability of the bacterial genome. As major rearrangements are thought to frequently operate by homologous recombination between inverted repeats, repeat avoidance is frequently associated with genome stability [47].

The N47 metagenome contained repetitive elements larger than 300 bp covering 12.2% of the sequence for window size 300 (table S4.6). The mean repeat coverage of prokaryotic genomes by repeats equal or longer than 300 nucleotides, is 6.9% [48]. These authors also found a very weak positive correlation between repeat coverage and genome size [48]. According to this, N47 should have approximately 7.6% coverage by repeats equal or longer than 300 bp. However, the N47 genome showed an astonishing higher percentage of repetitive sequences. Nevertheless, the high amount of repetitive sequences in N47 (3471 larger than 300 bp) leads to the conclusion that the metagenome is presently very dynamic and probably adapting to changing environmental conditions, respectively niches. The metagenome was not concentrated by genome streamlining or neutral gene loss as it is proposed for relatively constant environments [49].

#### **4.3.8 Over- and underrepresented domains within N47**

Protein domains are distinct units of molecular evolution, generally connected to particular aspects of molecular function, for example catalysis or binding. Usually, they stand for discrete units of three-dimensional structure [50]. Therefore, remarkable over- or underrepresented domains regarding an organism's proteome compared to other proteomes allows drawing conclusions about particular functions playing major or minor role for the organism. For the three taxonomic levels analyzed (*Proteobacteria*, *delta/epsilon subdivision*, *Deltaproteobacteria*) four transposase domains were overrepresented: IPR001207, IPR002559, IPR002560, and PF07592. In the whole metagenome, the amount of proteins containing transposase domains is significantly enriched (data not shown). Such transposable elements (TEs) are widely distributed in bacteria and supposed to enhance the ability of genome evolution being a major source for genetic diversity and allowing for response to environmental changes [51].

#### **4.3.9 Identification of existing gene clusters and expression during growth on substrates**

Insight into the metabolic potential of N47 during growth on PAHs was gained by depicting its 5231 predicted proteins in the corresponding KEGG PATHWAY maps, where 101 different pathways were hit. To this end, N47 was grown on the three PAHs naphthalene, 2-methylnaphthalene, and 2-naphthoic acid and the proteomes were analyzed. During growth with naphthalene as carbon source 854 proteins could be identified, 782 with 2-methylnaphthalene, and 1064 with 2-naphthoic acid. Altogether, 1177 distinct proteins could be detected. However, as mentioned in the methods section, probably not all expressed proteins could be analyzed. Subsequently, those proteins were also matched onto the KEGG PATHWAY maps resulting in a multi colouring scheme, which is given in the supplementary material. These maps were evaluated manually.

#### **4.3.10 Genes for central catabolism and anabolism of nucleic acid, amino acids, sugars and lipids**

In the N47 metagenome, all enzymes of the KEGG PATHWAY maps related to nucleotide anabolism and amino acid metabolism were found and nearly completely detected by the proteome measurements. This indicates that N47 has the potential to synthesize all nucleotides and amino acids and does not show auxotrophy.

Regarding sugar metabolism, N47 possesses genes for degradation and production of D-mannose, D-fructose, D-galactose,  $\alpha$ -D-glucose-1P, starch, glycogen, and peptidoglycan, which were nearly completely expressed during growth on all three substrates. It has already been shown that N47 grows on glucose, pyruvate, and acetate [28]. For D-mannose, D-fructose, and D-galactose no transport system could be identified in N47. Therefore a possible growth on those substrates has to be tested.

The pentose phosphate pathway can be divided into an oxidative irreversible part and non-oxidative (reductive) reversible part [52]. N47 is holding the latter one, where C4, C5, C6, and C7 sugars are transformed into each other and no reduction equivalents are produced. The main enzymes were shown to be expressed (EC numbers: 4.1.2.13, 2.2.1.2, 2.2.1.1, 5.1.3.1, 5.3.1.6, 2.2.1.1, and 2.7.6.1). This mirrored that N47 is frequently using every sugar conversion reaction of the non-oxidative part of the pentose phosphate pathway during growth on PAHs.

Regarding lipid metabolism, N47 has genes for synthesis of the following unsaturated fatty acids: Eicosatrienoic acid (ETE) (C<sub>20</sub>,  $\omega$ 3,6,9), docosapentaenoic acid (DPA) (C<sub>22</sub>,  $\omega$ 3,6,9,12,15), eicosadienoic acid (C<sub>20</sub>,  $\omega$ 6,9), docosadienoic acid (C<sub>22</sub>,  $\omega$ 6,9), behenic acid

(C<sub>22</sub>), lignoceric acid (C<sub>24</sub>), eicosenoic acid (C<sub>20</sub>, ω<sub>9</sub>), erucic acid (C<sub>22</sub>, ω<sub>9</sub>), nervonic acid (C<sub>24</sub>, ω<sub>9</sub>), which were all expressed. N47 has genes to build the following lipopolysaccharides: Phosphoethanolamine with an additional phosphor atom (PEtN-P), heptose α 1 (HEPα1), 3-deoxy-D-manno-oct-2-iloopyranosonic acid (KDO). However, the enzymes could only be identified partly. N47 possesses the genes for synthesis of cardiolipin, phosphatidylglycerol, phosphatidyl-L-serine, and phosphatidylethanolamine, but expression of those glycerophospholipid genes was rarely measured under the conditions tested. The genes for the synthesis of different terpenoid backbones (monoterpenoid, diterpenoid, and carotenoid) were present except the final enzymatic step in the pathway. Among the present genes, only a few were detected as being expressed. Genes for biosynthesis of tetrahymanol are present and were expressed, for the steroid hopane they are present and were mostly measured.

#### **4.3.11 Hydrocarbon metabolism**

Since nearly all completely sequenced pathways for PAH degradation belong to aerobic degradation all hits of N47, which is an obligate anaerobe, in the respective KEGG PATHWAY maps are single hits in complex pathways and not significant. Similarities between aerobic and anaerobic aromatic hydrocarbon degradation enzymes are so small that they are not significant for the corresponding pathways. Only for the “benzoate degradation via CoA ligation” pathway recorded in KEGG, the KEGG route from toluene to benzoyl-CoA is completely present and expressed on all three tested substrates. This sub-pathway is part of the pathway already described for 2-methylnaphthalene degradation in culture N47 [28]. No other pathways for anaerobic aromatic hydrocarbon degradation could be identified in the metagenome sequence of N47. Furthermore, the comparison of the proteomes for the three different substrates did not show significant differences that would allow identifying enzymes for e.g. the initial activation reaction of naphthalene.

#### **4.3.12 Butanoate fermentation**

Butanol production during microbial fermentation was already described 150 years ago and the biochemical pathways for e.g. *Clostridium acetobutylicum* have been firmly established [53-57]. N47 coded for all necessary enzymes of pyruvate fermentation to butanoic acid as depicted in Jones *et al* 1986 [58]. The only difference is located in the first enzymatic step – the transformation of pyruvate to acetyl-CoA – which is catalyzed by pyruvate-ferredoxin oxidoreductase (EC: 1.2.7.1) in *C. acetobutylicum*. N47 has genes for a pyruvate formate-

lyase (EC: 2.3.1.54) instead, which has not been identified as expressed, however. All other enzymes for butanol production were present and expressed in N47, namely: acetyl-CoA C-acetyltransferase (EC: 2.3.1.9), 3-hydroxybutyryl-CoA dehydrogenase (EC: 1.1.1.157), crotonase (EC: 4.2.1.17), butyryl-CoA dehydrogenase (EC: 1.3.99.2), phosphate butyryltransferase (EC: 2.3.1.19), and butyrate kinase (EC: 2.7.2.7).

However, as all reactions catalyzing the conversion from acetyl-CoA to butanoate are reversible, N47 might be able to grow with butyric acid as carbon source.

#### **4.3.13 Mobility and signalling**

All necessary genes for bacterial chemotaxis are present in the metagenome (KEGG PATHWAY map 02030), but only about 25% could be detected as protein products on all three substrates and additional 25% were detected with 2-naphthoic acid as growth substrate only. Furthermore, nearly all genes for flagellar assembly (KEGG PATHWAY map 02040) were found, but only a few were identified as expressed. This fits to the observation that the cells of N47 agglomerate at the bottom of the bottles, when grown in batch culture. As all additives of the medium in the batch culture are dissolved in excess and equally distributed there is actually no need for chemotaxis, as it has been shown for example for bacterial cultures under nutrient limiting conditions [59-61].

Further systems enabling bacteria to react on environmental stimuli are the different two-component systems transmitting environmental stimuli into the cell. In N47, no complete set of genes of such two-component systems has been found.

#### **4.3.14 Transport systems**

Furthermore, N47 possesses genes for 14 of the 76 known ABC transporter systems. However, none of them was detected to be expressed which was not surprising for growth in batch cultures on other substrates. Surprisingly, none of the genes known for the two ABC transporter systems for sulfate is present in N47. Nevertheless, N47 possesses the major facilitator superfamily-type transporters (Sulp family) [62] for sulfate transport, containing InterPro domain IPR001902, which is a known sulfate anion transporter. The corresponding ORF (292723\_290600\_-\_sel010e01) was expressed on all three substrates.

Type II secretion is one of five known protein secretion systems in gram-negative bacteria, which allow for the export of proteins to the extracellular milieu or the outer membrane [63,64]. Type II protein secretion is a two-step process: First the translocation across the inner membrane by Sec or Tat pathway and second the transport from the periplasm to the exterior

[64]. All three described complexes are present in N47. The Tat (twin arginine targeting) system could not be detected during growth, but for the type II secretion and Sec-SRP roughly half of the proteins could be measured as expressed. Therefore it is concluded that N47 is using Sec-SRP with the type II secretion to export proteins during growth on PAHs.

#### 4.3.15 Vitamins and antibiotics

N47 is potentially able to synthesize 9 different essential vitamins, thiamine, riboflavin, pyridoxine, nicotinate / niacin, nicotinamide, pantothenic acid, biotin, folate, and cobalmin (table 4.2). All genes needed for production of vitamins which are not added to the growth medium were expressed during growth (riboflavin and nicotinate / niacin). It has been shown earlier, that N47 is growing also without any vitamin additive which fits to the proteo-genomic analysis presented here.

<b>genes for production of vitamins in N47</b>	<b>contained in the growth medium</b>	<b>genes expressed during growth</b>
thiamine	yes	no
riboflavin	no	yes
pyridoxine	yes	no
nicotinate / niacin	no	yes
nicotinamide	yes	no
pantothenic acid	yes	yes
biotin	yes	no
folate	yes	no
cobalamin	yes	no

Table 4.2: Genes for vitamin synthesis of N47 possessed and expressed during growth.

#### 4.3.16 Energy metabolism

As a sulfate-reducing culture, N47 contains the genes for  $\alpha$  and  $\beta$  subunit of the dissimilatory sulfite reductase (dsrAB) which were expressed during growth with sulfate as terminal electron acceptor. The dissimilatory sulfite reductase was not shown to be present in N47 according to the colouring of KEGG PATHWAY map 00920, because there is no appropriate

orthologous group defined yet in KEGG. Nevertheless, when blasting the sulfite reductase sequence of *Desulfovibrio desulfuricans* (GenBank IDs: CAC09930.1 and CAC09931.1) against the N47 metagenome sequence the *dsr* gene was retrieved with an e-value of 0, a bit score larger than 630, and the alignment length equals the predicted enzyme length.

Furthermore, N47 possesses genes for reduction of nitrate to ammonium which is well known for many sulfate-reducers [65], such as *Desulfobulbus* [66], *Desulforhopalus* [67], *Desulfobacterium* [68], and *Desulfovibrio* [65,69,70]. In contrast to those organisms, which all have been shown to have the ability to utilize nitrate as terminal electron acceptor, N47 did not grow with  $\text{NO}_3^-$  as sole terminal electron acceptor.

In sulfate-reducing bacteria, numerous enzymes catalyzing redox-reactions as well as potentially electron-carrying proteins and menaquinones have been found and electron transport chains have been proposed. However, there is no unifying theory of electron transport in sulfate-reducing bacteria [71]. N47 expressed the NADH dehydrogenase complex as well as parts of the succinate dehydrogenase / fumarate reductase complex. Those  $\text{H}^+$ -pumping complexes have already been shown in other sulfate-reducing bacteria [71].

Different types of cytochromes have been indentified in sulfate-reducing bacteria [72-74]. N47 possesses the genes for a cytochrome *bd* complex. However, cytochrome *bd*-I oxidase subunit I was detected only, when N47 was grown on 2-naphthoic acid. The aerobic microorganism *Azotobacter vinelandii* has the ability to fix nitrogen via nitrogenase [75]. Nitrogenase is oxygen-labile and therefore a system is needed to lower the intracellular oxygen while nitrogenase is active. One strategy of *A. vinelandii* is the use of the cytochrome *bd* complex as a respiratory protection oxidase keeping the intracellular oxygen concentration at low level [76-78]. This leads to the hypothesis that the cytochrome *bd* complex is used as  $\text{O}_2$ -protection system in the obligate anaerobe N47. Furthermore, N47 possesses the enzymes catalase and superoxide dismutase as protection systems against oxidative stress.

Chemical energy conservation in N47 can be performed by a regular F-type ATPase complex which has been detected expressed during growth. Such an ATPase of similar structure can be found in every organism forming or cleaving ATP coupled to proton translocation [79].

N47 possesses the Embden-Meyerhof pathway of glycolysis and a gluconeogenesis pathway. These are connected via pyruvate metabolism, which is a key step in central energy and anabolic metabolisms in most microorganisms [80].

For oxidation of acetate, N47 has genes for the tricarboxylic acid cycle (TCA cycle) which is used by some Desulfobacteriaceae such as *Desulfobacter postgatei* [81,82] and *Desulfuromonas acetoxidans* [83]. Nevertheless, they use a menaquinone containing electron

transport chain to overcome the difference in redox potential between the terminal electron acceptor and succinate [84,85]. Similar to *D. postgatei* and *D. acetoxidans*, N47 is probably lacking the 2-oxoglutarate dehydrogenase, which is a key enzyme of the complete TCA cycle [86]. For example in *Rhodobacter sphaeroides* KD131, the gene for 2-oxoglutarate dehydrogenase is in genomic neighbourhood with the genes for the TCA cycle enzymes citrate synthase, succinate dehydrogenase, and malate dehydrogenase. In N47, those three enzymes are located in the same region on the contig selsg002P03.q1c whereas 2-oxoglutarate dehydrogenase is not present. Instead, N47 is expressing all enzymes, which enable *D. acetoxidans* and *D. postgatei* to operate the TCA cycle [87]. Namely they contain a NADP-specific isocitrate dehydrogenase (EC: 1.1.1.42), a 2-oxoglutarate ferredoxin oxidoreductase (EC: 1.2.7.3), a membrane-bound succinate oxidoreductase (EC: 1.3.99.1), and NAD-dependent malate dehydrogenase (EC: 1.1.1.37). Additionally, N47 expresses a citrate synthase (EC: 2.3.3.1) instead of ATP citrate lyase (EC: 2.3.3.8) as shown in *D. postgatei* but catalyzing the same reaction, an aconitate hydratase (EC: 4.2.1.3), a succinyl-CoA synthetase (EC: 6.2.1.5), and a fumarate hydratase (EC: 4.2.1.2) (also shown in *D. postgatei*) which are completely closing the TCA cycle. Furthermore, a phosphoenolpyruvate carboxykinase (EC: 4.1.1.32) is expressed, which connects the TCA cycle to the glycolysis / gluconeogenesis pathway.

A second possibility to interpret the presence of those enzymes in N47 has been shown in *Desulfobacter hydrogenophilus*, which grows lithoautotrophically on H<sub>2</sub>, CO<sub>2</sub>, and sulfate using the reversal of the above described pathway to assimilate CO<sub>2</sub> to acetate [88]. Nevertheless, *D. hydrogenophilus* can also use acetate and sulfate as sole energy source for heterotrophic growth using the TCA cycle for complete oxidation [86,88]. *D. hydrogenophilus* can thus switch between a heteroorganotrophic and a lithoautotrophic metabolism of growth. The same might be possible also in N47, because the presence of the three enzymes ATP citrate lyase, 2-oxoglutarate ferredoxin oxidoreductase, and fumarate reductase are indicative for a functioning reductive TCA cycle [89]. Some enzymes involved in that cycle are sensitive to oxygen, for this reason it only occurs in anaerobes or microaerophiles. So far, it has been detected in *Hydrogenobacter*, *Aquifex*, some sulfate-reducers, and several thermophilic archeal strains [90] and is the only confirmed autotrophic pathway in  $\epsilon$ -proteobacteria [89].

<b>enzyme originally proposed by Thauer 1988</b>	<b>EC number</b>	<b>enzyme in N47</b>	<b>EC number</b>	<b>detected</b>
acetyl-CoA synthase	6.2.1.1	acetyl-CoA synthase	6.2.1.1	yes
pyruvate synthase	1.2.7.1	pyruvate formate-lyase	2.3.1.54	no
phosphoenolpyruvate synthase	2.7.9.2	phosphoenolpyruvate synthase	2.7.9.2	no
phosphoenolpyruvate synthase	2.7.9.2	pyruvate, phosphate dikinase	2.7.9.1	yes
phosphoenolpyruvate carboxylase	4.1.1.31	phosphoenolpyruvate carboxykinase	4.1.1.32	yes

Table 4.3: Pyruvate synthase pathway for TCA cycle intermediate replenishment originally proposed by Thauer and present in N47. Additionally proteins are marked in the last column, when detected during growth.

The TCA cycle also provides 2-oxoglutarate, succinyl-CoA, and oxaloacetate for the biosynthesis of various cell compounds, such as amino acids. The intermediates have therefore to be replenished to maintain the activity of the cycle [91,92]. Anaerobes possessing the TCA cycle are using the pyruvate synthase pathway as anaplerotic sequence [87]. Genes for all enzymes to replenish the TCA cycle proposed by Thauer 1988 or equivalents were identified on the genome and were mostly expressed during growth on PAHs (table 4.3). This showed that N47 has the ability to replenish the intermediates of the TCA cycle.

The only non-cyclic pathway for autotrophic CO<sub>2</sub> fixation known so far is the reductive acetyl-CoA pathway, also called Wood-Ljungdahl pathway [90,93]. The key enzyme of this pathway is the carbon monoxide dehydrogenase / acetyl-CoA synthase complex [94,95] which is also encoded and expressed in N47 (EC: 1.2.7.4, 1.2.99.2, and EC: 23.1.1.69).

This enzyme complex is meant to reduce two molecules of CO<sub>2</sub> independently if it is used for CO<sub>2</sub> fixation. The first CO<sub>2</sub> is reduced to build 5,10-methylenetetrahydrofolate and the second CO<sub>2</sub> to form CO. The two C1-units are fused to acetyl-CoA [94]. However, carbon monoxide dehydrogenase can also catalyze the reverse reaction to oxidize acetate units which is used by many strictly anaerobic sulfate-reducers.

N47 possesses the genes for an additional pathway synthesizing 5,10-methylenetetrahydrofolate starting from GTP, but the step from dihydroneopterin to 2-amino-4-hydroxy-6-hydroxymethyl-7,8-dihydropteridine-P<sub>2</sub> (EC: 4.1.2.25) is missing. As the pathway was not measured to be expressed during growth on any of the three substrates and

every enzyme is coded on a different contig, it seems likely that the missing enzyme dihydroneopterin aldolase is located somewhere in the gaps of the metagenome.

Nevertheless, this showed that N47 has all prerequisites to autotrophically fix CO<sub>2</sub> via a reductive acetyl-CoA pathway or oxidize acetate via carbon monoxide dehydrogenase. Furthermore, CO-dehydrogenase activity has already been measured in cells grown on naphthalene and 2-methylnaphthalene [96].

Remarkably, N47 is the first bacterium known that contains the reductive acetyl-CoA / CO-dehydrogenase pathway and a complete TCA cycle at the same time. Even more surprisingly, it is also simultaneously expressing both pathways during growth on the PAHs naphthalene, 2-methylnaphthalene and 2-naphthoic acid.

#### 4.4 References

1. Cerniglia CE: **Biodegradation of polycyclic aromatic hydrocarbons**. *Biodegradation* 1992, **3**:351-368.
2. Anderson R, Lovley D: **Ecology and biochemistry of *in situ* groundwater bioremediation**. *Adv Microb Ecol* 1997, **15**:289 - 350.
3. Chakraborty R, Coates JD: **Anaerobic degradation of monoaromatic hydrocarbons**. *Appl Microbiol Biot* 2004, **64**:437-446.
4. Harayama S, Kok M, Neidle EL: **Functional and evolutionary relationships among diverse oxygenases**. *Annu Rev Microbiol* 1992, **46**:565-601.
5. Christensen TH, Kjeldsen P, Albrechtsen H-Jr, Heron G, Nielsen PH, Bjerg PL, Holm PE: **Attenuation of landfill leachate pollutants in aquifers**. *Crit Rev Env Sci Tech* 1994, **24**:119 - 202.
6. Heider J, Fuchs G: **Anaerobic metabolism of aromatic compounds**. *Eur J Biochem* 1997, **243**:577-596.
7. Boll M, Fuchs G, Heider J: **Anaerobic oxidation of aromatic compounds and hydrocarbons**. *Curr Opin Chem Biol* 2002, **6**:604-611.
8. Gibson J, S. Harwood C: **Metabolic diversity in aromatic compound utilization by anaerobic microbes**. *Annu Rev Microbiol* 2002, **56**:345-369.
9. Meckenstock RU, Safinowski M, Griebl C: **Anaerobic degradation of polycyclic aromatic hydrocarbons**. *FEMS Microbiol Ecol* 2004, **49**:27-36.
10. Foght J: **Anaerobic biodegradation of aromatic hydrocarbons: Pathways and prospects**. *J Mol Microb Biotech* 2008, **15**:93-120.
11. Carmona M, Zamarro MT, Blazquez B, Durante-Rodriguez G, Juarez JF, Valderrama JA, Barragan MJL, Garcia JL, Diaz E: **Anaerobic catabolism of aromatic compounds: a genetic and genomic view**. *Microbiol Mol Biol R* 2009, **73**:71-+.
12. Larimer FW, Chain P, Hauser L, Lamerdin J, Malfatti S, Do L, Land ML, Pelletier DA, Beatty JT, Lang AS, et al.: **Complete genome sequence of the metabolically versatile photosynthetic bacterium *Rhodospseudomonas palustris***. *Nat Biotechnol* 2004, **22**:55-61.

13. Boll M: **Dearomatizing benzene ring reductases.** *J Mol Microb Biotech* 2005, **10**:132-142.
14. Rabus R: **Functional genomics of an anaerobic aromatic-degrading denitrifying bacterium, strain EbN1.** *Appl Microbiol Biot* 2005, **68**:580-587.
15. Butler JE, He Q, Nevin KP, He ZL, Zhou JZ, Lovley DR: **Genomic and microarray analysis of aromatics degradation in *Geobacter metallireducens* and comparison to a *Geobacter* isolate from a contaminated field site.** *BMC Genomics* 2007, **8**.
16. Salinero KK, Keller K, Feil WS, Feil H, Trong S, Di Bartolo G, Lapidus A: **Metabolic analysis of the soil microbe *Dechloromonas aromatica* str. RCB: indications of a surprisingly complex life-style and cryptic anaerobic pathways for aromatic degradation.** *BMC Genomics* 2009, **10**.
17. Rabus R, Kube M, Heider J, Beck A, Heitmann K, Widdel F, Reinhardt R: **The genome sequence of an anaerobic aromatic-degrading denitrifying bacterium, strain EbN1.** *Arch Microbiol* 2005, **183**:27-36.
18. Wohlbrand L, Wilkes H, Halder T, Rabus R: **Anaerobic degradation of p-ethylphenol by *Aromatoleum aromaticum* strain EbN1: Pathway, regulation, and involved proteins.** *J Bacteriol* 2008, **190**:5699-5709.
19. Kuhner S, Wohlbrand L, Fritz I, Wruck W, Hultschig C, Hufnagel P, Kube M, Reinhardt R, Rabus R: **Substrate-dependent regulation of anaerobic degradation pathways for toluene and ethylbenzene in a denitrifying bacterium, strain EbN1.** *J Bacteriol* 2005, **187**:1493-1503.
20. Wohlbrand L, Kallerhoff B, Lange D, Hufnagel P, Thiermann J, Reinhardt R, Rabus R: **Functional proteomic view of metabolic regulation in *Aromatoleum aromaticum* strain EbN1.** *Proteomics* 2007, **7**:2222-2239.
21. Durante-Rodriguez G, Zamarro MT, Garcia JL, Diaz E, Carmona M: **New insights into the BzdR-mediated transcriptional regulation of the anaerobic catabolism of benzoate in *Azoarcus* sp CIB.** *Microbiol-SGM* 2008, **154**:306-316.
22. Coates JD, Chakraborty R, Lack JG, O'Connor SM, Cole KA, Bender KS, Achenbach LA: **Anaerobic benzene oxidation coupled to nitrate reduction in pure culture by two strains of *Dechloromonas*.** *Nature* 2001, **411**:1039-1043.
23. Chakraborty R, O'Connor SM, Chan E, Coates JD: **Anaerobic degradation of benzene, toluene, ethylbenzene, and xylene compounds by *Dechloromonas* strain RCB.** *Appl Environ Microb* 2005, **71**:8649-8655.
24. Sun J, Sayyar B, Butler JE, Pharkya P, Fahland TR, Famili I, Schilling CH, Lovley DR, Mahadevan R: **Genome-scale constraint-based modeling of *Geobacter metallireducens*.** *BMC Syst Biol* 2009, **3**.
25. Aklujkar M, Krushkal J, DiBartolo G, Lapidus A, Land ML, Lovley DR: **The genome sequence of *Geobacter metallireducens*: features of metabolism, physiology and regulation common and dissimilar to *Geobacter sulfurreducens*.** *BMC Microbiol* 2009, **9**.
26. Juarez JF, Zamarro MT, Barragan MJL, Blazquez B, Boll M, Kuntze K, Garcia JL, Diaz E, Carmona M: **Identification of the *Geobacter metallireducens* BamVW two-component system, involved in transcriptional regulation of aromatic degradation.** *Appl Environ Microbiol* 2010, **76**:383-385.
27. Meckenstock RU, Annweiler E, Michaelis W, Richnow HH, Schink B: **Anaerobic naphthalene degradation by a sulfate-reducing enrichment culture.** *Appl Environ Microbiol* 2000, **66**:2743-2747.
28. Selesi D, Jehmlich N, von Bergen M, Schmidt F, Rattei T, Tischler P, Lueders T, Meckenstock RU: **Combined genomic and proteomic approaches identify gene**

- clusters involved in anaerobic 2-methylnaphthalene degradation in the sulfate-reducing enrichment culture N47.** *J Bacteriol* 2010, **192**:295-306.
29. Safinowski M, Meckenstock RU: **Enzymatic reactions in anaerobic 2-methylnaphthalene degradation by the sulphate-reducing enrichment culture N47.** *FEMS Microbiol Lett* 2004, **240**:99-104.
  30. Cline JD: **Spectrophotometric determination of hydrogen sulfide in natural waters.** *Limnol Oceanogr* 1969, **14**:454 - 458.
  31. Walter MC, Rattei T, Arnold R, Guldener U, Munsterkotter M, Nenova K, Kastenmuller G, Tischler P, Wolling A, Volz A, et al.: **PEDANT covers all complete RefSeq genomes.** *Nucl Acids Res* 2009, **37**:D408-D411.
  32. Benson DA, Karsch-Mizrachi I, Lipman DJ, Ostell J, Wheeler DL: **GenBank.** *Nucl Acids Res* 2008, **36**:D25-30.
  33. Sayers EW, Barrett T, Benson DA, Bryant SH, Canese K, Chetvernin V, Church DM, DiCuccio M, Edgar R, Federhen S, et al.: **Database resources of the National Center for Biotechnology Information.** *Nucl Acids Res* 2009, **37**:D5-15.
  34. Altschul SF, Gish W, Miller W, Myers EW, Lipman DJ: **Basic local alignment search tool.** *J Mol Biol* 1990, **215**:403-410.
  35. Arnold R, Rattei T, Tischler P, Truong M-D, Stumpflen V, Mewes W: **SIMAP--The similarity matrix of proteins.** *Bioinformatics* 2005, **21**:ii42-46.
  36. Jensen LJ, Julien P, Kuhn M, von Mering C, Muller J, Doerks T, Bork P: **eggNOG: automated construction and annotation of orthologous groups of genes.** *Nucl Acids Res* 2008, **36**:D250-254.
  37. The UniProt C: **The universal protein resource (UniProt) in 2010.** *Nucl Acids Res* 2010, **38**:D142-148.
  38. Kurtz S, Schleiermacher C: **REPuter: fast computation of maximal repeats in complete genomes.** *Bioinformatics* 1999, **15**:426-427.
  39. Quevillon E, Silventoinen V, Pillai S, Harte N, Mulder N, Apweiler R, Lopez R: **InterProScan: protein domains identifier.** *Nucl Acids Res* 2005, **33**:W116-W120.
  40. Zehr BD, Savin TJ, Hall RE: **A one-step, low background Coomassie staining procedure for polyacrylamide gels.** *Anal Biochem* 1989, **182**:157-159.
  41. Keller A, Nesvizhskii AI, Kolker E, Aebersold R: **Empirical statistical model to estimate the accuracy of peptide identifications made by MS/MS and database search.** *Anal Chem* 2002, **74**:5383-5392.
  42. Nesvizhskii AI, Keller A, Kolker E, Aebersold R: **A statistical model for identifying proteins by tandem mass spectrometry.** *Anal Chem* 2003, **75**:4646-4658.
  43. Wu LF, Han DK: **Overcoming the dynamic range problem in mass spectrometry-based shotgun proteomics.** *Expert Rev Proteomic* 2006, **3**:611-619.
  44. Kanehisa M, Goto S: **KEGG: Kyoto encyclopedia of genes and genomes.** *Nucl Acids Res* 2000, **28**:27-30.
  45. Krumsiek J, Arnold R, Rattei T: **Gepard: a rapid and sensitive tool for creating dotplots on genome scale.** *Bioinformatics* 2007, **23**:1026-1028.
  46. Schneiker S, Perlova O, Kaiser O, Gerth K, Alici A, Altmeyer MO, Bartels D, Bekel T, Beyer S, Bode E, et al.: **Complete genome sequence of the myxobacterium *Sorangium cellulosum*.** *Nat Biotech* 2007, **25**:1281-1289.
  47. Achaz G, Coissac E, Netter P, Rocha EPC: **Associations between inverted repeats and the structural evolution of bacterial genomes.** *Genetics* 2003, **164**:1279-1289.
  48. Treangen TJ, Abraham AL, Touchon M, Rocha EPC: **Genesis, effects and fates of repeats in prokaryotic genomes.** *FEMS Microbiol Rev* 2009, **33**:539-571.
  49. Koonin EV, Wolf YI: **Genomics of bacteria and archaea: the emerging dynamic view of the prokaryotic world.** *Nucl Acids Res* 2008, **36**:6688-6719.

50. Marchler-Bauer A, Anderson JB, Cherukuri PF, DeWeese-Scott C, Geer LY, Gwadz M, He S, Hurwitz DI, Jackson JD, Ke Z, et al.: **CDD: a conserved domain database for protein classification**. *Nucl Acids Res* 2005, **33**:D192-196.
51. Kidwell MG, Lisch DR: **Transposable elements and host genome evolution**. *Trends Ecol Evol* 2000, **15**:95-99.
52. Kruger NJ, von Schaewen A: **The oxidative pentose phosphate pathway: structure and organisation**. *Curr Opin Plant Biol* 2003, **6**:236-246.
53. Doelle HW: **Bacterial metabolism, 2nd ed.** Academic Press, Inc., New York 1975.
54. Gottschalk G: **Bacterial metabolism**. Springer Verlag, New York 1979.
55. Hartmanis MGN, Gatenbeck S: **Intermediary metabolism in *Clostridium acetobutylicum*: Levels of enzymes involved in the formation of acetate and butyrate**. *Appl Environ Microbiol* 1984, **47**:1277-1283.
56. Häggström L: **Acetone-butanol fermentation and its variants**. *Biotechnol Adv* 1985, **3**:13-28.
57. Rogers P, Allen IL: **Genetics and biochemistry of clostridium relevant to development of fermentation processes**. In *Advances in Applied Microbiology*. Edited by: Academic Press; 1986:1-60. vol Volume 31.]
58. Jones DT, Woods DR: **Acetone-butanol fermentation revisited**. *Microb Rev* 1986, **50**:484 - 524.
59. Terracciano JS, Canale-Parola E: **Enhancement of chemotaxis in *Spirochaeta aurantia* grown under conditions of nutrient limitation**. *J Bacteriol* 1984, **159**:173-178.
60. Ford RM, Lauffenburger DA: **A simple expression for quantifying bacterial chemotaxis using capillary assay data: application to the analysis of enhanced chemotactic responses from growth-limited cultures**. *Math Biosci* 1992, **109**:127-149.
61. Wadhams GH, Armitage JP: **Making sense of it all: bacterial chemotaxis**. *Nat Rev Mol Cell Biol* 2004, **5**:1024-1037.
62. Kertesz MA: **Bacterial transporters for sulfate and organosulfur compounds**. *Res Microbiol* 2001, **152**:279-290.
63. Maria S: **Biology of type II secretion**. *Mol Microbiol* 2001, **40**:271-283.
64. Cianciotto NP: **Type II secretion: a protein secretion system for all seasons**. *Trends Microbiol* 2005, **13**:581-588.
65. Lopez-Cortes A, Fardeau M-L, Fauque G, Joulain C, Ollivier B: **Reclassification of the sulfate- and nitrate-reducing bacterium *Desulfovibrio vulgaris* subsp. oxamicus as *Desulfovibrio oxamicus* sp. nov., comb. nov.** *Int J Syst Evol Microbiol* 2006, **56**:1495-1499.
66. Widdel F, Pfennig N: **Studies on dissimilatory sulfate-reducing bacteria that decompose fatty acids II. Incomplete oxidation of propionate by *Desulfobulbus propionicus* gen. nov., sp. nov.** *Arch Microbiol* 1982, **131**:360-365.
67. Lie TJ, Clawson ML, Godchaux W, Leadbetter ER: **Sulfidogenesis from 2-aminoethanesulfonate (taurine) fermentation by a morphologically unusual sulfate-reducing bacterium, *Desulforhopalus singaporensis* sp. nov.** *Appl Environ Microbiol* 1999, **65**:3328-3334.
68. Szewzyk R, Pfennig N: **Complete oxidation of catechol by the strictly anaerobic sulfate-reducing *Desulfobacterium catecholicum* sp. nov.** *Arch Microbiol* 1987, **147**:163-168.
69. Keith SM, Herbert RA: **Dissimilatory nitrate reduction by a strain of *Desulfovibrio desulfuricans***. *FEMS Microbiol Lett* 1983, **18**:55-59.

70. Dalsgaard T, Bak F: **Nitrate reduction in a sulfate-reducing bacterium, *Desulfovibrio desulfuricans*, isolated from rice paddy soil: Sulfide inhibition, kinetics, and regulation.** *Appl Environ Microbiol* 1994, **60**:291-297.
71. Rabus R, Hansen T, Widdel F: **Dissimilatory sulfate- and sulfur-reducing prokaryotes.** In *The Prokaryotes*. Edited by; 2006:659-768.
72. LeGall J, Fauque G: **Dissimilatory reduction of sulfur compounds.** *A.J.B. Zehnder Biology of Anaerobic Microorganisms*. John Wiley & Sons. New York. 1988:587 - 639.
73. Widdel F: **Microbiology and ecology of sulfate- and sulfur-reducing bacteria.** *A.J.B. Zehnder Biology of Anaerobic Microorganisms*. John Wiley & Sons. New York. 1988:469 - 585.
74. Fauque G, LeGall J, Barton L: **Sulfate-reducing and sulfur-reducing bacteria.** *J.M. Shively and L.L. Barton Variations in Autotrophic Life*. Academic Press. London 1991:271 - 337.
75. Bishop PE, Jarlenski DM, Hetherington DR: **Evidence for an alternative nitrogen fixation system in *Azotobacter vinelandii*.** *P Natl Acad Sci USA* 1980, **77**:7342-7346.
76. Kelly MJ, Poole RK, Yates MG, Kennedy C: **Cloning and mutagenesis of genes encoding the cytochrome *bd* terminal oxidase complex in *Azotobacter vinelandii*: mutants deficient in the cytochrome *d* complex are unable to fix nitrogen in air.** *J Bacteriol* 1990, **172**:6010-6019.
77. Kolonay JF, Jr., Moshiri F, Gennis RB, Kaysser TM, Maier RJ: **Purification and characterization of the cytochrome *bd* complex from *Azotobacter vinelandii*: comparison to the complex from *Escherichia coli*.** *J Bacteriol* 1994, **176**:4177-4181.
78. Belevich I, Borisov VB, Bloch DA, Konstantinov AA, Verkhovskiy MI: **Cytochrome *bd* from *Azotobacter vinelandii*: Evidence for high-affinity oxygen binding.** *Biochemistry-US* 2007, **46**:11177-11184.
79. Boyer PD: **The ATP synthase - A splendid molecular machine.** *Annu Rev Biochem* 1997, **66**:717-749.
80. Menzel K, Ahrens K, Zeng AP, Deckwer WD: **Kinetic, dynamic, and pathway studies of glycerol metabolism by *Klebsiella pneumoniae* in anaerobic continuous culture: IV. Enzymes and fluxes of pyruvate metabolism.** *Biotechnol Bioeng* 1998, **60**:617-626.
81. Brandis-Heep A, Gebhardt NA, Thauer RK, Widdel F, Pfennig N: **Anaerobic acetate oxidation to CO<sub>2</sub> by *Desulfobacter postgatei*.** *Arch Microbiol* 1983, **136**:222-229.
82. Gebhardt NA, Linder D, Thauer RK: **Anaerobic acetate oxidation to CO<sub>2</sub> by *Desulfobacter postgatei*.** *Arch Microbiol* 1983, **136**:230-233.
83. Gebhardt NA, Thauer RK, Linder D, Kaulfers P-M, Pfennig N: **Mechanism of acetate oxidation to CO<sub>2</sub> with elemental sulfur in *Desulfuromonas acetoxidans*.** *Arch Microbiol* 1985, **141**:392-398.
84. Paulsen J, Kröger A, Thauer RK: **ATP-driven succinate oxidation in the catabolism of *Desulfuromonas acetoxidans*.** *Arch Microbiol* 1986, **144**:78-83.
85. Möller D, Schauder R, Fuchs G, Thauer RK: **Acetate oxidation to CO<sub>2</sub> via a citric acid cycle involving an ATP-citrate lyase: a mechanism for the synthesis of ATP via substrate level phosphorylation in *Desulfobacter postgatei* growing on acetate and sulfate.** *Arch Microbiol* 1987, **148**:202-207.
86. Schauder R, Eikmanns B, Thauer RK, Widdel F, Fuchs G: **Acetate oxidation to CO<sub>2</sub> in anaerobic bacteria via a novel pathway not involving reactions of the citric acid cycle.** *Arch Microbiol* 1986, **145**:162-172.
87. Thauer RK: **Citric-acid cycle, 50 years on.** *Eur J Biochem* 1988, **176**:497-508.

88. Schauder R, Widdel F, Fuchs G: **Carbon assimilation pathways in sulfate-reducing bacteria II. Enzymes of a reductive citric acid cycle in the autotrophic *Desulfobacter hydrogenophilus*.** *Arch Microbiol* 1987, **148**:218-225.
89. Hugler M, Wirsén CO, Fuchs G, Taylor CD, Sievert SM: **Evidence for autotrophic CO<sub>2</sub> fixation via the reductive tricarboxylic acid cycle by members of the epsilon subdivision of proteobacteria.** *J Bacteriol* 2005, **187**:3020-3027.
90. Thauer RK: **Microbiology - A fifth pathway of carbon fixation.** *Science* 2007, **318**:1732-1733.
91. Kornberg HL: **Anaplerotic sequences and their role in metabolism.** *Essays Biochem* 1966, **2**:1 - 31.
92. Owen OE, Kalhan SC, Hanson RW: **The key role of anaplerosis and cataplerosis for citric acid cycle function.** *J Biol Chem* 2002, **277**:30409-30412.
93. Wood HG, Ragsdale SW, Pezacka E: **The acetyl-CoA pathway: a newly discovered pathway of autotrophic growth.** *Trends Biochem Sci* 1986, **11**:14-18.
94. Wood HG: **Life with CO or CO<sub>2</sub> and H<sub>2</sub> as a source of carbon and energy [published erratum appears in FASEB J 1991 May;5(8):2216].** *FASEB J* 1991, **5**:156-163.
95. Hügler M, Huber H, Stetter KO, Fuchs G: **Autotrophic CO<sub>2</sub> fixation pathways in archaea (Crenarchaeota).** *Arch Microbiol* 2003, **179**:160-173.
96. Safinowski M, Meckenstock RU: **Methylation is the initial reaction in anaerobic naphthalene degradation by a sulfate-reducing enrichment culture.** *Environ Microbiol* 2006, **8**:347-352.





## **5.**

# **General Conclusion and Outlook**

## 5.1 Conclusion and Outlook

Regarding the processes during natural attenuation of aromatic hydrocarbon spills, anaerobic degradation of naphthalene is an important one, as naphthalene represents the smallest non-substituted polycyclic aromatic hydrocarbon (PAH) and is therefore investigated as model substance. However, up to now biodegradation of naphthalene is hardly assessable by conventional methods, the initial activation mechanism of anaerobic naphthalene degradation is still unclear, as well as the knowledge about physiology and metabolic potential of those bacteria is scarce.

Therefore, this is the first study which analyzed a metagenomic sequence of an anaerobic naphthalene-degrading bacterium screening for its metabolic potential. Subsequently, its physiology was explored by sequencing and comparing the proteome during the growth on three different PAHs. Additionally this offered insight concluding for the first reaction step in anaerobic naphthalene degradation. Compound Specific Isotope Analysis (CSIA) could not further support the hypothesis, but it could be shown to be an alternative in assessing biodegradation of naphthalene qualitatively and quantitatively by measuring hydrogen fractionation for the first time.

The annotation of the assembled metagenome of a sulphate-reducing, naphthalene-degrading *deltaproteobacterium* N47 indicated the ability for butanoate fermentation as well as CO<sub>2</sub> fixation via the reductive acetyl-CoA pathway. Both possibilities of growth have not been proven by laboratorial experiments yet. Even though N47 is not growing with NO<sub>3</sub><sup>-</sup> as terminal electron acceptor, the metagenome revealed the capacity to reduce nitrate to ammonium. A potential benefit has to be clarified, or if it is an ancient artefact. Furthermore, N47 was capable to switch between operation of TCA cycle and reductive TCA cycle enabling for heteroorganotrophic and lithoautotrophic growth. Together with the other options of growth mode it mirrors the ability of N47 to adapt to a changing environment as it possess the ability for energy gain under different given conditions. Noticeable N47 is the first eubacterium established containing the reductive acetyl-CoA pathway and the reductive TCA cycle at the same time.

A clear indication for the scarce knowledge in the field of metabolic potential and physiology of especially PAH-degrading bacteria were the many unique putative genes encoded in N47. These are candidates coding for up to now non-elucidated pathways and reactions. This

depicts the necessity for additional insights into potential processes and physiology of anaerobically PAH-degrading bacteria by genomic and proteomic methods.

Turning the focus further down to reaction pathways, the initial activation mechanism for anaerobic naphthalene degradation is still ambiguous. Presently, two hypotheses are discussed. One is a methylation of naphthalene to 2-methylnaphthalene [1,2] subsequently following the recently completely elucidated anaerobic 2-methylnaphthalene degradation pathway [3-5]. The second suggestion is a direct carboxylation of naphthalene to 2-naphthoic acid [6,7].

The comparison of combination of proteomic analyses of naphthalene-, 2-methylnaphthalene-, and 2-naphthoic acid-grown N47 cells by SDS PAGE (sodium dodecyl sulphate-polyacrylamide gel electrophoresis) with MS/MS (mass spectrometry) and 2-DGE (two-dimensional gel electrophoresis) with MS/MS supported the conclusion of carboxylation as initial activation reaction. This hypothesis is based on three findings:

- specific up-regulation of carboxylase related polypeptides in naphthalene-grown cells, compared to 2-methylnaphthalene-grown
- significant sequence similarity and gene structure to those encoding for anaerobic benzene carboxylase catalyzing a similar reaction
- absence of gamma- and delta-subunits as present in the closest related enzyme phenylphosphate carboxylase needed for the phosphatase reaction

Nevertheless, for a final proof of a putative naphthalene carboxylase responsible for the initial activation mechanism, it has to be purified and the activity to be measured. Furthermore, a mutant of the organism lacking those genes has to lose its ability to anaerobically degrade naphthalene. Anyway, the hints for carboxylation are convincing.

Even though CSIA has been shown to offer the possibility to pinpoint degradation pathways of organic contaminants [8,9], in the case of naphthalene it was barely possible. The main obstacle was that it could not be excluded that the initial reaction is split into two consecutive steps resulting in different fractionation depending on which step is rate-limiting.

Anyhow, natural attenuation of organic pollutants in the environment has already been determined by CSIA [10-12]. The carbon isotope fractionation during anaerobic naphthalene degradation has been shown to be too small to serve as robust tool for biodegradation assessment in this study as well as in a former one [13]. In contrast, the measurement of hydrogen isotope fractionation demonstrated the potential leading to a stable quantification of anaerobic naphthalene degradation in the fields by using laboratory derived reference values.

There are many unsolved issues and questions remaining, as for example the direct proof of the initial activation mechanism of anaerobic naphthalene degradation. Which metabolic properties in the genome are artefacts? What are the putative unique genes in N47 coding for? Is a quantitative and qualitative assessment of natural attenuation by CSIA also possible for PAHs containing more than two condensed aromatic rings?

Nevertheless, the investigations done in this work and the accordingly gained insights enlightened the fate of naphthalene during anaerobic biodegradation and the physiology of the responsible bacteria, even though much work has to be done for solving the complete picture.

## 5.2 References

1. Meckenstock RU, Annweiler E, Michaelis W, Richnow HH, Schink B: **Anaerobic naphthalene degradation by a sulfate-reducing enrichment culture**. *Applied and Environmental Microbiology* 2000, **66**:2743-2747.
2. Safinowski M, Meckenstock RU: **Methylation is the initial reaction in anaerobic naphthalene degradation by a sulfate-reducing enrichment culture**. *Environmental Microbiology* 2006, **8**:347-352.
3. Annweiler E, Materna A, Safinowski M, Kappler A, Richnow HH, Michaelis W, Meckenstock RU: **Anaerobic degradation of 2-methylnaphthalene by a sulfate-reducing enrichment culture**. *Applied and Environmental Microbiology* 2000, **66**:5329-5333.
4. Safinowski M, Meckenstock RU: **Enzymatic reactions in anaerobic 2-methylnaphthalene degradation by the sulphate-reducing enrichment culture N 47**. *Fems Microbiology Letters* 2004, **240**:99-104.
5. Selesi D, Jehmlich N, von Bergen M, Schmidt F, Rattei T, Tischler P, Lueders T, Meckenstock RU: **Combined Genomic and Proteomic Approaches Identify Gene Clusters Involved in Anaerobic 2-Methylnaphthalene Degradation in the Sulfate-Reducing Enrichment Culture N47**. *Journal of Bacteriology* 2010, **192**:295-306.
6. Zhang XM, Young LY: **Carboxylation as an initial reaction in the anaerobic metabolism of naphthalene and phenanthrene by sulfidogenic consortia**. *Applied and Environmental Microbiology* 1997, **63**:4759-4764.
7. Musat F, Galushko A, Jacob J, Widdel F, Kube M, Reinhardt R, Wilkes H, Schink B, Rabus R: **Anaerobic degradation of naphthalene and 2-methylnaphthalene by strains of marine sulfate-reducing bacteria**. *Environmental Microbiology* 2009, **11**:209-219.
8. Elsner M, Zwank L, Hunkeler D, Schwarzenbach RP: **A new concept linking observable stable isotope fractionation to transformation pathways of organic pollutants**. *Environ Sci Technol* 2005, **39**:6896-6916.
9. Zwank L, Berg M, Elsner M, Schmidt TC, Schwarzenbach RP, Haderlein SB: **New evaluation scheme for two-dimensional isotope analysis to decipher biodegradation processes: Application to groundwater contamination by MTBE**. *Environ Sci Technol* 2005, **39**:1018-1029.

10. Lollar BS, Slater GF, Sleep B, Witt M, Klecka GM, Harkness M, Spivack J: **Stable carbon isotope evidence for intrinsic bioremediation of tetrachloroethene and trichloroethene at area 6, Dover Air Force Base.** *Environ Sci Technol* 2001, **35**:261-269.
11. Meckenstock RU, Morasch B, Griebler C, Richnow HH: **Stable isotope fractionation analysis as a tool to monitor biodegradation in contaminated aquifers.** *Journal of Contaminant Hydrology* 2004, **75**:215-255.
12. Abe Y, Hunkeler D: **Does the Rayleigh equation apply to evaluate field isotope data in contaminant hydrogeology?** *Environ Sci Technol* 2006, **40**:1588-1596.
13. Griebler C, Safinowski M, Vieth A, Richnow HH, Meckenstock RU: **Combined application of stable carbon isotope analysis and specific metabolites determination for assessing in situ degradation of aromatic hydrocarbons in a tar oil-contaminated aquifer.** *Environ Sci Technol* 2004, **38**:617-631.



## **Supplementary material chapter 2**

### GC/MS operation mode:

The injector temperature was 220°C and helium (grade 5.0) served as carrier gas with a flow rate of 1 ml/min and a split ratio of 1 : 10. The oven temperature was set to 40°C and held for 3 minutes. Afterwards the temperature was risen at 9.6 °C/min to 150°C and subsequently at a rate of 100.0 °C/min to 310°C where it was kept for 4 minutes. The mass spectrometer was operated in single ion monitoring (SIM) mode. Quantification was accomplished at the masses  $m/z = 91, 92, 127, 128$  using a 5 point calibration of naphthalene in cyclohexane.

### Compound specific isotope ratio measurements:

Compound specific isotope ratios were measured using a TRACE GC Ultra gas chromatograph (GC) (Thermo Fisher Scientific; Milan, Italy), coupled to a Finnigan<sup>TM</sup> MAT 253 IRMS (Thermo Fisher Scientific; Bremen, Germany) connected by a Finnigan<sup>TM</sup> GC Combustion III Interface. The temperature of the combustion oven was 940°C for carbon isotope analysis. For hydrogen isotope analysis a pyrolytic interface was used with the pyrolysis oven set to 1440°C. The GC was equipped with a programmable temperature vaporizer (PTV) injector (Optic3, ATAS GL International B.V.; Veldhoven, Netherlands) with cryofocussing option by liquid N<sub>2</sub>. A purge and trap concentrator Tekmar VelocityXPT<sup>TM</sup> together with an autosampler Tekmar AQUATEk 70 (Tekmar-Dohrmann; Mason, Ohio, USA) were connected online to the PTV injector of the GC-IRMS. Operation of the purge & trap system including cryofocussing of analytes in the injector was accomplished according to (61).

For carbon isotope analysis of benzene the GC was equipped with a Vocol<sup>TM</sup> capillary column (30m x 0.25, 1.5 µm film thickness, Supelco, Bellefonte, PA, USA) connected to fused-silica pre- and postcolumns (FS-Methyl-Sil, 2 m x 0.32 mm and 1 m x 0.32 mm, respectively; CS Chromatographie Service GmbH, Langerwehe, Germany). The GC-oven was programmed from 40°C (hold: 4 min), ramp 8°C min<sup>-1</sup> to 100°C, ramp 30°C min<sup>-1</sup> to 220°C (hold: 5 min). In contrast, for the carbon isotope analysis of naphthalene the GC was equipped with a DB-624 capillary column (60 m x 0.25 mm, 1.4 µm film thickness from Supelco; Bellefonte, Pennsylvania, USA) connected to fused-silica pre- and postcolumns (FS-Methyl-Sil, 2 m x 0.32 mm and 1 m x 0.32 mm respectively, CS Chromatographie Service GmbH; Langerwehe, Germany). The GC oven was initially set to 50°C for 4 min, then heated with 10°C min<sup>-1</sup> to 120°C, with 3°C min<sup>-1</sup> to 140°C, and with 15°C min<sup>-1</sup> to 250°C where it was held for 12 min.

Hydrogen isotope analysis was not possible under the same conditions because of high backgrounds caused by elevated water concentrations in the system. GC analysis was therefore accomplished with a Supelcowax<sup>TM</sup> capillary column (30 m x 0.25 mm, 0.5  $\mu\text{m}$  film thickness, Supelco, Bellefonte, Pennsylvania, USA). For benzene measurements the GC-oven was programmed from 40°C (hold: 0.5 min), ramp 3°C min<sup>-1</sup> to 45°C (hold: 5min), ramp 4°C min<sup>-1</sup> to 95°C, ramp 20°C min<sup>-1</sup> to 200°C (5 min). For naphthalene measurements the GC oven was initially set to 50°C for 1 min, then heated with 10°C min<sup>-1</sup> to 80°C and with 8°C min<sup>-1</sup> to 240°C where it was held for 10 min. Helium of grade 5 served in both cases as carrier gas. Depending on the concentration in the samples of benzene (404  $\mu\text{M}$  to 8  $\mu\text{M}$ ) or naphthalene (202  $\mu\text{M}$  to 1,9  $\mu\text{M}$ ) the split ratio was set between 8 and 120. The isotope ratios are expressed in the  $\delta$ -notation ( $\delta^{13}\text{C}$  and  $\delta^2\text{H}$ ) according to equation 2.

For the carbon isotope analysis of naphthalene by GC-IRMS, a laboratory CO<sub>2</sub> standard was used as calibration gas. This laboratory standard had been calibrated to V-PDB by reference CO<sub>2</sub> standards (RM 8562, RM 8563, RM 8564). In contrast, hydrogen isotope analysis of naphthalene was performed using a laboratory H<sub>2</sub> monitoring gas, which had not been calibrated against an international standard. For this reason changes in hydrogen isotope ratios are given as relative differences  $\Delta\delta^2\text{H} = \delta^2\text{H}_t - \delta^2\text{H}_0$  where  $\delta^2\text{H}_0$  is the mean isotope value of the control bottles at time point zero. All samples were measured in duplicate. Reproducibility for  $\delta^{13}\text{C}$  and  $\delta^2\text{H}$  was always better than 0.5‰ and 5‰.



## **Supplementary material chapter 4**

Table S4.1: 50 universal bacterial COGs used to assess N47 metagenome completeness.

Pcar_0002	Pcar_0686	Pcar_0723	Pcar_1555	Pcar_2002
Pcar_0004	Pcar_0690	Pcar_0726	Pcar_1618	Pcar_2210
Pcar_0005	Pcar_0691	Pcar_0727	Pcar_1650	Pcar_2315
Pcar_0100	Pcar_0698	Pcar_0728	Pcar_1694	Pcar_2348
Pcar_0101	Pcar_0699	Pcar_0742	Pcar_1741	Pcar_2489
Pcar_0107	Pcar_0701	Pcar_1222	Pcar_1899	Pcar_2532
Pcar_0197	Pcar_0707	Pcar_1413	Pcar_1918	Pcar_2581
Pcar_0326	Pcar_0713	Pcar_1418	Pcar_1920	Pcar_2692
Pcar_0550	Pcar_0716	Pcar_1421	Pcar_1921	Pcar_2698
Pcar_0588	Pcar_0720	Pcar_1422	Pcar_1969	Pcar_2864
Pcar_0592	Pcar_0721	Pcar_1423	Pcar_1995	Pcar_3143
Pcar_0682	Pcar_0722	Pcar_1553	Pcar_2000	

Table S4.2: Number of predicted proteins of N47 showing significant similarities to already known bacterial proteins using different e-value cutoffs and databases to assess the conservation of the predicted proteome.

database	e-value cutoff	1e-02	1e-03	1e-10
SwissProt	nr of proteins	3681 (70%)	3237 (62%)	2439 (47%)
UniProtKB	nr of proteins	4523 (86%)	4474 (86%)	4213 (81%)

Table S4.3: Unique genes for proteomes of the taxon delta/epsilon subdivisions according to COG calculation.

organism name	nr of unique genes
<i>Anaeromyxobacter dehalogenans</i> 2CP-1	174
<i>Anaeromyxobacter dehalogenans</i> 2CP-C	190
<i>Anaeromyxobacter</i> sp. Fw109-5	406
<i>Anaeromyxobacter</i> sp. K	135
<i>Arcobacter butzleri</i> RM4018	195
<i>Bdellovibrio bacteriovorus</i> HD100	1113
<i>Campylobacter concisus</i> 13826	280
<i>Campylobacter curvus</i> 525.92	224
<i>Campylobacter fetus</i> subsp. fetus 82-40	112
<i>Campylobacter hominis</i> ATCC BAA-381	312
<i>Campylobacter jejuni</i> RM1221	134
<i>Campylobacter jejuni</i> subsp. doylei 269.97	141
<i>Campylobacter jejuni</i> subsp. jejuni 81116	33
<i>Campylobacter jejuni</i> subsp. jejuni 81-176	109
<i>Campylobacter jejuni</i> subsp. jejuni NCTC 11168	44
<i>Campylobacter lari</i> RM2100	53
<i>Desulfatibacillum alkenivorans</i> AK-01	1001
<i>Desulfobacterium autotrophicum</i> HRM2	907
<i>Desulfococcus oleovorans</i> Hxd3	352
<i>Desulfotalea psychrophila</i> LSv54	697
<i>Desulfovibrio desulfuricans</i> subsp. desulfuricans str. ATCC 27774	238
<i>Desulfovibrio desulfuricans</i> subsp. desulfuricans str. G20	741
<i>Desulfovibrio vulgaris</i> str. Miyazaki F	144
<i>Desulfovibrio vulgaris</i> subsp. vulgaris DP4	88
<i>Desulfovibrio vulgaris</i> subsp. vulgaris str. Hildenborough	505
<i>Geobacter bemidjiensis</i> Bem	365
<i>Geobacter lovleyi</i> SZ	398
<i>Geobacter metallireducens</i> GS-15	202
<i>Geobacter</i> sp. FRC-32	310
<i>Geobacter sulfurreducens</i> PCA	274
<i>Geobacter uraniumreducens</i> Rf4	356
<i>Helicobacter acinonychis</i> str. Sheeba	268
<i>Helicobacter hepaticus</i> ATCC 51449	325
<i>Helicobacter pylori</i> 26695	81
<i>Helicobacter pylori</i> G27	54
<i>Helicobacter pylori</i> HPAG1	60
<i>Helicobacter pylori</i> J99	30
<i>Helicobacter pylori</i> P12	63
<i>Helicobacter pylori</i> Shi470	135
<i>Lawsonia intracellularis</i> PHE/MN1-00	55
<i>Myxococcus xanthus</i> DK 1622	2141
N47	1867
<i>Nautilia profundicola</i> AmH	127
<i>Nitratiruptor</i> sp. SB155-2	103
<i>Pelobacter carbinolicus</i> DSM 2380	512
<i>Pelobacter propionicus</i> DSM 2379	463
<i>Sorangium cellulosum</i> So ce 56	3164
<i>Sulfurimonas denitrificans</i> DSM 1251	137
<i>Sulfurovum</i> sp. NBC37-1	275
<i>Syntrophobacter fumaroxidans</i> MPOB	719
<i>Syntrophus aciditrophicus</i> SB	736
<i>Wolinella succinogenes</i> DSM 1740	129

Table S4.4: Unique genes for proteomes of the taxon Deltaproteobacteria according to COG calculation.

organism name	nr of unique genes
<i>Anaeromyxobacter dehalogenans</i> 2CP-1	179
<i>Anaeromyxobacter dehalogenans</i> 2CP-C	195
<i>Anaeromyxobacter</i> sp. Fw109-5	420
<i>Anaeromyxobacter</i> sp. K	139
<i>Bdellovibrio bacteriovorus</i> HD100	1231
<i>Desulfatibacillum alkenivorans</i> AK-01	1076
<i>Desulfobacterium autotrophicum</i> HRM2	1004
<i>Desulfococcus oleovorans</i> Hxd3	399
<i>Desulfotalea psychrophila</i> LSv54	780
<i>Desulfovibrio desulfuricans</i> subsp. <i>desulfuricans</i> str. ATCC 27774	260
<i>Desulfovibrio desulfuricans</i> subsp. <i>desulfuricans</i> str. G20	769
<i>Desulfovibrio vulgaris</i> str. Miyazaki F	146
<i>Desulfovibrio vulgaris</i> subsp. <i>vulgaris</i> DP4	95
<i>Desulfovibrio vulgaris</i> subsp. <i>vulgaris</i> str. Hildenborough	511
<i>Geobacter bemidjiensis</i> Bem	392
<i>Geobacter lovleyi</i> SZ	437
<i>Geobacter metallireducens</i> GS-15	221
<i>Geobacter</i> sp. FRC-32	341
<i>Geobacter sulfurreducens</i> PCA	287
<i>Geobacter uraniumreducens</i> Rf4	388
<i>Lawsonia intracellularis</i> PHE/MN1-00	66
<i>Myxococcus xanthus</i> DK 1622	2266
N47	1949
<i>Pelobacter carbinolicus</i> DSM 2380	554
<i>Pelobacter propionicus</i> DSM 2379	506
<i>Sorangium cellulosum</i> So ce 56	3315
<i>Syntrophobacter fumaroxidans</i> MPOB	758
<i>Syntrophus aciditrophicus</i> SB	770

Table S4.5: Number of paralogous genes per genome for taxa delta/epsilon subdivisions and Deltaproteobacteria.

taxon	organism name	# paralogues	# cluster	Ø per cluster	# genes of org	% paralogues per org
δ-proteo	<i>Anaeromyxobacter dehalogenans</i> 2CP-1	702	259	2.71042471	4473	15.69416499
δ-proteo	<i>Anaeromyxobacter dehalogenans</i> 2CP-C	684	240	2.85	4346	15.73861022
δ-proteo	<i>Anaeromyxobacter</i> sp. Fw109-5	769	277	2.776173285	4466	17.21898791
δ-proteo	<i>Anaeromyxobacter</i> sp. K	736	261	2.819923372	4457	16.51334979
δ/ε subdiv	<i>Arcobacter butzleri</i> RM4018	213	77	2.766233766	2259	9.428950863
δ-proteo	<i>Bdellovibrio bacteriovorus</i> HD100	294	117	2.512820513	3588	8.193979933
δ/ε subdiv	<i>Campylobacter concisus</i> 13826	158	66	2.393939394	1985	7.959697733
δ/ε subdiv	<i>Campylobacter curvus</i> 525.92	99	43	2.302325581	1931	5.126877266
δ/ε subdiv	<i>Campylobacter fetus</i> subsp. fetus 82-40	97	39	2.487179487	1719	5.64281559
δ/ε subdiv	<i>Campylobacter hominis</i> ATCC BAA-381	95	39	2.435897436	1687	5.631298162
δ/ε subdiv	<i>Campylobacter jejuni</i> RM1221	94	40	2.35	1838	5.114254625
δ/ε subdiv	<i>Campylobacter jejuni</i> subsp. doylei 269.97	143	64	2.234375	1731	8.261120739
δ/ε subdiv	<i>Campylobacter jejuni</i> subsp. jejuni 81116	75	29	2.586206897	1626	4.612546125
δ/ε subdiv	<i>Campylobacter jejuni</i> subsp. jejuni 81-176	93	40	2.325	1758	5.290102389
δ/ε subdiv	<i>Campylobacter jejuni</i> subsp. jejuni NCTC 11168	79	33	2.393939394	1629	4.849600982
δ/ε subdiv	<i>Campylobacter lari</i> RM2100	85	35	2.428571429	1545	5.501618123
δ-proteo	<i>Desulfatibacillum alkenivorans</i> AK-01	989	337	2.934718101	5252	18.83092155
δ-proteo	<i>Desulfobacterium autotrophicum</i> HRM2	841	279	3.014336918	4943	17.01395913
δ-proteo	<i>Desulfococcus oleovorans</i> Hxd3	387	153	2.529411765	3265	11.85298622
δ-proteo	<i>Desulfotalea psychrophila</i> Lsv54	368	145	2.537931034	3234	11.37909709
δ-proteo	<i>Desulfovibrio desulfuricans</i> subsp. desulfuricans str. ATCC 27774	217	82	2.646341463	2356	9.210526316
δ-proteo	<i>Desulfovibrio desulfuricans</i> subsp. desulfuricans str. G20	631	238	2.651260504	3775	16.71523179
δ-proteo	<i>Desulfovibrio vulgaris</i> str. Miyazaki F	397	126	3.150793651	3180	12.48427673
δ-proteo	<i>Desulfovibrio vulgaris</i> subsp. vulgaris DP4	420	157	2.675159236	3091	13.58783565
δ-proteo	<i>Desulfovibrio vulgaris</i> subsp. vulgaris str. Hildenborough	469	173	2.710982659	3531	13.28235627
δ-proteo	<i>Geobacter bemidjiensis</i> Bem	773	278	2.78057554	4018	19.23842708
δ-proteo	<i>Geobacter lovleyi</i> SZ	705	254	2.775590551	3685	19.13161465
δ-proteo	<i>Geobacter metallireducens</i> GS-15	630	213	2.957746479	3532	17.83691959
δ-proteo	<i>Geobacter</i> sp. FRC-32	646	239	2.70292887	3798	17.00895208
δ-proteo	<i>Geobacter sulfurreducens</i> PCA	525	180	2.916666667	3445	15.2394775
δ-proteo	<i>Geobacter uraniumreducens</i> Rf4	958	337	2.84272997	4357	21.98760615

δ/ε subdiv	<i>Helicobacter acinonychis</i> str. Sheeba	127	60	2.116666667	1618	7.849196539
δ/ε subdiv	<i>Helicobacter hepaticus</i> ATCC 51449	102	42	2.428571429	1875	5.44
δ/ε subdiv	<i>Helicobacter pylori</i> 26695	119	46	2.586956522	1576	7.550761421
δ/ε subdiv	<i>Helicobacter pylori</i> G27	95	38	2.5	1504	6.316489362
δ/ε subdiv	<i>Helicobacter pylori</i> HPAG1	110	43	2.558139535	1544	7.124352332
δ/ε subdiv	<i>Helicobacter pylori</i> J99	108	44	2.454545455	1489	7.25319006
δ/ε subdiv	<i>Helicobacter pylori</i> P12	105	41	2.56097561	1578	6.653992395
δ/ε subdiv	<i>Helicobacter pylori</i> Shi470	101	45	2.244444444	1569	6.43722116
δ-proteo	<i>Lawsonia intracellularis</i> PHE/MN1-00	50	22	2.272727273	1180	4.237288136
δ-proteo	<i>Myxococcus xanthus</i> DK 1622	1248	434	2.875576037	7331	17.02359842
δ-proteo	N47	1375	360	3.819444444	5231	26.28560505
δ/ε subdiv	<i>Nautilia profundicola</i> AmH	78	34	2.294117647	1730	4.50867052
δ/ε subdiv	<i>Nitratiruptor</i> sp. SB155-2	95	42	2.261904762	1843	5.154639175
δ-proteo	<i>Pelobacter carbinolicus</i> DSM 2380	509	196	2.596938776	3352	15.1849642
δ-proteo	<i>Pelobacter propionicus</i> DSM 2379	794	301	2.637873754	3804	20.87276551
δ-proteo	<i>Sorangium cellulosum</i> So ce 56	2218	689	3.2191582	9384	23.63597613
δ/ε subdiv	<i>Sulfurimonas denitrificans</i> DSM 1251	139	65	2.138461538	2097	6.628516929
δ/ε subdiv	<i>Sulfurovum</i> sp. NBC37-1	257	113	2.274336283	2438	10.5414274
δ-proteo	<i>Syntrophobacter fumaroxidans</i> MPOB	769	289	2.660899654	4064	18.92224409
δ-proteo	<i>Syntrophus aciditrophicus</i> SB	437	169	2.585798817	3168	13.79419192
δ/ε subdiv	<i>Wolinella succinogenes</i> DSM 1740	180	70	2.571428571	2042	8.814887365

Table S4.6: Percentage of repetitive metagenomic sequence according to the categories given by REPuter (Kurtz 1999) evaluated for different window sizes for the minimal repeat length.

repeat category	window size 100 coverage [%] of metagenome	window size 300 coverage [%] of metagenome	window size 500 coverage [%] of metagenome
complement (C)	0.0	0.0	0.0
forward (F)	12.6	10.8	9.1
palindromic (P)	11.4	9.6	8.4
reverse (R)	0.0	0.0	0.0
F & P	13.9	12.2	10.6
C & F & P & R	13.9	12.2	10.6

Additional material on CD: Coloured\_KEGG\_maps.tar.gz, containing all multicoloured KEGG PATHWAY maps as .png files used for evaluation and colour coding.pdf, explaining the evaluation of the used colour code.





## Clarifications

Chapter 2: “C and H stable isotope fractionation during strictly anaerobic naphthalene and benzene degradation: mechanistic implications and potential to assess natural attenuation.”

The contributions of the PhD candidate to this work were the following:

The concept for the experiment was developed by Prof. Dr. Rainer Meckenstock, Dr. Martin Elsner, Dr. Nidal Abu Laban and the PhD candidate. The experimental design was done by Dr. Nidal Abu Laban and the PhD candidate. The preparation, sampling and concentration measurements for the benzene-degrading cultures were done by Dr. Nidal Abu Laban. The preparation, sampling and concentration for the naphthalene-degrading cultures were done by the PhD candidate. The GC-IRMS measurements for both substances were done together with Nadezda Kadlec and Armin Meyer. The evaluation, statistical data analyses and their graphical illustration were done by the PhD candidate independently. Prof. Dr. Rainer Meckenstock, Dr. Martin Elsner and the PhD candidate interpreted and discussed the results together. The draft of the manuscript was written by the PhD candidate independently and the comments of Prof. Dr. Rainer Meckenstock and Dr. Martin Elsner included afterwards. The manuscript was submitted by the corresponding author Prof. Dr. Rainer Meckenstock to the ACS Journal *Environmental Science and Technology*.

Chapter 3: “Identification of new potential enzymes involved in anaerobic naphthalene degradation by the sulphate-reducing enrichment culture N47.”

The contributions of the PhD candidate to this work were the following:

The experimental design and idea for the experiment were conceived by Dr. Draženka Selesi and the PhD candidate and complemented by Prof. Dr. Rainer Meckenstock. Cultivation of bacteria, sample preparation for subsequent 2-DGE, MALDI-TOF-MS and T-RFLP and data evaluation were done by Dr. Draženka Selesi. The PhD candidate performed the cultivation of bacteria, sample preparation for subsequent SDS PAGE, ESI LTQ Orbitrap XL MS and T-RFLP and data evaluation. The results were discussed by all three authors together and combined to a manuscript by the PhD candidate. Proof reading was done by both co-authors. The manuscript was submitted by the corresponding author Prof. Dr. Rainer Meckenstock to the Springer Journal *Archives of Microbiology*.

Chapter 4: “Genomic insights in the metabolic potential of the polycyclic aromatic hydrocarbon degrading sulphate-reducing culture N47.”

The contributions of the PhD candidate to this work were the following:

The ideas and concept for the experimental design were carried out by Prof. Dr. Rainer Meckenstock, Prof. Dr. Thomas Rattei, Dr. Draženka Selesi and the PhD candidate. The cultivation of culture N47 was done by Dr. Draženka Selesi. Sequencing and assembly were done by diverse external companies. The genome annotation was done by Patrick Tischler, Dr. Draženka Selesi, the PhD candidate and Prof. Dr. Thomas Rattei. The KEGG pathway maps were multicoloured by an in-house tool by Thomas Weinmaier. All other genomic analyses were performed by Patrick Tischler and the PhD candidate. The evaluation and analyses of the data were achieved by the PhD candidate. The interpretations and conclusions drawn by the PhD candidate were refined by Prof. Dr. Thomas Rattei and Prof. Dr. Rainer Meckenstock. Finally, the manuscript was written by the PhD candidate and proof read by all co-authors. The manuscript was submitted by the corresponding author Prof. Dr. Rainer Meckenstock to the Wiley-Blackwell Journal *Environmental Microbiology*.

## **Danksagung**

Um eine solche Arbeit anfangen, durchführen und v.a. erfolgreich beenden zu können, bedarf es der Unterstützung vieler Personen auf dem Weg dorthin. Diesen Leuten möchte ich an dieser Stelle für ihre unterschiedliche Art und Weise der Hilfe danken.

Großer Dank gilt vor allem meinem Doktorvater und Institutsleiter Prof. Dr. Rainer Meckenstock, der mir ermöglichte diese Arbeit anzutreten und das Vertrauen in mich setzte sie zu einem erfolgreichen Ende zu führen. Er brachte mir stets die fachliche, konzeptionelle und nicht zuletzt finanzielle Unterstützung entgegen um meine Forschungen erfolgreich gestalten zu können um schließlich diese Arbeit verfassen zu können. Insbesondere möchte ich Dir für die sehr intensive und stets zielgerichtete Betreuung in den letzten Monaten danken.

Ebenso sehr großen Dank richte ich an Dr. Draženka Selesi, die mich in den ersten 3 Jahren meiner Arbeit intensiv betreut hat und auch nach ihrer Zeit am Institut immer mit Rat und Tat zur Seite stand. Ohne ihre Hilfe und Unterstützung wäre diese Arbeit nie zustande gekommen. Ich danke dir für die Zeit, das Engagement, das Vertrauen und die Motivation, welche du mir stets geschenkt hast. Vor allem die vielen aufmunternden Worte werden mir immer in positiver Erinnerung bleiben. Nicht zu vergessen so mancher Abend, den wir um die Häuser gezogen sind. Getreu dem Motto „Schaff was!“ möchte ich dir liebe Draženka nochmals vielen lieben Dank sagen!!

Großer Dank richtet sich auch an meine Kollegen die mich sowohl fachlich als auch menschlich immer unterstützt haben: Martin Elsner, Claudia Kellermann, Armin Meyer, Thomas Rattei, Patrick Tischler, Thomas Weinmaier. Dankeschön.

Ein ganz spezieller Dank geht an meine Container-Crew Armino Schlomäiée, Bibie the evil lab dragon und Viktor P.Ä. Raggefängg und außerdem der ewigen Königin Muno, Fürstin der Finsternis, Johnny Pornetti, Plauzolita und Maggoö für die vielen lustigen Stunden die wir hier und außerhalb zusammen verbracht haben.

Mein Dank geht auch an alle anderen IGÖ'ler, Helmholtzer und WZWler, die für eine freundschaftliche und produktive Atmosphäre an den Instituten gesorgt haben.

Mein ganz privater Dank geht an Clemens, Evelyn, Günthna, Johannes, Markus, Martin, Roman, Sarah, Sebastian, Verena und alle die ich vergessen habe namentlich zu erwähnen - ihr wisst wofür.

Nicht zuletzt möchte ich mich ganz herzlich bei meiner Familie bedanken, die mich immer und zu jeder Zeit in jeder erdenklichen Form unterstützt hat. Ohne ihren permanenten

Rückhalt und ihre Hilfe wäre ich niemals an den Punkt gekommen an dem ich jetzt stehe.  
Vielen lieben Dank für Alles an Agnes, Annerose, Detlef, Hedi, Hermann, Margot, Regina,  
Richard, Roland und meiner geliebten Shushu.

## Curriculum Vitae

04.03.1981 geboren in Dachau

1991 – 2000 Abitur am Josef-Hofmiller-Gymnasium in Freising, Deutschland

2001 – 2006 Bioinformatikdiplom an der Technischen Universität München und an der Ludwig-Maximilians-Universität in München, Deutschland

2005 – 2006 Diplomarbeit an der Technischen Universität München am Lehrstuhl für Genomorientierte Bioinformatik:

“Development of methods for the functional analyses of bacterial genomes by comparative genomics and application to Chlamydial genomes”

betreut durch Prof. Dr. Thomas Rattei und Prof. Dr. Hans-Werner Mewes

2006 – 2010 Doktorand in der Arbeitsgruppe anaerober Abbau am Institut für Grundwasserökologie in Neuherberg, betreut durch Dr. Draženka Selesi und Prof. Dr. Rainer Meckenstock